The Astrophysical Journal 966:137 32pp), 2024 May 1 https: doi.org 10.3847 1538-4357 ad27d3

Search for Gravitational wave Transients Associated with Magnetar Bursts in Advanced LIGO and Advanced Virgo Data from the Third Observing Run

R. Abbott[1], H. Abe[2], F. Acernese[3,4], K. Ackley[5], N. Adhikari[6], R. X. Adhikari[1], V. K. Adkins[7], V. B. Adya[8], C. Affeldt[9,10], D. Agarwal[11], M. Agathos[12,13], K. Agatsuma[14], N. Aggarwal[15], O. D. Aguiar[16], L. Aiello[17], A. Ain[18], P. Ajith[19], T. Akutsu[20,21], S. Albanesi[22,23], R. A. Alfaidi[24], A. Allocca[4,25], P. A. Altin[8], A. Amato[26], C. Anand[5], S. Anand[1], A. Ananyeva[1], S. B. Anderson[1], W. G. Anderson[6], M. Ando[27,28], T. Andrade[29], N. Andres[30], M. Andrés-Carcasona[31], T. Andri [32], S. V. Angelova[33], S. Ansoldi[34,35], J. M. Antelis[36], S. Antier[37,38], T. Apostolatos[39], E. Z. Appavuravther[40,41], S. Appert[1], S. K. Apple[42], K. Arai[1], A. Araya[43], M. C. Araya[1], J. S. Areeda[44], M. Arène[45], N. Aritomi[20], N. Arnaud[46,47], M. Arogeti[48], S. M. Aronson[7], H. Asada[49], Y. Asali[50], G. Ashton[51], Y. Aso[52,53], M. Assiduo[54,55], S. Assis de Souza Melo[47], S. M. Aston[56], P. Astone[57], F. Aubin[55], K. AultONeal[36], C. Austin[7], S. Babak[45], F. Badaracco[58], M. K. M. Bader[59], C. Badger[60], S. Bae[61], Y. Bae[62], A. M. Baer[63], S. Bagnasco[23], Y. Bai[1], J. Baird[45], R. Bajpai[64], T. Baka[65], M. Ball[66], G. Ballardin[47], S. W. Ballmer[67], A. Balsamo[63], G. Baltus[68], S. Banagiri[15], B. Banerjee[32], D. Bankar[11], J. C. Barayoga[1], C. Barbieri[69,70,71], B. C. Barish[1], D. Barker[72], P. Barneo[29], F. Barone[4,73], B. Barr[24], L. Barsotti[74], M. Barsuglia[45], D. Barta[75], J. Bartlett[72], M. A. Barton[24], I. Bartos[76], S. Basak[19], R. Bassiri[77], A. Basti[18,78], M. Bawaj[40,79], J. C. Bayley[24], M. Bazzan[80,81], B. R. Becher[82], B. Bécsy[83], V. M. Bedakihale[84], F. Beirnaert[85], M. Bejger[86], I. Belahcene[46], V. Benedetto[87], D. Beniwal[88], M. G. Benjamin[89], T. F. Bennett[90], J. D. Bentley[14], M. BenYaala[33], S. Bera[11], M. Berbel[91], F. Bergamin[9,10], B. K. Berger[77], S. Bernuzzi[13], D. Bersanetti[92], A. Bertolini[59], J. Betzwieser[56], D. Beveridge[93], R. Bhandare[94], A. V. Bhandari[11], U. Bhardwaj[38,59], R. Bhatt[1], D. Bhattacharjee[95], S. Bhaumik[76], A. Bianchi[59,96], I. A. Bilenko[97], G. Billingsley[1], S. Bini[98,99], R. Birney[100], O. Birnholtz[101], S. Biscans[1,74], M. Bischi[54,55], S. Biscoveanu[74], A. Bisht[9,10], B. Biswas[11], M. Bitossi[18,47], M.-A. Bizouard[37], J. K. Blackburn[1], C. D. Blair[93], D. G. Blair[93], R. M. Blair[72], F. Bobba[102,103], N. Bode[9,10], M. Boër[37], G. Bogaert[37], M. Boldrini[57,104], G. N. Bolingbroke[88], L. D. Bonavena[80], F. Bondu[105], E. Bonilla[77], R. Bonnand[30], P. Booker[9,10], B. A. Boom[59], R. Bork[1], V. Boschi[18], N. Bose[106], S. Bose[11], V. Bossilkov[93], V. Boudart[68], Y. Bouffanais[80,81], A. Bozzi[47], C. Bradaschia[18], P. R. Brady[6], A. Bramley[56], A. Branch[56], M. Branchesi[32,107], J. E. Brau[66], M. Breschi[13], T. Briant[108], J. H. Briggs[24], A. Brillet[37], M. Brinkmann[9,10], P. Brockill[6], A. F. Brooks[1], J. Brooks[47], D. D. Brown[88], S. Brunett[1], G. Bruno[58], R. Bruntz[63], J. Bryant[14], F. Bucci[55], T. Bulik[109], H. J. Bulten[59], A. Buonanno[110,111], K. Burtnyk[72], R. Buscicchio[14], D. Buskulic[30], C. Buy[112], R. L. Byer[77], G. S. Cabourn Davies[51], G. Cabras[34,35], R. Cabrita[58], L. Cadonati[48], M. Caesar[113], G. Cagnoli[26], C. Cahillane[72], J. Calderón Bustillo[114], J. D. Callaghan[24], T. A. Callister[115,116], E. Calloni[4,25], J. Cameron[93], J. B. Camp[117], M. Canepa[92,118], S. Canevarolo[65], M. Cannavacciuolo[102], K. C. Cannon[28], H. Cao[88], Z. Cao[119], E. Capocasa[20,45], E. Capote[67], G. Carapella[102,103], F. Carbognani[47], M. Carlassara[9,10], J. B. Carlin[120], M. F. Carney[15], M. Carpinelli[47,121,122], G. Carrillo[66], G. Carullo[18,78], T. L. Carver[17], J. Casanueva Diaz[47], C. Casentini[123,124], G. Castaldi[125,126], S. Caudill[59,65], M. Cavaglià[95], F. Cavalier[46], R. Cavalieri[47], G. Cella[18], P. Cerdá-Durán[127], E. Cesarini[124], W. Chaibi[37], S. Chalathadka Subrahmanya[128], E. Champion[129], C.-H. Chan[130], C. Chan[28], C. L. Chan[131], K. Chan[131], M. Chan[132], K. Chandra[106], I. P. Chang[130], P. Chanial[47], S. Chao[130], C. Chapman-Bird[24], P. Charlton[133], E. A. Chase[15], E. Chassande-Mottin[45], C. Chatterjee[93], Debarati Chatterjee[11], Deep Chatterjee[6], M. Chaturvedi[94], S. Chaty[45], C. Chen[134,135], D. Chen[52], H. Y. Chen[74], J. Chen[130], K. Chen[136], X. Chen[93], Y.-B. Chen[137], Y.-R. Chen[138], Z. Chen[17], H. Cheng[76], C. K. Cheong[131], H. Y. Cheung[131], H. Y. Chia[76], F. Chiadini[103,139], C-Y. Chiang[140], G. Chiarini[81], R. Chierici[141], A. Chincarini[92], M. L. Chiofalo[18,78], A. Chiummo[47], R. K. Choudhary[93], S. Choudhary[11], N. Christensen[37], Q. Chu[93], Y-K. Chu[140], S. S. Y. Chua[8], K. W. Chung[60], G. Ciani[80,81], P. Ciecielag[86], M. Cieślar[86], M. Cifaldi[123,124], A. A. Ciobanu[88], R. Ciol [81,142], F. Cipriano[37], F. Clara[72], J. A. Clark[1,48], P. Clearwater[143], S. Clesse[144], F. Cleva[37], E. Coccia[32,107], E. Codazzo[32], P.-F. Cohadon[108], D. E. Cohen[46], M. Colleoni[145], C. G. Collette[146], A. Colombo[69,70], M. Colpi[69,70], C. M. Compton[72], M. Constancio, Jr.[16], L. Conti[81], S. J. Cooper[14], P. Corban[56], T. R. Corbitt[7], I. Cordero-Carrión[147], S. Corezzi[40,79], K. R. Corley[50], N. J. Cornish[83], D. Corre[46], A. Corsi[148], S. Cortese[47], C. A. Costa[16], R. Cotesta[111], R. Cottingham[56], M. W. Coughlin[149], J.-P. Coulon[37], S. T. Countryman[50], B. Cousins[150], P. Couvares[1], D. M. Coward[93], M. J. Cowart[56], D. C. Coyne[1], R. Coyne[151], J. D. E. Creighton[6], T. D. Creighton[89], A. W. Criswell[149], M. Croquette[108], S. G. Crowder[152], J. R. Cudell[68], T. J. Cullen[7], A. Cumming[24], R. Cummings[24], L. Cunningham[24], E. Cuoco[18,47,153], M. Cury o[109], P. Dabadie[26], T. Dal Canton[46], S. Dall Osso[32], G. Dálya[85,154], A. Dana[77], B. D Angelo[92,118], S. Danilishin[59,155], S. D Antonio[124], K. Danzmann[9,10], C. Darsow-Fromm[128], A. Dasgupta[84], L. E. H. Datrier[24], Sayak Datta[11], Sayantani Datta[156], V. Dattilo[47], I. Dave[94], M. Davier[46], D. Davis[1], M. C. Davis[113], E. J. Daw[157], R. Dean[113], D. DeBra[77], M. Deenadayalan[11], J. Degallaix[158], M. De Laurentis[4,25], S. Deléglise[108], V. Del Favero[129], F. De Lillo[58], N. De Lillo[24], D. Dell Aquila[121], W. Del Pozzo[18,78], L. M. DeMarchi[15], F. De Matteis[123,124], V. D Emilio[17], N. Demos[74], T. Dent[114], A. Depasse[58], R. De Pietri[159,160], R. De Rosa[4,25], C. De Rossi[47], R. DeSalvo[125,126,161], R. De Simone[139], S. Dhurandhar[11], M. C. Díaz[89], N. A. Didio[67], T. Dietrich[111], L. Di Fiore[4], C. Di Fronzo[14], C. Di Giorgio[102,103], F. Di Giovanni[127], M. Di Giovanni[32],

T. Di Girolamo[4,25], A. Di Lieto[18,78], A. Di Michele[79], B. Ding[146], S. Di Pace[57,104], I. Di Palma[57,104], F. Di Renzo[18,78], A. K. Divakarla[76], A. Dmitriev[14], Z. Doctor[15], L. Donahue[162], L. D Onofrio[4,25], F. Donovan[74], K. L. Dooley[17], S. Doravari[11], M. Drago[57,104], J. C. Driggers[72], Y. Drori[1], J.-G. Ducoin[46], P. Dupej[24], U. Dupletsa[32], O. Durante[102,103], D. D Urso[121,122], P.-A. Duverne[46], S. E. Dwyer[72], C. Eassa[72], P. J. Easter[5], M. Ebersold[163], T. Eckhardt[128], G. Eddolls[24], B. Edelman[66], T. B. Edo[1], O. Edy[51], A. Effler[56], S. Eguchi[132], J. Eichholz[8], S. S. Eikenberry[76], M. Eisenmann[20,30], R. A. Eisenstein[74], A. Ejlli[17], E. Engelby[44], Y. Enomoto[27], L. Errico[4,25], R. C. Essick[164], H. Estellés[145], D. Estevez[165], Z. Etienne[166], T. Etzel[1], M. Evans[74], T. M. Evans[56], T. Evstafyeva[12], B. E. Ewing[150], F. Fabrizi[54,55], F. Faedi[55], V. Fafone[32,123,124], H. Fair[67], S. Fairhurst[17], P. C. Fan[162], A. M. Farah[167], S. Farinon[92], B. Farr[66], W. M. Farr[115,116], E. J. Fauchon-Jones[17], G. Favaro[80], M. Favata[168], M. Fays[68], M. Fazio[169], J. Feicht[1], M. M. Fejer[77], E. Fenyvesi[75,170], D. L. Ferguson[171], A. Fernandez-Galiana[74], I. Ferrante[18,78], T. A. Ferreira[16], F. Fidecaro[18,78], P. Figura[109], A. Fiori[18,78], I. Fiori[47], M. Fishbach[15], R. P. Fisher[63], R. Fittipaldi[103,172], V. Fiumara[103,173], R. Flaminio[20,30], E. Floden[149], H. K. Fong[28], J. A. Font[127,174], B. Fornal[161], P. W. F. Forsyth[8], A. Franke[128], S. Frasca[57,104], F. Frasconi[18], J. P. Freed[36], Z. Frei[154], A. Freise[59,96], O. Freitas[175], R. Frey[66], P. Fritschel[74], V. V. Frolov[56], G. G. Fronzé[23], Y. Fujii[176], Y. Fujikawa[177], Y. Fujimoto[178], P. Fulda[76], M. Fyffe[56], H. A. Gabbard[24], B. U. Gadre[111], J. R. Gair[111], J. Gais[131], S. Galaudage[5], R. Gamba[13], D. Ganapathy[74], A. Ganguly[11], D. Gao[179], S. G. Gaonkar[11], B. Garaventa[92,118], C. García Núñez[100], C. García-Quirós[145], F. Garu[4,25], B. Gateley[72], V. Gayathri[76], G.-G. Ge[179], G. Gemme[92], A. Gennai[18], J. George[94], O. Gerberding[128], L. Gergely[180], P. Gewecke[128], S. Ghonge[48], Abhirup Ghosh[111], Archisman Ghosh[85], Shaon Ghosh[168], Shrobana Ghosh[17], Tathagata Ghosh[11], B. Giacomazzo[69,70,71], L. Giacoppo[57,104], J. A. Giaime[7,56], K. D. Giardina[56], D. R. Gibson[100], C. Gier[33], M. Giesler[181], P. Giri[18,78], F. Gissi[87], S. Gkaitatzis[18,78], J. Glanzer[7], A. E. Gleckl[44], P. Godwin[150], E. Goetz[182], R. Goetz[76], N. Gohlke[9,10], J. Golomb[1], B. Goncharov[32], G. González[7], M. Gosselin[47], R. Gouaty[30], D. W. Gould[8], S. Goyal[19], B. Grace[8], A. Grado[4,183], V. Graham[24], M. Granata[158], V. Granata[102], A. Grant[24], S. Gras[74], P. Grassia[1], C. Gray[72], R. Gray[24], G. Greco[40], A. C. Green[76], R. Green[17], A. M. Gretarsson[36], E. M. Gretarsson[36], D. Grif th[1], W. L. Grif ths[17], H. L. Griggs[48], G. Grignani[40,79], A. Grimaldi[98,99], E. Grimes[36], S. J. Grimm[32,107], H. Grote[17], S. Grunewald[111], P. Gruning[46], A. S. Gruson[44], D. Guerra[127], G. M. Guidi[54,55], A. R. Guimaraes[7], G. Guixé[29], H. K. Gulati[84], A. M. Gunny[74], H.-K. Guo[161], Y. Guo[59], Anchal Gupta[1], Anuradha Gupta[184], I. M. Gupta[150], P. Gupta[59,65], S. K. Gupta[106], R. Gustafson[185], F. Guzman[186], S. Ha[187], I. P. W. Hadiputrawan[136], L. Haegel[45], S. Haino[140], O. Halim[35], E. D. Hall[74], E. Z. Hamilton[163], G. Hammond[24], W.-B. Han[188], M. Haney[163], J. Hanks[72], C. Hanna[150], M. D. Hannam[17], O. Hannuksela[59,65], H. Hansen[72], T. J. Hansen[36], J. Hanson[56], T. Harder[37], K. Haris[59,65], J. Harms[32,107], G. M. Harry[42], I. W. Harry[51], D. Hartwig[128], K. Hasegawa[189], B. Haskell[86], C.-J. Haster[74], J. S. Hathaway[129], K. Hattori[190], K. Haughian[24], H. Hayakawa[191], K. Hayama[132], F. J. Hayes[24], J. Healy[129], A. Heidmann[108], A. Heidt[9,10], M. C. Heintze[56], J. Heinze[9,10], J. Heinzel[74], H. Heitmann[37], F. Hellman[192], P. Hello[46], A. F. Helmling-Cornell[66], G. Hemming[47], M. Hendry[24], I. S. Heng[24], E. Hennes[59], J. Hennig[193], M. H. Hennig[193], C. Henshaw[48], A. G. Hernandez[90], F. Hernandez Vivanco[5], M. Heurs[9,10], A. L. Hewitt[194], S. Higginbotham[17], S. Hild[59,155], P. Hill[33], Y. Himemoto[195], A. S. Hines[186], N. Hirata[20], C. Hirose[177], T-C. Ho[136], S. Hochheim[9,10], D. Hofman[158], J. N. Hohmann[128], D. G. Holcomb[113], N. A. Holland[8], I. J. Hollows[157], Z. J. Holmes[88], K. Holt[56], D. E. Holz[167], Q. Hong[130], J. Hough[24], S. Hourihane[1], E. J. Howell[93], C. G. Hoy[17], D. Hoyland[14], A. Hreibi[9,10], B-H. Hsieh[189], H-F. Hsieh[196], C. Hsiung[134], Y. Hsu[130], H-Y. Huang[140], P. Huang[179], Y-C. Huang[138], Y.-J. Huang[140], Yiting Huang[152], Yiwen Huang[74], M. T. Hübner[5], A. D. Huddart[197], B. Hughey[36], D. C. Y. Hui[198], V. Hui[30], S. Husa[145], S. H. Huttner[24], R. Huxford[150], T. Huynh-Dinh[56], S. Ide[199], B. Idzkowski[109], A. Iess[123,124], K. Inayoshi[200], Y. Inoue[136], P. Iosif[201], M. Isi[74], K. Isleif[128], K. Ito[202], Y. Itoh[178,203], B. R. Iyer[19], V. JaberianHamedan[93], T. Jacqmin[108], P.-E. Jacquet[108], S. J. Jadhav[204], S. P. Jadhav[11], T. Jain[12], A. L. James[17], A. Z. Jan[171], K. Jani[205], J. Janquart[59,65], K. Janssens[37,206], N. N. Janthalur[204], P. Jaranowski[207], D. Jariwala[76], R. Jaume[145], A. C. Jenkins[60], K. Jenner[88], C. Jeon[208], W. Jia[74], J. Jiang[76], H.-B. Jin[209,210], G. R. Johns[63], R. Johnston[24], A. W. Jones[93], D. I. Jones[211], P. Jones[14], R. Jones[24], P. Joshi[150], L. Ju[93], A. Jue[161], P. Jung[62], K. Jung[187], J. Junker[9,10], V. Juste[165], K. Kaihotsu[202], T. Kajita[212], M. Kakizaki[190], C. V. Kalaghatgi[17,59,65,213], V. Kalogera[15], B. Kamai[1], M. Kamiizumi[191], N. Kanda[178,203], S. Kandhasamy[11], G. Kang[214], J. B. Kanner[1], Y. Kao[130], S. J. Kapadia[19], D. P. Kapasi[8], C. Karathanasis[31], S. Karki[95], R. Kashyap[150], M. Kasprzack[1], W. Kastaun[9,10], T. Kato[189], S. Katsanevas[47], E. Katsavounidis[74], W. Katzman[56], T. Kaur[93], K. Kawabe[72], K. Kawaguchi[189], F. Kéfélian[37], D. Keitel[145], J. S. Key[215], S. Khadka[77], F. Y. Khalili[97], S. Khan[17], T. Khanam[148], E. A. Khazanov[216], N. Khetan[32,107], M. Khursheed[94], N. Kijbunchoo[8], A. Kim[15], C. Kim[208], J. C. Kim[217], J. Kim[218], K. Kim[208], W. S. Kim[62], Y.-M. Kim[187], C. Kimball[15], N. Kimura[191], M. Kinley-Hanlon[24], R. Kirchhoff[9,10], J. S. Kissel[72], S. Klimenko[76], T. Klinger[12], A. M. Knee[182], T. D. Knowles[166], N. Knust[9,10], E. Knyazev[74], Y. Kobayashi[178], P. Koch[9,10], G. Koekoek[59,155], K. Kohri[219], K. Kokeyama[220], S. Koley[32], P. Kolitsidou[17], M. Kolstein[31], K. Komori[74], V. Kondrashov[1], A. K. H. Kong[196], A. Kontos[82], N. Koper[9,10], M. Korobko[128], M. Kovalam[93], N. Koyama[177], D. B. Kozak[1], C. Kozakai[52], V. Kringel[9,10], N. V. Krishnendu[9,10], A. Królak[221,222], G. Kuehn[9,10], F. Kuei[130], P. Kuijer[59], S. Kulkarni[184], A. Kumar[204], Prayush Kumar[19], Rahul Kumar[72], Rakesh Kumar[84], J. Kume[28], K. Kuns[74], Y. Kuromiya[202], S. Kuroyanagi[223,224], K. Kwak[187], G. Lacaille[24], P. Lagabbe[30], D. Laghi[112], E. Lalande[225], M. Lalleman[206], T. L. Lam[131], A. Lamberts[37,226], M. Landry[72], B. B. Lane[74], R. N. Lang[74], J. Lange[171], B. Lantz[77], I. La Rosa[30], A. Lartaux-Vollard[46],

P. D. Lasky[5], M. Laxen[56], A. Lazzarini[1], C. Lazzaro[80,81], P. Leaci[57,104], S. Leavey[9,10], S. LeBohec[161], Y. K. Lecoeuche[182], E. Lee[189], H. M. Lee[227], H. W. Lee[217], K. Lee[228], R. Lee[138], I. N. Legred[1], J. Lehmann[9,10], A. Lemaitre[229], M. Lenti[55,230], M. Leonardi[20], E. Leonova[38], N. Leroy[46], N. Letendre[30], C. Levesque[225], Y. Levin[5], J. N. Leviton[185], K. Leyde[45], A. K. Y. Li[1], B. Li[130], J. Li[15], K. L. Li[231], P. Li[232], T. G. F. Li[131], X. Li[137], C-Y. Lin[233], E. T. Lin[196], F-K. Lin[140], F-L. Lin[234], H. L. Lin[136], L. C.-C. Lin[231], F. Linde[59,213], S. D. Linker[90,125,126], J. N. Linley[24], T. B. Littenberg[235], G. C. Liu[134], J. Liu[93], K. Liu[130], X. Liu[6], F. Llamas[89], R. K. L. Lo[1], T. Lo[130], L. T. London[38,74], A. Longo[236], D. Lopez[163], M. Lopez Portilla[65], M. Lorenzini[123,124], V. Loriette[237], M. Lormand[56], G. Losurdo[18], T. P. Lott[48], J. D. Lough[9,10], C. O. Lousto[129], G. Lovelace[44], J. F. Lucaccioni[238], H. Lück[9,10], D. Lumaca[123,124], A. P. Lundgren[51], L.-W. Luo[140], J. E. Lynam[63], M. Ma arif[136], R. Macas[51], J. B. Machtinger[15], M. MacInnis[74], D. M. Macleod[17], I. A. O. MacMillan[1], A. Macquet[37], I. Magaña Hernandez[6], C. Magazzù[18], R. M. Magee[1], R. Maggiore[14], M. Magnozzi[92,118], S. Mahesh[166], E. Majorana[57,104], I. Maksimovic[237], S. Maliakal[1], A. Malik[94], N. Man[37], V. Mandic[149], V. Mangano[57,104], B. R. Mannix[66], G. L. Mansell[72,74], M. Manske[6], M. Mantovani[47], M. Mapelli[80,81], F. Marchesoni[40,41,239], D. Marín Pina[29], F. Marion[30], Z. Mark[137], S. Márka[50], Z. Márka[50], C. Markakis[12], A. S. Markosyan[77], A. Markowitz[1], E. Maros[1], A. Marquina[147], S. Marsat[45], F. Martelli[54,55], I. W. Martin[24], R. M. Martin[168], M. Martinez[31], V. A. Martinez[76], V. Martinez[26], K. Martinovic[60], D. V. Martynov[14], E. J. Marx[74], H. Masalehdan[128], K. Mason[74], E. Massera[157], A. Masserot[30], M. Masso-Reid[24], S. Mastrogiovanni[45], A. Matas[111], M. Mateu-Lucena[145], F. Matichard[1,74], M. Matiushechkina[9,10], N. Mavalvala[74], J. J. McCann[93], R. McCarthy[72], D. E. McClelland[8], P. K. McClincy[150], S. McCormick[56], L. McCuller[74], G. I. McGhee[24], S. C. McGuire[56], C. McIsaac[51], J. McIver[182], T. McRae[8], S. T. McWilliams[166], D. Meacher[6], M. Mehmet[9,10], A. K. Mehta[111], Q. Meijer[65], A. Melatos[120], D. A. Melchor[44], G. Mendell[72], A. Menendez-Vazquez[31], C. S. Menoni[169], R. A. Mercer[6], L. Mereni[158], K. Merfeld[66,148], E. L. Merilh[56], J. D. Merritt[66], M. Merzougui[37], S. Meshkov[1,294], C. Messenger[24], C. Messick[74], P. M. Meyers[120], F. Meylahn[9,10], A. Mhaske[11], A. Miani[98,99], H. Miao[14], I. Michaloliakos[76], C. Michel[158], Y. Michimura[27], H. Middleton[120], D. P. Mihaylov[111], L. Milano[25,295], A. L. Miller[58], A. Miller[90], B. Miller[38,59], M. Millhouse[120], J. C. Mills[17], E. Milotti[35,240], Y. Minenkov[124], N. Mio[241], Ll. M. Mir[31], M. Miravet-Tenés[127], A. Mishkin[76], C. Mishra[242], T. Mishra[76], T. Mistry[157], S. Mitra[11], V. P. Mitrofanov[97], G. Mitselmakher[76], R. Mittleman[74], O. Miyakawa[191], K. Miyo[191], S. Miyoki[191], Geoffrey Mo[74], L. M. Modafferi[145], E. Moguel[238], K. Mogushi[95], S. R. P. Mohapatra[74], S. R. Mohite[6], I. Molina[44], M. Molina-Ruiz[192], M. Mondin[90], M. Montani[54,55], C. J. Moore[14], J. Moragues[145], D. Moraru[72], F. Morawski[86], A. More[11], C. Moreno[36], G. Moreno[72], Y. Mori[202], S. Morisaki[6], N. Morisue[178], Y. Moriwaki[190], B. Mours[165], C. M. Mow-Lowry[59,96], S. Mozzon[51], F. Muciaccia[57,104], Arunava Mukherjee[243], D. Mukherjee[150], Soma Mukherjee[89], Subroto Mukherjee[84], Suvodip Mukherjee[38,164], N. Mukund[9,10], A. Mullavey[56], J. Munch[88], E. A. Muñiz[67], P. G. Murray[24], R. Musenich[92,118], S. Muusse[88], S. L. Nadji[9,10], K. Nagano[244], A. Nagar[23,245], K. Nakamura[20], H. Nakano[246], M. Nakano[189], Y. Nakayama[202], V. Napolano[47], I. Nardecchia[123,124], T. Narikawa[189], H. Narola[65], L. Naticchioni[57], B. Nayak[90], R. K. Nayak[247], B. F. Neil[93], J. Neilson[87,103], A. Nelson[186], T. J. N. Nelson[56], M. Nery[9,10], P. Neubauer[238], A. Neunzert[215], K. Y. Ng[74], S. W. S. Ng[88], C. Nguyen[45], P. Nguyen[66], T. Nguyen[74], L. Nguyen Quynh[248], J. Ni[149], W.-T. Ni[138,179,209], S. A. Nichols[7], T. Nishimoto[189], A. Nishizawa[28], S. Nissanke[38,59], E. Nitoglia[141], F. Nocera[47], M. Norman[17], C. North[17], S. Nozaki[190], G. Nurbek[89], L. K. Nuttall[51], Y. Obayashi[189], J. Oberling[72], B. D. O Brien[76], J. O Dell[197], E. Oelker[24], W. Ogaki[189], G. Oganesyan[32,107], J. J. Oh[62], K. Oh[198], S. H. Oh[62], M. Ohashi[191], T. Ohashi[178], M. Ohkawa[177], F. Ohme[9,10], H. Ohta[28], M. A. Okada[16], Y. Okutani[199], C. Olivetto[47], K. Oohara[189,249], R. Oram[56], B. O Reilly[56], R. G. Ormiston[149], N. D. Ormsby[63], R. O Shaughnessy[129], E. O Shea[181], S. Oshino[191], S. Ossokine[111], C. Osthelder[1], S. Otabe[2], D. J. Ottaway[88], H. Overmier[56], A. E. Pace[150], G. Pagano[18,78], R. Pagano[7], M. A. Page[93], G. Pagliaroli[32,107], A. Pai[106], S. A. Pai[94], S. Pal[247], J. R. Palamos[66], O. Palashov[216], C. Palomba[57], H. Pan[130], K.-C. Pan[138,196], P. K. Panda[204], P. T. H. Pang[59,65], C. Pankow[15], F. Pannarale[57,104], B. C. Pant[94], F. H. Panther[93], F. Paoletti[18], A. Paoli[47], A. Paolone[57,250], G. Pappas[201], A. Parisi[134], H. Park[6], J. Park[251], W. Parker[56], D. Pascucci[59,85], A. Pasqualetti[47], R. Passaquieti[18,78], D. Passuello[18], M. Patel[63], M. Pathak[88], B. Patricelli[18,47], A. S. Patron[7], S. Paul[66], E. Payne[5], M. Pedraza[1], R. Pedurand[103], M. Pegoraro[81], A. Pele[56], F. E. Peña Arellano[191], S. Penano[77], S. Penn[252], A. Perego[98,99], A. Pereira[26], T. Pereira[253], C. J. Perez[72], C. Périgois[30], C. C. Perkins[76], A. Perreca[98,99], S. Perriès[141], D. Pesios[201], J. Petermann[128], D. Petterson[1], H. P. Pfeiffer[111], H. Pham[56], K. A. Pham[149], K. S. Phukon[59,213], H. Phurailatpam[131], O. J. Piccinni[57], M. Pichot[37], M. Piendibene[18,78], F. Piergiovanni[54,55], L. Pierini[57,104], V. Pierro[87,103], G. Pillant[47], M. Pillas[46], F. Pilo[18], L. Pinard[158], C. Pineda-Bosque[90], I. M. Pinto[87,103,254], M. Pinto[47], B. J. Piotrzkowski[6], K. Piotrzkowski[58], M. Pirello[72], M. D. Pitkin[194], A. Placidi[40,79], E. Placidi[57,104], M. L. Planas[145], W. Plastino[236,255], C. Pluchar[256], R. Poggiani[18,78], E. Polini[30], D. Y. T. Pong[131], S. Ponrathnam[11], E. K. Porter[45], R. Poulton[47], A. Poverman[82], J. Powell[143], M. Pracchia[30], T. Pradier[165], A. K. Prajapati[84], K. Prasai[77], R. Prasanna[204], G. Pratten[14], M. Principe[87,103,254], G. A. Prodi[99,257], L. Prokhorov[14], P. Prosposito[123,124], L. Prudenzi[111], A. Puecher[59,65], M. Punturo[40], F. Puosi[18,78], P. Puppo[57], M. Pürrer[111], H. Qi[17], N. Quartey[63], V. Quetschke[89], P. J. Quinonez[36], R. Quitzow-James[95], F. J. Raab[72], G. Raaijmakers[38,59], H. Radkins[72], N. Radulesco[37], P. Raffai[154], S. X. Rail[225], S. Raja[94], C. Rajan[94], K. E. Ramirez[56], T. D. Ramirez[44], A. Ramos-Buades[111], J. Rana[150], P. Rapagnani[57,104],

A. Ray[6], V. Raymond[17], N. Raza[182], M. Razzano[18,78], J. Read[44], L. A. Rees[42], T. Regimbau[30], L. Rei[92], S. Reid[33], S. W. Reid[63], D. H. Reitze[1,76], P. Relton[17], A. Renzini[1], P. Rettegno[22,23], B. Revenu[45], A. Reza[59], M. Rezac[44], F. Ricci[57,104], D. Richards[197], J. W. Richardson[258], L. Richardson[186], G. Riemenschneider[22,23], K. Riles[185], S. Rinaldi[18,78], K. Rink[182], N. A. Robertson[1], R. Robie[1], F. Robinet[46], A. Rocchi[124], S. Rodriguez[44], L. Rolland[30], J. G. Rollins[1], M. Romanelli[105], R. Romano[3,4], C. L. Romel[72], A. Romero[31], I. M. Romero-Shaw[5], J. H. Romie[56], S. Ronchini[32,107], L. Rosa[4,25], C. A. Rose[6], D. Rosińska[109], M. P. Ross[259], S. Rowan[24], S. J. Rowlinson[14], S. Roy[65], Santosh Roy[11], Soumen Roy[260], D. Rozza[121,122], P. Ruggi[47], K. Ruiz-Rocha[205], K. Ryan[72], S. Sachdev[150], T. Sadecki[72], J. Sadiq[114], S. Saha[196], Y. Saito[191], K. Sakai[261], M. Sakellariadou[60], S. Sakon[150], O. S. Sala a[69,70,71], F. Salces-Carcoba[1], L. Salconi[47], M. Saleem[149], F. Salemi[98,99], A. Samajdar[70], E. J. Sanchez[1], J. H. Sanchez[44], L. E. Sanchez[1], N. Sanchis-Gual[262], J. R. Sanders[263], A. Sanuy[29], T. R. Saravanan[11], N. Sarin[5], B. Sassolas[158], H. Satari[93], B. S. Sathyaprakash[17,150], O. Sauter[76], R. L. Savage[72], V. Savant[11], T. Sawada[178], H. L. Sawant[11], S. Sayah[158], D. Schaetzl[1], M. Scheel[137], J. Scheuer[15], M. G. Schiworski[88], P. Schmidt[14], S. Schmidt[65], R. Schnabel[128], M. Schneewind[9,10], R. M. S. Scho eld[66], A. Schönbeck[128], B. W. Schulte[9,10], B. F. Schutz[9,10,17], E. Schwartz[17], J. Scott[24], S. M. Scott[8], M. Seglar-Arroyo[30], Y. Sekiguchi[264], D. Sellers[56], A. S. Sengupta[260], D. Sentenac[47], E. G. Seo[131], V. Sequino[4,25], A. Sergeev[216], Y. Setyawati[9,10,65], T. Shaffer[72], M. S. Shahriar[15], M. A. Shaikh[19], B. Shams[161], L. Shao[200], A. Sharma[32,107], P. Sharma[94], P. Shawhan[110], N. S. Shcheblanov[229], A. Sheela[242], Y. Shikano[265,266], M. Shikauchi[28], H. Shimizu[267], K. Shimode[191], H. Shinkai[268], T. Shishido[53], A. Shoda[20], D. H. Shoemaker[74], D. M. Shoemaker[171], S. ShyamSundar[94], M. Sieniawska[58], D. Sigg[72], L. Silenzi[40,41], L. P. Singer[117], D. Singh[150], M. K. Singh[19], N. Singh[109], A. Singha[59,155], A. M. Sintes[145], V. Sipala[121,122], V. Skliris[17], B. J. J. Slagmolen[8], T. J. Slaven-Blair[93], J. Smetana[14], J. R. Smith[44], L. Smith[24], R. J. E. Smith[5], J. Soldateschi[55,230,269], S. N. Somala[270], K. Somiya[2], I. Song[196], K. Soni[11], V. Sordini[141], F. Sorrentino[92], N. Sorrentino[18,78], R. Soulard[37], T. Souradeep[11,271], E. Sowell[148], V. Spagnuolo[59,155], A. P. Spencer[24], M. Spera[80,81], P. Spinicelli[47], A. K. Srivastava[84], V. Srivastava[67], K. Staats[15], C. Stachie[37], F. Stachurski[24], D. A. Steer[45], J. Steinlechner[59,155], S. Steinlechner[59,155], N. Stergioulas[201], D. J. Stops[14], M. Stover[238], K. A. Strain[24], L. C. Strang[120], G. Stratta[57,272], M. D. Strong[7], A. Strunk[72], R. Sturani[253], A. L. Stuver[113], M. Suchenek[86], S. Sudhagar[11], V. Sudhir[74], R. Sugimoto[244,273], H. G. Suh[6], A. G. Sullivan[50], T. Z. Summerscales[274], L. Sun[8], S. Sunil[84], A. Sur[86], J. Suresh[28], P. J. Sutton[17], Takamasa Suzuki[177], Takanori Suzuki[2], Toshikazu Suzuki[189], B. L. Swinkels[59], M. J. Szczepańczyk[76], P. Szewczyk[109], M. Tacca[59], H. Tagoshi[189], S. C. Tait[24], H. Takahashi[275], R. Takahashi[20], S. Takano[27], H. Takeda[27], M. Takeda[178], C. J. Talbot[33], C. Talbot[1], K. Tanaka[276], Taiki Tanaka[189], Takahiro Tanaka[277], A. J. Tanasijczuk[58], S. Tanioka[191], D. B. Tanner[76], D. Tao[1], L. Tao[76], R. D. Tapia[150], E. N. Tapia San Martín[59], C. Taranto[123], A. Taruya[278], J. D. Tasson[162], R. Tenorio[145], J. E. S. Terhune[113], L. Terkowski[128], M. P. Thirugnanasambandam[11], M. Thomas[56], P. Thomas[72], E. E. Thompson[48], J. E. Thompson[17], S. R. Thondapu[94], K. A. Thorne[56], E. Thrane[5], Shubhanshu Tiwari[163], Srishti Tiwari[11], V. Tiwari[17], A. M. Toivonen[149], A. E. Tolley[51], T. Tomaru[20], T. Tomura[191], M. Tonelli[18,78], Z. Tornasi[24], A. Torres-Forné[127], C. I. Torrie[1], I. Tosta e Melo[122], D. Töyrä[8], A. Trapananti[40,41], F. Travasso[40,41], G. Traylor[56], M. Trevor[110], M. C. Tringali[47], A. Tripathee[185], L. Troiano[103,279], A. Trovato[45], L. Trozzo[4,191], R. J. Trudeau[1], D. Tsai[130], K. W. Tsang[59,65,280], T. Tsang[281], J-S. Tsao[234], M. Tse[74], R. Tso[137], S. Tsuchida[178], L. Tsukada[150], D. Tsuna[28], T. Tsutsui[28], K. Turbang[206,282], M. Turconi[37], D. Tuyenbayev[178], A. S. Ubhi[14], N. Uchikata[189], T. Uchiyama[191], R. P. Udall[1], A. Ueda[283], T. Uehara[284,285], K. Ueno[28], G. Ueshima[286], C. S. Unnikrishnan[287], A. L. Urban[7], T. Ushiba[191], A. Utina[59,155], G. Vajente[1], A. Vajpeyi[5], G. Valdes[186], M. Valentini[98,99,184], V. Valsan[6], N. van Bakel[59], M. van Beuzekom[59], M. van Dael[59,288], J. F. J. van den Brand[59,96,155], C. Van Den Broeck[59,65], D. C. Vander-Hyde[67], H. van Haevermaet[206], J. V. van Heijningen[58], M. H. P. M. van Putten[289], N. van Remortel[206], M. Vardaro[59,213], A. F. Vargas[120], V. Varma[111], M. Vasúth[75], A. Vecchio[14], G. Vedovato[81], J. Veitch[24], P. J. Veitch[88], J. Venneberg[9,10], G. Venugopalan[1], D. Verkindt[30], P. Verma[222], Y. Verma[94], S. M. Vermeulen[17], D. Veske[50], F. Vetrano[54], A. Viceré[54,55], S. Vidyant[67], A. D. Viets[290], A. Vijaykumar[19], V. Villa-Ortega[114], J.-Y. Vinet[37], A. Virtuoso[35,240], S. Vitale[74], H. Vocca[40,79], E. R. G. von Reis[72], J. S. A. von Wrangel[9,10], C. Vorvick[72], S. P. Vyatchanin[97], L. E. Wade[238], M. Wade[238], K. J. Wagner[129], R. C. Walet[59], M. Walker[63], G. S. Wallace[33], L. Wallace[1], J. Wang[179], J. Z. Wang[185], W. H. Wang[89], R. L. Ward[8], J. Warner[72], M. Was[30], T. Washimi[20], N. Y. Washington[1], J. Watchi[146], B. Weaver[72], C. R. Weaving[51], S. A. Webster[24], M. Weinert[9,10], A. J. Weinstein[1], R. Weiss[74], C. M. Weller[259], R. A. Weller[205], F. Wellmann[9,10], L. Wen[93], P. Weßels[9,10], K. Wette[8], J. T. Whelan[129], D. D. White[44], B. F. Whiting[76], C. Whittle[74], D. Wilken[9,10], D. Williams[24], M. J. Williams[24], A. R. Williamson[51], J. L. Willis[1], B. Willke[9,10], D. J. Wilson[256], C. C. Wipf[1], T. Wlodarczyk[111], G. Woan[24], J. Woehler[9,10], J. K. Wofford[129], D. Wong[182], I. C. F. Wong[131], M. Wright[24], C. Wu[138], D. S. Wu[9,10], H. Wu[138], D. M. Wysocki[6], L. Xiao[1], T. Yamada[267], H. Yamamoto[1], K. Yamamoto[1], T. Yamamoto[191], K. Yamashita[202], R. Yamazaki[199], F. W. Yang[161], K. Z. Yang[149], L. Yang[169], Y.-C. Yang[130], Y. Yang[291], Yang Yang[76], M. J. Yap[8], D. W. Yeeles[17], S.-W. Yeh[138], A. B. Yelikar[129], M. Ying[130], J. Yokoyama[27,28], T. Yokozawa[191], J. Yoo[181], T. Yoshioka[202], Hang Yu[137], Haocun Yu[74], H. Yuzurihara[189], A. Zadrożny[222], M. Zanolin[36], S. Zeidler[292], T. Zelenova[47], J.-P. Zendri[81], M. Zevin[167], M. Zhan[179], H. Zhang[234],

J. Zhang[93], L. Zhang[1], R. Zhang[76], T. Zhang[14], Y. Zhang[186], C. Zhao[93], G. Zhao[146], Y. Zhao[20,189], Yue Zhao[161], R. Zhou[192], Z. Zhou[15], X. J. Zhu[5], Z.-H. Zhu[119,232], M. E. Zucker[1,74], J. Zweizig[293], and
The LIGO Scienti c Collaboration, the Virgo Collaboration, and the KAGRA Collaboration

[1] LIGO Laboratory, California Institute of Technology, Pasadena, CA 91125, USA
[2] Graduate School of Science, Tokyo Institute of Technology, Meguro-ku, Tokyo 152-8551, Japan
[3] Dipartimento di Farmacia, Università di Salerno, I-84084 Fisciano, Salerno, Italy
[4] INFN, Sezione di Napoli, Complesso Universitario di Monte S. Angelo, I-80126 Napoli, Italy
[5] OzGrav, School of Physics & Astronomy, Monash University, Clayton 3800, Victoria, Australia
[6] University of Wisconsin-Milwaukee, Milwaukee, WI 53201, USA
[7] Louisiana State University, Baton Rouge, LA 70803, USA
[8] OzGrav, Australian National University, Canberra, Australian Capital Territory 0200, Australia
[9] Max Planck Institute for Gravitational Physics Albert Einstein Institute), D-30167 Hannover, Germany
[10] Leibniz Universität Hannover, D-30167 Hannover, Germany
[11] Inter-University Centre for Astronomy and Astrophysics, Pune 411007, India
[12] University of Cambridge, Cambridge CB2 1TN, UK
[13] Theoretisch-Physikalisches Institut, Friedrich-Schiller-Universität Jena, D-07743 Jena, Germany
[14] University of Birmingham, Birmingham B15 2TT, UK
[15] Northwestern University, Evanston, IL 60208, USA
[16] Instituto Nacional de Pesquisas Espaciais, 12227-010 São José dos Campos, São Paulo, Brazil
[17] Cardiff University, Cardiff CF24 3AA, UK
[18] INFN, Sezione di Pisa, I-56127 Pisa, Italy
[19] International Centre for Theoretical Sciences, Tata Institute of Fundamental Research, Bengaluru 560089, India
[20] Gravitational Wave Science Project, National Astronomical Observatory of Japan NAOJ), Mitaka City, Tokyo 181-8588, Japan
[21] Advanced Technology Center, National Astronomical Observatory of Japan NAOJ), Mitaka City, Tokyo 181-8588, Japan
[22] Dipartimento di Fisica, Università degli Studi di Torino, I-10125 Torino, Italy
[23] INFN, Sezione di Torino, I-10125 Torino, Italy
[24] SUPA, University of Glasgow, Glasgow G12 8QQ, UK
[25] Università di Napoli "Federico II," Complesso Universitario di Monte S. Angelo, I-80126 Napoli, Italy
[26] Université de Lyon, Université Claude Bernard Lyon 1, CNRS, Institut Lumière Matière, F-69622 Villeurbanne, France
[27] Department of Physics, The University of Tokyo, Bunkyo-ku, Tokyo 113-0033, Japan
[28] Research Center for the Early Universe RESCEU), The University of Tokyo, Bunkyo-ku, Tokyo 113-0033, Japan
[29] Institut de Ciències del Cosmos ICCUB), Universitat de Barcelona, C Martí i Franquès 1, Barcelona 08028, Spain
[30] Univ. Savoie Mont Blanc, CNRS, Laboratoire d Annecy de Physique des Particules—IN2P3, F-74000 Annecy, France
[31] Institut de Física d Altes Energies IFAE), Barcelona Institute of Science and Technology, and ICREA, E-08193 Barcelona, Spain
[32] Gran Sasso Science Institute GSSI), I-67100 L Aquila, Italy
[33] SUPA, University of Strathclyde, Glasgow G1 1XQ, UK
[34] Dipartimento di Scienze Matematiche, Informatiche e Fisiche, Università di Udine, I-33100 Udine, Italy
[35] INFN, Sezione di Trieste, I-34127 Trieste, Italy
[36] Embry-Riddle Aeronautical University, Prescott, AZ 86301, USA
[37] Artemis, Université Côte d Azur, Observatoire de la Côte d Azur, CNRS, F-06304 Nice, France
[38] GRAPPA, Anton Pannekoek Institute for Astronomy and Institute for High-Energy Physics, University of Amsterdam, Science Park 904, 1098 XH Amsterdam, Netherlands
[39] National and Kapodistrian University of Athens, School of Science Building, 2nd floor, Panepistimiopolis, 15771 Ilissia, Greece
[40] INFN, Sezione di Perugia, I-06123 Perugia, Italy
[41] Università di Camerino, Dipartimento di Fisica, I-62032 Camerino, Italy
[42] American University, Washington, DC 20016, USA
[43] Earthquake Research Institute, The University of Tokyo, Bunkyo-ku, Tokyo 113-0032, Japan
[44] California State University Fullerton, Fullerton, CA 92831, USA
[45] Université de Paris, CNRS, Astroparticule et Cosmologie, F-75006 Paris, France
[46] Université Paris-Saclay, CNRS IN2P3, IJCLab, 91405 Orsay, France
[47] European Gravitational Observatory EGO), I-56021 Cascina, Pisa, Italy
[48] Georgia Institute of Technology, Atlanta, GA 30332, USA
[49] Department of Mathematics and Physics, Graduate School of Science and Technology, Hirosaki University, Hirosaki, Aomori 036-8561, Japan
[50] Columbia University, New York, NY 10027, USA
[51] University of Portsmouth, Portsmouth PO1 3FX, UK
[52] Kamioka Branch, National Astronomical Observatory of Japan NAOJ), Kamioka-cho, Hida City, Gifu 506-1205, Japan
[53] The Graduate University for Advanced Studies SOKENDAI), Mitaka City, Tokyo 181-8588, Japan
[54] Università degli Studi di Urbino "Carlo Bo," I-61029 Urbino, Italy
[55] INFN, Sezione di Firenze, I-50019 Sesto Fiorentino, Firenze, Italy
[56] LIGO Livingston Observatory, Livingston, LA 70754, USA
[57] INFN, Sezione di Roma, I-00185 Roma, Italy
[58] Université catholique de Louvain, B-1348 Louvain-la-Neuve, Belgium
[59] Nikhef, Science Park 105, 1098 XG Amsterdam, Netherlands
[60] King s College London, University of London, London WC2R 2LS, UK
[61] Korea Institute of Science and Technology Information, Daejeon 34141, Republic of Korea
[62] National Institute for Mathematical Sciences, Daejeon 34047, Republic of Korea
[63] Christopher Newport University, Newport News, VA 23606, USA
[64] School of High Energy Accelerator Science, The Graduate University for Advanced Studies SOKENDAI), Tsukuba City, Ibaraki 305-0801, Japan
[65] Institute for Gravitational and Subatomic Physics GRASP), Utrecht University, Princetonplein 1, 3584 CC Utrecht, Netherlands
[66] University of Oregon, Eugene, OR 97403, USA
[67] Syracuse University, Syracuse, NY 13244, USA
[68] Université de Liège, B-4000 Liège, Belgium
[69] Università degli Studi di Milano-Bicocca, I-20126 Milano, Italy
[70] INFN, Sezione di Milano-Bicocca, I-20126 Milano, Italy

[71] INAF, Osservatorio Astronomico di Brera sede di Merate, I-23807 Merate, Lecco, Italy
[72] LIGO Hanford Observatory, Richland, WA 99352, USA
[73] Dipartimento di Medicina, Chirurgia e Odontoiatria "Scuola Medica Salernitana,"Università di Salerno, I-84081 Baronissi, Salerno, Italy
[74] LIGO Laboratory, Massachusetts Institute of Technology, Cambridge, MA 02139, USA
[75] Wigner RCP, RMKI, H-1121 Budapest, Konkoly Thege Miklós út 29-33, Hungary
[76] University of Florida, Gainesville, FL 32611, USA
[77] Stanford University, Stanford, CA 94305, USA
[78] Università di Pisa, I-56127 Pisa, Italy
[79] Università di Perugia, I-06123 Perugia, Italy
[80] Università di Padova, Dipartimento di Fisica e Astronomia, I-35131 Padova, Italy
[81] INFN, Sezione di Padova, I-35131 Padova, Italy
[82] Bard College, Annandale-On-Hudson, NY 12504, USA
[83] Montana State University, Bozeman, MT 59717, USA
[84] Institute for Plasma Research, Bhat, Gandhinagar 382428, India
[85] Universiteit Gent, B-9000 Gent, Belgium
[86] Nicolaus Copernicus Astronomical Center, Polish Academy of Sciences, 00-716, Warsaw, Poland
[87] Dipartimento di Ingegneria, Università del Sannio, I-82100 Benevento, Italy
[88] OzGrav, University of Adelaide, Adelaide, South Australia 5005, Australia
[89] The University of Texas Rio Grande Valley, Brownsville, TX 78520, USA
[90] California State University, Los Angeles, Los Angeles, CA 90032, USA
[91] Departamento de Matemáticas, Universitat Autònoma de Barcelona, Edi cio C Facultad de Ciencias 08193 Bellaterra Barcelona), Spain
[92] INFN, Sezione di Genova, I-16146 Genova, Italy
[93] OzGrav, University of Western Australia, Crawley, Western Australia 6009, Australia
[94] RRCAT, Indore, Madhya Pradesh 452013, India
[95] Missouri University of Science and Technology, Rolla, MO 65409, USA
[96] Vrije Universiteit Amsterdam, 1081 HV Amsterdam, Netherlands
[97] Lomonosov Moscow State University, Moscow 119991, Russia
[98] Università di Trento, Dipartimento di Fisica, I-38123 Povo, Trento, Italy
[99] INFN, Trento Institute for Fundamental Physics and Applications, I-38123 Povo, Trento, Italy
[100] SUPA, University of the West of Scotland, Paisley PA1 2BE, UK
[101] Bar-Ilan University, Ramat Gan, 5290002, Israel
[102] Dipartimento di Fisica "E.R. Caianiello,"Università di Salerno, I-84084 Fisciano, Salerno, Italy
[103] INFN, Sezione di Napoli, Gruppo Collegato di Salerno, Complesso Universitario di Monte S. Angelo, I-80126 Napoli, Italy
[104] Università di Roma "La Sapienza," I-00185 Roma, Italy
[105] Univ Rennes, CNRS, Institut FOTON—UMR6082, F-3500 Rennes, France
[106] Indian Institute of Technology Bombay, Powai, Mumbai 400 076, India
[107] INFN, Laboratori Nazionali del Gran Sasso, I-67100 Assergi, Italy
[108] Laboratoire Kastler Brossel, Sorbonne Université, CNRS, ENS-Université PSL, Collège de France, F-75005 Paris, France
[109] Astronomical Observatory Warsaw University, 00-478 Warsaw, Poland
[110] University of Maryland, College Park, MD 20742, USA
[111] Max Planck Institute for Gravitational Physics Albert Einstein Institute), D-14476 Potsdam, Germany
[112] L2IT, Laboratoire des 2 In nis—Toulouse, Université de Toulouse, CNRS IN2P3, UPS, F-31062 Toulouse Cedex 9, France
[113] Villanova University, Villanova, PA 19085, USA
[114] IGFAE, Universidade de Santiago de Compostela, Galicia 15782 Spain
[115] Stony Brook University, Stony Brook, NY 11794, USA
[116] Center for Computational Astrophysics, Flatiron Institute, New York, NY 10010, USA
[117] NASA Goddard Space Flight Center, Greenbelt, MD 20771, USA
[118] Dipartimento di Fisica, Università degli Studi di Genova, I-16146 Genova, Italy
[119] Department of Astronomy, Beijing Normal University, Beijing 100875, People s Republic of China
[120] OzGrav, University of Melbourne, Parkville, Victoria 3010, Australia
[121] Università degli Studi di Sassari, I-07100 Sassari, Italy
[122] INFN, Laboratori Nazionali del Sud, I-95125 Catania, Italy
[123] Università di Roma Tor Vergata, I-00133 Roma, Italy
[124] INFN, Sezione di Roma Tor Vergata, I-00133 Roma, Italy
[125] University of Sannio at Benevento, I-82100 Benevento, Italy
[126] INFN, Sezione di Napoli, I-80100 Napoli, Italy
[127] Departamento de Astronomía y Astrofísica, Universitat de València, E-46100 Burjassot, València, Spain
[128] Universität Hamburg, D-22761 Hamburg, Germany
[129] Rochester Institute of Technology, Rochester, NY 14623, USA
[130] National Tsing Hua University, Hsinchu City, 30013 Taiwan, People s Republic of China
[131] The Chinese University of Hong Kong, Shatin, NT, Hong Kong
[132] Department of Applied Physics, Fukuoka University, Jonan, Fukuoka City, Fukuoka 814-0180, Japan
[133] OzGrav, Charles Sturt University, Wagga Wagga, New South Wales 2678, Australia
[134] Department of Physics, Tamkang University, Danshui Dist., New Taipei City 25137, Taiwan
[135] Department of Physics and Institute of Astronomy, National Tsing Hua University, Hsinchu 30013, Taiwan
[136] Department of Physics, Center for High Energy and High Field Physics, National Central University, Zhongli District, Taoyuan City 32001, Taiwan
[137] CaRT, California Institute of Technology, Pasadena, CA 91125, USA
[138] Department of Physics, National Tsing Hua University, Hsinchu 30013, Taiwan
[139] Dipartimento di Ingegneria Industriale DIIN), Università di Salerno, I-84084 Fisciano, Salerno, Italy
[140] Institute of Physics, Academia Sinica, Nankang, Taipei 11529, Taiwan
[141] Université Lyon, Université Claude Bernard Lyon 1, CNRS, IP2I Lyon IN2P3, UMR 5822, F-69622 Villeurbanne, France
[142] INAF, Osservatorio Astronomico di Padova, I-35122 Padova, Italy
[143] OzGrav, Swinburne University of Technology, Hawthorn VIC 3122, Australia
[144] Université libre de Bruxelles, Avenue Franklin Roosevelt 50-1050 Bruxelles, Belgium

[145] IAC3–IEEC, Universitat de les Illes Balears, E-07122 Palma de Mallorca, Spain
[146] Université Libre de Bruxelles, Brussels 1050, Belgium
[147] Departamento de Matemáticas, Universitat de València, E-46100 Burjassot, València, Spain
[148] Texas Tech University, Lubbock, TX 79409, USA
[149] University of Minnesota, Minneapolis, MN 55455, USA
[150] The Pennsylvania State University, University Park, PA 16802, USA
[151] University of Rhode Island, Kingston, RI 02881, USA
[152] Bellevue College, Bellevue, WA 98007, USA
[153] Scuola Normale Superiore, Piazza dei Cavalieri, 7-56126 Pisa, Italy
[154] Eötvös University, Budapest 1117, Hungary
[155] Maastricht University, P.O. Box 616, 6200 MD Maastricht, Netherlands
[156] Chennai Mathematical Institute, Chennai 603103, India
[157] The University of Shef eld, Shef eld S10 2TN, UK
[158] Université Lyon, Université Claude Bernard Lyon 1, CNRS, Laboratoire des Matériaux Avancés LMA), IP2I Lyon IN2P3, UMR 5822, F-69622 Villeurbanne, France
[159] Dipartimento di Scienze Matematiche, Fisiche e Informatiche, Università di Parma, I-43124 Parma, Italy
[160] INFN, Sezione di Milano Bicocca, Gruppo Collegato di Parma, I-43124 Parma, Italy
[161] The University of Utah, Salt Lake City, UT 84112, USA
[162] Carleton College, North eld, MN 55057, USA
[163] University of Zurich, Winterthurerstrasse 190, 8057 Zurich, Switzerland
[164] Perimeter Institute, Waterloo, ON N2L 2Y5, Canada
[165] Université de Strasbourg, CNRS, IPHC UMR 7178, F-67000 Strasbourg, France
[166] West Virginia University, Morgantown, WV 26506, USA
[167] University of Chicago, Chicago, IL 60637, USA
[168] Montclair State University, Montclair, NJ 07043, USA
[169] Colorado State University, Fort Collins, CO 80523, USA
[170] Institute for Nuclear Research, Bem t er 18 c, H-4026 Debrecen, Hungary
[171] University of Texas, Austin, TX 78712, USA
[172] CNR-SPIN, c o Università di Salerno, I-84084 Fisciano, Salerno, Italy
[173] Scuola di Ingegneria, Università della Basilicata, I-85100 Potenza, Italy
[174] Observatori Astronòmic, Universitat de València, E-46980 Paterna, València, Spain
[175] Centro de Física das Universidades do Minho e do Porto, Universidade do Minho, Campus de Gualtar, PT-4710-057 Braga, Portugal
[176] Department of Astronomy, The University of Tokyo, Mitaka City, Tokyo 181-8588, Japan
[177] Faculty of Engineering, Niigata University, Nishi-ku, Niigata City, Niigata 950-2181, Japan
[178] Department of Physics, Graduate School of Science, Osaka City University, Sumiyoshi-ku, Osaka City, Osaka 558-8585, Japan
[179] State Key Laboratory of Magnetic Resonance and Atomic and Molecular Physics, Innovation Academy for Precision Measurement Science and Technology APM), Chinese Academy of Sciences, Xiao Hong Shan, Wuhan 430071, People s Republic of China
[180] University of Szeged, Dóm tér 9, Szeged 6720, Hungary
[181] Cornell University, Ithaca, NY 14850, USA
[182] University of British Columbia, Vancouver, BC V6T 1Z4, Canada
[183] INAF, Osservatorio Astronomico di Capodimonte, I-80131 Napoli, Italy
[184] The University of Mississippi, University, MS 38677, USA
[185] University of Michigan, Ann Arbor, MI 48109, USA
[186] Texas A&M University, College Station, TX 77843, USA
[187] Ulsan National Institute of Science and Technology, Ulsan 44919, Republic of Korea
[188] Shanghai Astronomical Observatory, Chinese Academy of Sciences, Shanghai 200030, People s Republic of China
[189] Institute for Cosmic Ray Research ICRR), KAGRA Observatory, The University of Tokyo, Kashiwa City, Chiba 277-8582, Japan
[190] Faculty of Science, University of Toyama, Toyama City, Toyama 930-8555, Japan
[191] Institute for Cosmic Ray Research ICRR), KAGRA Observatory, The University of Tokyo, Kamioka-cho, Hida City, Gifu 506-1205, Japan
[192] University of California, Berkeley, CA 94720, USA
[193] Maastricht University, 6200 MD, Maastricht, Netherlands
[194] Lancaster University, Lancaster LA1 4YW, UK
[195] College of Industrial Technology, Nihon University, Narashino City, Chiba 275-8575, Japan
[196] Institute of Astronomy, National Tsing Hua University, Hsinchu 30013, Taiwan
[197] Rutherford Appleton Laboratory, Didcot OX11 0DE, UK
[198] Department of Astronomy & Space Science, Chungnam National University, Yuseong-gu, Daejeon 34134, Republic of Korea
[199] Department of Physical Sciences, Aoyama Gakuin University, Sagamihara City, Kanagawa 252-5258, Japan
[200] Kavli Institute for Astronomy and Astrophysics, Peking University, Haidian District, Beijing 100871, People s Republic of China
[201] Aristotle University of Thessaloniki, University Campus, 54124 Thessaloniki, Greece
[202] Graduate School of Science and Engineering, University of Toyama, Toyama City, Toyama 930-8555, Japan
[203] Nambu Yoichiro Institute of Theoretical and Experimental Physics NITEP), Osaka City University, Sumiyoshi-ku, Osaka City, Osaka 558-8585, Japan
[204] Directorate of Construction, Services & Estate Management, Mumbai 400094, India
[205] Vanderbilt University, Nashville, TN 37235, USA
[206] Universiteit Antwerpen, Prinsstraat 13, 2000 Antwerpen, Belgium
[207] University of Bia ystok, 15-424 Bia ystok, Poland
[208] Ewha Womans University, Seoul 03760, Republic of Korea
[209] National Astronomical Observatories, Chinese Academic of Sciences, Chaoyang District, Beijing, People s Republic of China
[210] School of Astronomy and Space Science, University of Chinese Academy of Sciences, Chaoyang District, Beijing, People s Republic of China
[211] University of Southampton, Southampton SO17 1BJ, UK
[212] Institute for Cosmic Ray Research ICRR), The University of Tokyo, Kashiwa City, Chiba 277-8582, Japan
[213] Institute for High-Energy Physics, University of Amsterdam, Science Park 904, 1098 XH Amsterdam, Netherlands
[214] Chung-Ang University, Seoul 06974, Republic of Korea
[215] University of Washington Bothell, Bothell, WA 98011, USA
[216] Institute of Applied Physics, Nizhny Novgorod, 603950, Russia

[217] Inje University Gimhae, South Gyeongsang 50834, Republic of Korea
[218] Department of Physics, Myongji University, Yongin 17058, Republic of Korea
[219] Institute of Particle and Nuclear Studies IPNS), High Energy Accelerator Research Organization KEK), Tsukuba City, Ibaraki 305-0801, Japan
[220] School of Physics and Astronomy, Cardiff University, Cardiff CF24 3AA, UK
[221] Institute of Mathematics, Polish Academy of Sciences, 00656 Warsaw, Poland
[222] National Center for Nuclear Research, 05-400 Świerk-Otwock, Poland
[223] Instituto de Fisica Teorica, 28049 Madrid, Spain
[224] Department of Physics, Nagoya University, Chikusa-ku, Nagoya, Aichi 464-8602, Japan
[225] Université de Montréal Polytechnique, Montreal, Quebec H3T 1J4, Canada
[226] Laboratoire Lagrange, Université Côte d Azur, Observatoire Côte d Azur, CNRS, F-06304 Nice, France
[227] Seoul National University, Seoul 08826, Republic of Korea
[228] Sungkyunkwan University, Seoul 03063, Republic of Korea
[229] NAVIER, École des Ponts, Univ Gustave Eiffel, CNRS, Marne-la-Vallée, France
[230] Università di Firenze, Sesto Fiorentino I-50019, Italy
[231] Department of Physics, National Cheng Kung University, Tainan City 701, Taiwan
[232] School of Physics and Technology, Wuhan University, Wuhan, Hubei, 430072, People s Republic of China
[233] National Center for High-performance computing, National Applied Research Laboratories, Hsinchu Science Park, Hsinchu City 30076, Taiwan
[234] Department of Physics, National Taiwan Normal University, Sec. 4, Taipei 116, Taiwan
[235] NASA Marshall Space Flight Center, Huntsville, AL 35811, USA
[236] INFN, Sezione di Roma Tre, I-00146 Roma, Italy
[237] ESPCI, CNRS, F-75005 Paris, France
[238] Kenyon College, Gambier, OH 43022, USA
[239] School of Physics Science and Engineering, Tongji University, Shanghai 200092, People s Republic of China
[240] Dipartimento di Fisica, Università di Trieste, I-34127 Trieste, Italy
[241] Institute for Photon Science and Technology, The University of Tokyo, Bunkyo-ku, Tokyo 113-8656, Japan
[242] Indian Institute of Technology Madras, Chennai 600036, India
[243] Saha Institute of Nuclear Physics, Bidhannagar, West Bengal 700064, India
[244] Institute of Space and Astronautical Science JAXA), Chuo-ku, Sagamihara City, Kanagawa 252-0222, Japan
[245] Institut des Hautes Etudes Scienti ques, F-91440 Bures-sur-Yvette, France
[246] Faculty of Law, Ryukoku University, Fushimi-ku, Kyoto City, Kyoto 612-8577, Japan
[247] Indian Institute of Science Education and Research, Kolkata, Mohanpur, West Bengal 741252, India
[248] Department of Physics, University of Notre Dame, Notre Dame, IN 46556, USA
[249] Graduate School of Science and Technology, Niigata University, Nishi-ku, Niigata City, Niigata 950-2181, Japan
[250] Consiglio Nazionale delle Ricerche—Istituto dei Sistemi Complessi, Piazzale Aldo Moro 5, I-00185 Roma, Italy
[251] Korea Astronomy and Space Science Institute KASI), Yuseong-gu, Daejeon 34055, Republic of Korea
[252] Hobart and William Smith Colleges, Geneva, NY 14456, USA
[253] International Institute of Physics, Universidade Federal do Rio Grande do Norte, Natal RN 59078-970, Brazil
[254] Museo Storico della Fisica e Centro Studi e Ricerche "Enrico Fermi," I-00184 Roma, Italy
[255] Dipartimento di Matematica e Fisica, Università degli Studi Roma Tre, I-00146 Roma, Italy
[256] University of Arizona, Tucson, AZ 85721, USA
[257] Università di Trento, Dipartimento di Matematica, I-38123 Povo, Trento, Italy
[258] University of California, Riverside, Riverside, CA 92521, USA
[259] University of Washington, Seattle, WA 98195, USA
[260] Indian Institute of Technology, Palaj, Gandhinagar, Gujarat 382355, India
[261] Department of Electronic Control Engineering, National Institute of Technology, Nagaoka College, Nagaoka City, Niigata 940-8532, Japan
[262] Departamento de Matemática da Universidade de Aveiro and Centre for Research and Development in Mathematics and Applications, Campus de Santiago, 3810-183 Aveiro, Portugal
[263] Marquette University, Milwaukee, WI 53233, USA
[264] Faculty of Science, Toho University, Funabashi City, Chiba 274-8510, Japan
[265] Graduate School of Science and Technology, Gunma University, Maebashi, Gunma 371-8510, Japan
[266] Institute for Quantum Studies, Chapman University, Orange, CA 92866, USA
[267] Accelerator Laboratory, High Energy Accelerator Research Organization KEK), Tsukuba City, Ibaraki 305-0801, Japan
[268] Faculty of Information Science and Technology, Osaka Institute of Technology, Hirakata City, Osaka 573-0196, Japan
[269] INAF, Osservatorio Astro sico di Arcetri, Largo E. Fermi 5, I-50125 Firenze, Italy
[270] Indian Institute of Technology Hyderabad, Sangareddy, Khandi, Telangana 502285, India
[271] Indian Institute of Science Education and Research, Pune, Maharashtra 411008, India
[272] Istituto di Astro sica e Planetologia Spaziali di Roma, Via del Fosso del Cavaliere, 100, 00133 Roma RM, Italy
[273] Department of Space and Astronautical Science, The Graduate University for Advanced Studies SOKENDAI), Sagamihara City, Kanagawa 252-5210, Japan
[274] Andrews University, Berrien Springs, MI 49104, USA
[275] Research Center for Space Science, Advanced Research Laboratories, Tokyo City University, Setagaya, Tokyo 158-0082, Japan
[276] Institute for Cosmic Ray Research ICRR), Research Center for Cosmic Neutrinos RCCN), The University of Tokyo, Kashiwa City, Chiba 277-8582, Japan
[277] Department of Physics, Kyoto University, Sakyou-ku, Kyoto City, Kyoto 606-8502, Japan
[278] Yukawa Institute for Theoretical Physics YITP), Kyoto University, Sakyou-ku, Kyoto City, Kyoto 606-8502, Japan
[279] Dipartimento di Scienze Aziendali—Management and Innovation Systems DISA-MIS), Università di Salerno, I-84084 Fisciano, Salerno, Italy
[280] Van Swinderen Institute for Particle Physics and Gravity, University of Groningen, Nijenborgh 4, 9747 AG Groningen, Netherlands
[281] Faculty of Science, Department of Physics, The Chinese University of Hong Kong, Shatin, N.T., Hong Kong
[282] Vrije Universiteit Brussel, Pleinlaan 2, 1050 Brussel, Belgium
[283] Applied Research Laboratory, High Energy Accelerator Research Organization KEK), Tsukuba City, Ibaraki 305-0801, Japan
[284] Department of Communications Engineering, National Defense Academy of Japan, Yokosuka City, Kanagawa 239-8686, Japan
[285] Department of Physics, University of Florida, Gainesville, FL 32611, USA
[286] Department of Information and Management Systems Engineering, Nagaoka University of Technology, Nagaoka City, Niigata 940-2188, Japan
[287] Tata Institute of Fundamental Research, Mumbai 400005, India
[288] Eindhoven University of Technology, Postbus 513, 5600 MB Eindhoven, Netherlands
[289] Department of Physics and Astronomy, Sejong University, Gwangjin-gu, Seoul 143-747, Republic of Korea
[290] Concordia University Wisconsin, Mequon, WI 53097, USA
[291] Department of Electrophysics, National Yang Ming Chiao Tung University, Hsinchu, Taiwan

[292] Department of Physics, Rikkyo University, Toshima-ku, Tokyo 171-8501, Japan
[293] LIGO Laboratory, California Institute of Technology, Pasadena, CA 91125, USA
Received 2022 October 22; revised 2023 November 22; accepted 2023 December 2; published 2024 April 30

Abstract

Gravitational waves are expected to be produced from neutron star oscillations associated with magnetar giant flares and short bursts. We present the results of a search for short-duration milliseconds to seconds) and long-duration ∼100 s) transient gravitational waves from 13 magnetar short bursts observed during Advanced LIGO, Advanced Virgo, and KAGRA s third observation run. These 13 bursts come from two magnetars, SGR 1935 +2154 and Swift J1818.0 1607. We also include three other electromagnetic burst events detected by Fermi-GBM which were identi ed as likely coming from one or more magnetars, but they have no association with a known magnetar. No magnetar giant flares were detected during the analysis period. We nd no evidence of gravitational waves associated with any of these 16 bursts. We place upper limits on the rms of the integrated incident gravitational-wave strain that reach $3.6 \times 10^{-23}/\sqrt{\mathrm{Hz}}$ at 100 Hz for the short-duration search and $1.1 \times 10^{-22}/\sqrt{\mathrm{Hz}}$ at 450 Hz for the long-duration search. For a ringdown signal at 1590 Hz targeted by the short-duration search the limit is set to $2.3 \times 10^{-22}/\sqrt{\mathrm{Hz}}$. Using the estimated distance to each magnetar, we derive upper limits on the emitted gravitational-wave energy of 1.5×10^{44} erg 1.0×10^{44} erg) for SGR 1935+2154 and 9.4×10^{43} erg 1.3×10^{44} erg) for Swift J1818.0 1607, for the short-duration long-duration) search. Assuming isotropic emission of electromagnetic radiation of the burst fluences, we constrain the ratio of gravitational-wave energy to electromagnetic energy for bursts from SGR 1935+2154 with the available fluence information. The lowest of these ratios is 4.5×10^{3}.

Uni ed Astronomy Thesaurus concepts: Magnetars 992); Gravitational waves 678); X-ray bursts 1814); Stellar oscillations 1617)

Supporting material: machine-readable tables

1. Introduction

Magnetars—highly magnetized neutron stars—exhibit intermittent bursts of hard X-rays and soft gamma-rays with typical peak luminosities 10^{43} erg s $^{-1}$ see Kaspi & Beloborodov 2017, for a review). Galactic Evans et al. 1980; Hurley et al. 1999, 2005; Mereghetti et al. 2005; Boggs et al. 2007) and extragalactic Mazets et al. 2008; Abadie et al. 2012; Burns et al. 2021; Svinkin et al. 2021) giant flares have peak luminosities up to ve orders of magnitude larger. Although the mechanisms that cause these bursts and giant flares are not well understood, many models predict accompanying gravitational-wave emission from excited core and or crust oscillations Ioka 2001; Ciol et al. 2011; Corsi & Owen 2011; Kashiyama & Ioka 2011; Zink et al. 2012). This hypothesis is enhanced by the identi cation of quasiperiodic oscillations QPOs) in the tails of giant flares Barat et al. 1983; Israel et al. 2005; Strohmayer & Watts 2005, 2006; Watts & Strohmayer 2006), and possibly fainter bursts Huppenkothen et al. 2014a, 2014b), which have been attributed to various oscillations of the stellar crust and core e.g., Duncan 1998; Messios et al. 2001; Piro 2005; Glampedakis et al. 2006; Strohmayer & Watts 2006; Levin 2007; Colaiuda & Kokkotas 2011; Glampedakis & Jones 2014).

Initial estimates for the potential gravitational-wave emission from giant flares were optimistic that the fundamental oscillation mode *f*-mode) of magnetars could be excited by the catastrophic rearrangement of the star s interior magnetic eld. These *f*-modes are excited at frequencies between ∼1 and 3 kHz, and could potentially emit up to $\sim 10^{49}$ erg Ioka 2001; Corsi & Owen 2011) for ∼100 ms Lindblom & Detweiler 1983; McDermott et al. 1988; Wen et al. 2019), making them detectable with the Advanced LIGO Aasi et al. 2015), Advanced Virgo Acernese et al. 2015), and KAGRA Akutsu et al. 2019, 2021) gravitational-wave observatories Abbott et al. 2018). Detailed calculations of the rearrangement of the neutron star s magnetic eld using analytic calculations Levin & van Hoven 2011) and numerical relativity simulations Ciol et al. 2011; Ciol & Rezzolla 2012; Zink et al. 2012; Tsokaros et al. 2021) yield more realistic estimates for the gravitational-wave energy emitted in the *f*-mode during these events. These models suggest that gravitational waves associated with Galactic magnetar flares are not observable with the current generation of observatories, but instead require the sensitivity of at least third-generation observatories such as the Einstein Telescope Punturo et al. 2010) or Cosmic Explorer Reitze et al. 2019; Evans et al. 2021), or dedicated kilohertz facilities such as the proposed NEMO observatory Ackley et al. 2020).

Other oscillation modes in the star, which are generally longer lived and at lower frequencies than the *f*-mode, may be excited. These include buoyancy modes *g*-modes) and Alfvén modes where the magnetic eld provides the oscillation restoring force. The latter of these modes has been suggested as potential long-lived gravitational-wave sources from magnetar giant flares Kashiyama & Ioka 2011; Zink et al. 2012), with the resonant frequency correlated to the initial rise time of the magnetar giant flare Hurley et al. 1999, 2005; Mazets et al. 2008). The damping time and mode excitation amplitude of these modes are largely unknown, making them interesting candidates for longer-lived gravitational-wave signals.

Only one Galactic giant flare has been observed coincident with a LIGO–Virgo observing run: the 2004 giant flare from SGR 1806 20. Upper limits on the gravitational-wave energy associated with the burst were determined to be between $\sim 10^{46}$ and 10^{52} erg, depending on the assumed waveform model

[294] Deceased, 2020 August.
[295] Deceased, 2021 April.

Table 1
List of Magnetar Short Bursts Considered for this Search from the Interplanetary Network Master Burst List Hurley 2021), and the Available Gravitational-wave Detectors: LHO H), LLO L), and Virgo V)

Burst	Source	Date	Time UTC)	Detectors	$E_{\rm EM}^{\rm iso}$ erg)	GCN Circulars
2651	SGR 1935+2154	2019 Nov 4	01:54:37	H V[a]		26169
2652	SGR 1935+2154	2019 Nov 4	02:53:31	H V	1.4×10^{39}	26163, 26151
2653	SGR 1935+2154	2019 Nov 4	04:26:55	H L V	1.1×10^{39}	26163
2654	SGR 1935+2154	2019 Nov 4	06:34:00	H L V		26153
2655	SGR 1935+2154	2019 Nov 4	09:17:53	H L	5.7×10^{39}	26163, 26154
2656	SGR 1935+2154	2019 Nov 4	10:44:26	H L	2.2×10^{40}	26242, 26163, 26158, 26157
2657	SGR 1935+2154	2019 Nov 4	12:38:38	H L V	2.7×10^{39}	26163
2660	SGR 1935+2154	2019 Nov 4	15:36:47	H V	1.2×10^{39}	
2661	SGR 1935+2154	2019 Nov 4	20:29:39	H V	1.3×10^{39}	26165, 26166
2665	SGR 1935+2154	2019 Nov 5	06:11:08	H V	7.8×10^{40}	26242
2668	SGR 1935+2154	2019 Nov 15	20:48:41	L V	7.7×10^{38}	
2669		2020 Feb 3	03:17:11	H L V		26980
2670		2020 Feb 3	03:44:03	H L V		26969, 26980
2671		2020 Feb 3	20:39:37	H L V		26980
2673	Swift J1818.0 1607	2020 Feb 28	22:19:32	L V		
2674	Swift J1818.0 1607	2020 Mar 12	21:16:47	H L V		27373

Notes. Three electromagnetic bursts 2669, 2670, and 2671) were not identi ed with a source and are thought to likely come from one or more magnetar s), as reported in GCN Circular 26980 Lesage 2020) and in the Fermi-GBM Meegan et al. 2009) onboard Trigger Catalog, available online https: heasarc.gsfc.nasa.gov W3Browse fermi fermigtrig.html). The isotropic electromagnetic energy $E_{\rm EM}^{\rm iso}$) is estimated from the fluence given in Lin et al. 2020) assuming a distance of 9.0 kpc for SGR 1935+2154. Distances to these sources with uncertainties Olausen & Kaspi 2014; the McGill Online Magnetar Catalog is available at https: www.physics.mcgill.ca pulsar magnetar main.html) are 9.0 ± 2.5 kpc for SGR 1935+2154 Zhong et al. 2020), 4.8 to 8.1 kpc for Swift J1818.0 1607 Karuppusamy et al. 2020), and 3.8 ± 0.5 kpc for 1 RXS J170849 Durant & van Kerkwijk 2006).
[a] Burst 2651 occurred 87 s before Virgo was in observation mode.

Kalmus et al. 2007; Abbott et al. 2008a; Kalmus 2009). A stacked search was performed on a series of bursts from the same magnetar occurring in the same minute, reducing the above upper limits to $\sim 10^{45}$ and 10^{50} erg assuming the same *f*-mode frequency and damping time for each burst Abbott et al. 2009; Kalmus 2009; Kalmus et al. 2009). Further searches for *f*-modes in 1279 bursts from six different magnetars yielded upper limits between $\sim 10^{44}$ and 10^{47} erg Abadie et al. 2011), while the rst search for *f*-modes in the advanced era of gravitational-wave interferometers yielded comparable upper limits for four bursts from two magnetars Abbott et al. 2019; Schale 2019). These energy upper limits are in the range of possible gravitational-wave energies given the most optimistic predictions Ioka 2001; Corsi & Owen 2011).

Longer-duration searches initially targeted the QPO frequencies in the tail of the giant flare of SGR 1806 20, with upper limits of various modes at 10^{46} erg Abbott et al. 2007; Matone & Márka 2007), comparable to the electromagnetic energy emitted from the giant flare. A study was performed on a method to detect gravitational waves targeting repeated QPOs Murphy et al. 2013). A search for long-duration gravitational waves from four magnetar bursts was performed using LIGO s sixth science run S6) data Quitzow-James 2016; Quitzow-James et al. 2017). The best upper limits from magnetar bursts come from recent observations in the Advanced LIGO–Virgo second observing run O2), with gravitational-wave energies constrained to less than $\sim 10^{44}$–10^{48} erg, again depending on the signal model, frequency, and damping time Abbott et al. 2019; Schale 2019). We previously placed limits on gravitational-wave emission from purported extragalactic magnetar giant flares Abbott et al. 2008b; Abadie et al. 2012),[296] with long-duration searches constraining the gravitational-wave energy emitted to between $\sim 10^{49}$ and 10^{52} erg for four different giant flares Macquet et al. 2021).

In this paper, we report on a search for gravitational waves coincident with 13 magnetar short bursts from SGR 1935 +2154, Swift J1818.0 1607, and three electromagnetic bursts from an unidenti ed source or sources) during the LIGO–Virgo–KAGRA third observing run O3). Targeted gravitational-wave searches associated with magnetar bursts can broadly be split in two categories following theoretical predictions of short-duration and long-duration signals. For each magnetar burst we carry out a short-duration and long-duration search. We nd no evidence of gravitational-wave signals and hence place upper limits on the gravitational-wave strain and energy for each burst considered.

[296] GRB 070222, included in a search targeting gamma-ray bursts Aasi et al. 2014), was later determined to likely be an extragalactic magnetar giant flare Burns et al. 2021; Macquet et al. 2021).

Table 2
On-source Window, Off-source Window, and Frequency Range of Searches Performed

Search	Pipeline	On-source Window s)	On-source Interval s)	Off-source Window s)	Frequency Range Hz)
Centered on source	X-pipeline	8	4, +4]	10,800	50–4000
Delayed on source	X-pipeline	500	+4, +504]	10,800	50–4000
Long duration	STAMP	1604	4, +1600]	59,040	24–2500

Note. The on-source interval is centered around the magnetar burst time.

2. Methodology

The O3 observing run extended from 2019 April 1 to 2020 March 27, with three gravitational-wave detectors taking data: LIGO Hanford Observatory LHO), LIGO Livingston Observatory LLO), and Virgo, all of which had been upgraded so that the binary neutron star inspiral ranges increased by a factor of 1.53 for LLO, 1.64 for LHO, and 1.73 for Virgo Davis et al. 2021) compared to their performance during O2. For each detector, several data quality checks are performed to mitigate terrestrial noise Davis et al. 2021). In addition, multidetector analyses are used to mitigate nonastrophysical features present in the data. In 2020 January, a new technique was implemented to mitigate the impact in LIGO detectors of scattered light, a transient noise coupled with ground motion. Data available for bursts that occurred in February and March show a lower transient noise rate.

The list of magnetar short bursts and giant flares from Hurley 2021) provides the source object and observation time for each burst. In both the long-duration and short-duration searches, we describe the data in which we look for a signal as the "on-source" window, while the time around this composing the background as the "off-source" window. Analysis requirements include at least two gravitational-wave detectors in observation mode, suf ciently good data quality, and suf cient data available in the burst s on-source window. Several bursts did not meet the two-detector criterion one detector available for bursts 2651, 2658, 2659, and 2667 in Hurley 2021; and none for 2662, 2663, and 2664), had poor data quality 2650 and 2672), or had very little data available in the on-source window 2650). Considering these requirements, 12 magnetar short bursts from known sources and three electromagnetic bursts thought to likely be magnetar short bursts from an unknown source or sources occurred when at least two detectors were in observation mode with suf ciently good data quality and are included in this search. In addition, although burst 2651 occurred when LHO was in observation mode and 87 s before Virgo was in observation mode LLO was not taking data), data were available for most of the long-duration search on-source window, thus the burst was analyzed by the long-duration search only. 11 of the short bursts were from SGR 1935+2154 Cummings et al. 2014), a magnetar that emitted a fast radio burst in 2020 April Kirsten et al. 2020), and two of the short bursts were from Swift J1818.0 1607, a magnetar discovered in 2020 Evans et al. 2020).

The source or sources of the remaining three electromagnetic bursts, detected by Fermi-GBM Meegan et al. 2009), are unknown as they have very poor sky localization. These three electromagnetic bursts were accompanied by a fourth burst which did not meet the two-detector condition necessary for our analysis, but all four of these bursts occurred in a 33 hr window of time between 2020 February 3 and February 4. Because of their temporal proximity, we search for a signal assuming that they were emitted by the same magnetar. Only two known Galactic magnetars are in the 3 sky position error region of all four electromagnetic bursts. In order to run a directional search and obtain the upper limits, we consider the source of these bursts to be 1 RXS J170849 at 3.8 kpc Durant & van Kerkwijk 2006), and note that the directional sensitivity of the detector network changes very little between neighboring sky positions. The sources, times, active detectors, and the isotropic electromagnetic energy $E_{\rm EM}^{\rm iso}$) of each burst included in this search are listed in Table 1; fluence information for some of the bursts from SGR 1935+2154 were obtained from Lin et al. 2020) and used to estimate $E_{\rm EM}^{\rm iso}$.

Table 3
False Alarm Statistic for the Most Signi cant Cluster Found for Each Burst by All Searches

Burst	Long-duration FBS	Centered 8 s) *p*-value	Delayed 500 s) *p*-value
2651	9.1×10^{1}		
2652	2.1×10^{1}	1.0	4.1×10^{1}
2653	7.7×10^{1}	1.8×10^{2}	3.5×10^{3}
2654	8.5×10^{1}	9.9×10^{2}	6.6×10^{1}
2655	7.8×10^{1}	1.0	7.3×10^{1}
2656	9.7×10^{1}	8.6×10^{3}	5.2×10^{1}
2657	1.6×10^{1}	6.7×10^{2}	4.8×10^{1}
2660	2.2×10^{2}	4.8×10^{1}	4.9×10^{1}
2661	9.0×10^{1}	1.9×10^{1}	7.4×10^{1}
2665	8.2×10^{1}		
2668	9.9×10^{1}	1.0	4.3×10^{1}
2669		1.0	6.3×10^{1}
2670		2.9×10^{1}	7.8×10^{1}
2671		3.4×10^{1}	
2673	6.8×10^{1}	1.0	4.8×10^{1}
2674	5.9×10^{1}	1.0	5.0×10^{2}

Note. FBS is reported for the long-duration search, and the *p*-value for the short-duration searches. A *p*-value of 1 indicates that there were no clusters in the on-source window that survive the cluster selection process. Table entries of " " indicate that no value is recorded, because no search was run. Bursts 2669–2671 are from the magnetar with no identi ed source, and the long-duration search was not conducted on these. Bursts 2651 and 2665 are missing segments of data from the on-source window such that the short-duration searches could not run, and burst 2671 has data missing in the delayed on-source window such that the delayed on-source search could not be run.

This table is available in machine-readable form.)

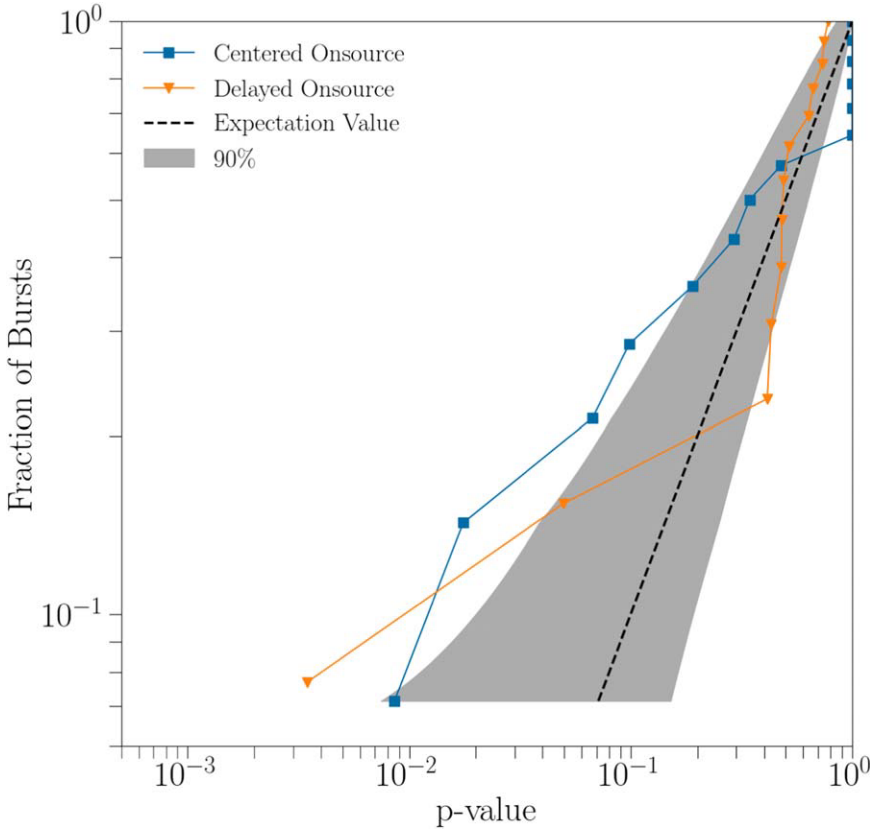

Figure 1. Cumulative distribution of the *p*-values of the most signi cant clusters found by the short-duration searches. The expectation value and 90 con dence interval are calculated numerically as in Abbott et al. 2023); the expectation value is calculated assuming a uniform distribution of *p*-values given by the null hypothesis), with each point having a 90 probability of landing in the shaded region. The lowest *p*-value in the delayed on-source search is 3.5×10^{3} from burst 2653, and is determined to be most likely an instrumental artifact through arguments invoking both astrophysics and the characteristics of the detector. Several centered on-source search clusters fall outside of the 90 con dence interval, which is not unlikely given how few data points there are, and many of them have properties inconsistent with what one would expect from an astrophysical source. Although the most signi cant of these, which appears in burst 2656, has a *p*-value 8.6×10^{3}) and a peak frequency 1577 Hz) which are consistent with expectations for an *f*-mode, we provide arguments for why this is not the case in Section 3.1.

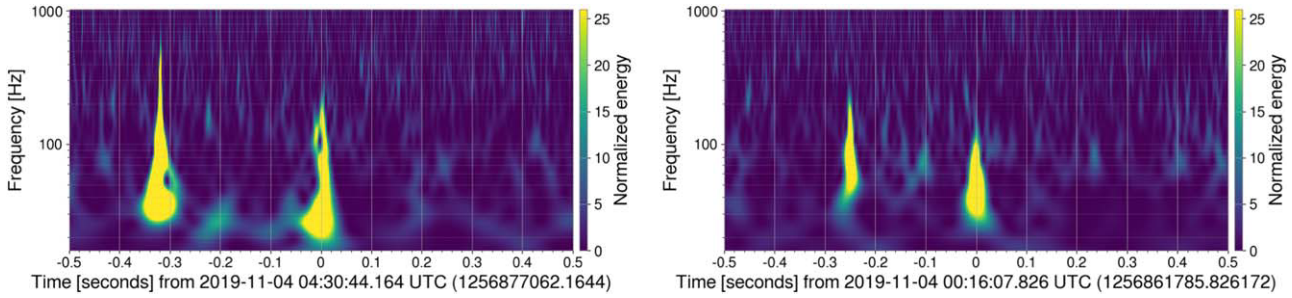

Figure 2. Spectrograms of the LHO data left) at the time of the most signi cant cluster found in the on-source window of burst 2653, and an instrumental artifact appearing also in the LHO data right). The time separation between these two events is ∼15,277 s, which is larger than the size of the background window in our analysis, and therefore the instrumental artifact was not included in the background. These two spectrograms display very similar structure, with similar double short-duration transients separated in both cases by ∼0.3 s. Several instrumental artifacts of this nature are found by Omicron Robinet et al. 2020) within the day of burst 2653. The second most signi cant cluster in the same delayed on-source analysis of burst 2653 also has this same double-peaked structure.

We follow Abbott et al. 2019) to search for short-duration signals as potentially emitted by *f*-modes) and long-duration signals such as might accompany an observed QPO). Each search combines the data from two or more when available in the case of the short-duration search) detectors into a time–frequency map and then forms groups of pixels, called clusters, to search for gravitational-wave signals. The three electromagnetic bursts without a known source are only analyzed with the short-duration search. The searches are described in the following sections.

2.1. Short duration Search

The search for short-duration transient gravitational waves milliseconds to seconds) is motivated by a potential signal associated with *f*-mode oscillations in the magnetar s core. Because the frequencies of the expected gravitational-wave signals can be as high as several kilohertz Wen et al. 2019; Ho et al. 2020), the search ranges in frequency from 50 to 4000 Hz, extending to higher frequencies than the other unmodeled searches most notably LIGO–Virgo–KAGRA s burst searches

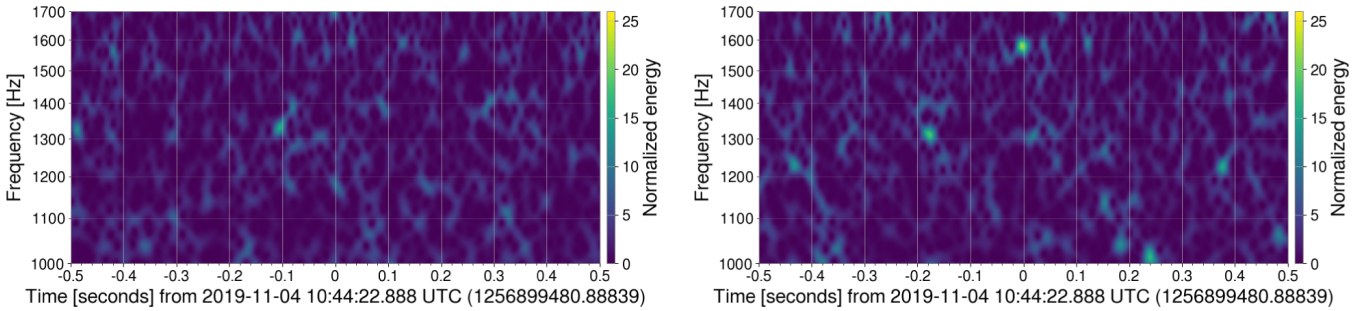

Figure 3. Spectrograms of the LHO left) and LLO right) data around the time of the most signi cant cluster found by the centered-window short-duration search of burst 2656. Even though the cluster is only barely visible in the LLO data, these spectrograms show that the ambient noise in each detector is in a normal state around the time of the flare.

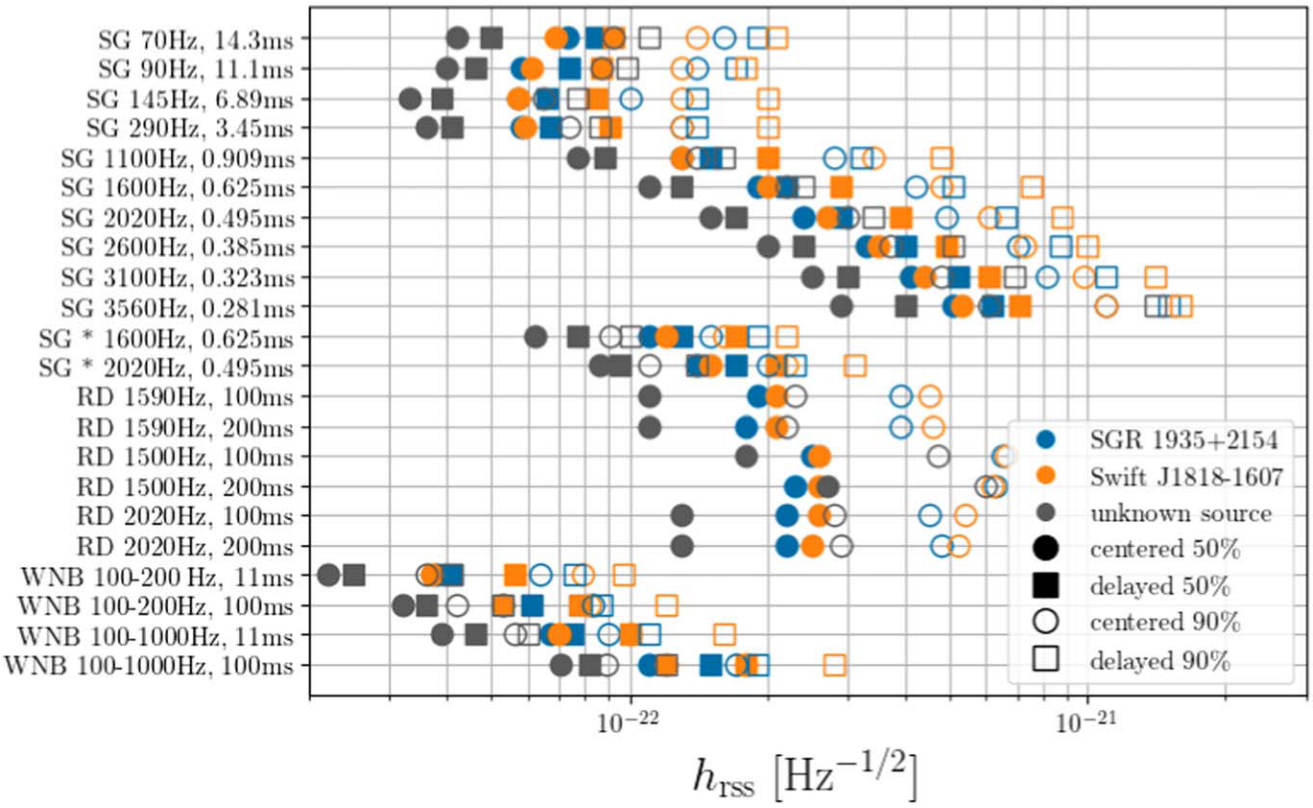

Figure 4. For each injection, we display the $h_{\rm rss}^{50\%}$ and $h_{\rm rss}^{90\%}$ values as measured by the most sensitive burst from each source in the short-duration search. The $h_{\rm rss}^{50\%}$ values are marked by lled-in shapes, and the $h_{\rm rss}^{90\%}$ values are not lled in. The vertical axis notes the waveform, where "SG" means sine-Gaussian and "RD" means ringdown. The frequency and duration of each injection are given as well. All of the sine-Gaussian and ringdown waveforms are eliptically polarized except for the ones denoted by " ," which are circularly polarized. The numerical values of $h_{\rm rss}^{50\%}$ can be found in Tables 6–8, while the numerical values of $h_{\rm rss}^{90\%}$ can be found in Tables 9–11.

associated with gamma-ray bursts, Abbott et al. 2021, 2022; and fast radio bursts, Abbott et al. 2023).

We analyze the data using X-pipeline: an unmodeled, coherent search pipeline Sutton et al. 2010; Was et al. 2012). The X-pipeline algorithm coherently combines the data from each detector in the network to produce a multiresolution time–frequency map displaying the energy in each pixel. The brightest 1 of these pixels are then selected, and neighboring bright pixels are combined into clusters, which are then assigned a ranking statistic. A large fraction of background clusters are rejected by vetos built from the coherent and incoherent power across the detector network. Other details on the parameters of the short-duration search are summarized in Appendix A.

The search for short-duration gravitational waves is comprised of two components: an 8 s on-source window centered on the magnetar burst time a "centered" on-source window) to optimize sensitivity when gravitational-wave emission is most probable, and a 500 s on-source window beginning just after the centered on-source window a "delayed" on-source window). The longer delayed on-source window is intended to search for short-duration signals emitted during the time following the burst, analogous to the QPOs that have been observed in some giant flares. For each on-source window, we calculate the signi cance of clusters using 3 hr of data taken symmetrically about the burst time with a gap of 16 s before and after the on-source window.

Table 4

Values of $h_{\rm rss}^{90\%}$ and $E_{\rm GW}^{90\%}$ for the Centered On-source Short-duration Search for Each Burst and for Two Types of Waveforms that Best Model the Gravitational Wave One Would Expect in Conjuncture with an *f*-mode: the Elliptically Polarized 1600 Hz sine-Gaussian Waveform and 100 ms Ringdown Waveform at Central Frequency 1590 Hz

Burst	Source	Ringdown			Sine-Gaussian		
		$h_{\rm rss}^{90\%}$ Hz $^{1\ 2}$)	$E_{\rm GW}^{90\%}$ erg)	$\frac{E_{\rm GW}^{90\%}}{E_{\rm EM}^{\rm iso}}$	$h_{\rm rss}^{90\%}$ Hz $^{1\ 2}$)	$E_{\rm GW}^{90\%}$ erg)	$\frac{E_{\rm GW}^{90\%}}{E_{\rm M}^{\rm ISO}}$
2652	SGR 1935+2154	1.2×10^{-21}	4.2×10^{48}	3.0×10^{9}	1.3×10^{-21}	5.4×10^{48}	3.8×10^{9}
2653	SGR 1935+2154	5.2×10^{-22}	8.3×10^{47}	7.3×10^{8}	5.5×10^{-22}	9.4×10^{47}	8.3×10^{8}
2654	SGR 1935+2154	1.0×10^{-21}	3.1×10^{48}		9.9×10^{-22}	3.1×10^{48}	
2655	SGR 1935+2154	3.9×10^{-22}	4.7×10^{47}	8.2×10^{7}	4.2×10^{-22}	5.5×10^{47}	9.6×10^{7}
2656	SGR 1935+2154	4.6×10^{-22}	6.7×10^{47}	3.0×10^{7}	4.5×10^{-22}	6.3×10^{47}	2.8×10^{7}
2657	SGR 1935+2154	4.9×10^{-22}	7.5×10^{47}	2.7×10^{8}	5.2×10^{-22}	8.4×10^{47}	3.1×10^{8}
2660	SGR 1935+2154	1.1×10^{-21}	3.6×10^{48}	3.0×10^{9}	8.8×10^{-22}	2.4×10^{48}	2.0×10^{9}
2661	SGR 1935+2154	7.4×10^{-22}	1.7×10^{48}	1.3×10^{9}	7.8×10^{-22}	1.9×10^{48}	1.4×10^{9}
2668	SGR 1935+2154	6.8×10^{-22}	1.4×10^{48}	1.9×10^{9}	6.5×10^{-22}	1.3×10^{48}	1.8×10^{9}
2669	unknown	2.5×10^{-22}	3.5×10^{46}		2.2×10^{-22}	2.6×10^{46}	
2670	unknown	2.3×10^{-22}	3.0×10^{46}		2.2×10^{-22}	2.8×10^{46}	
2671	unknown	4.1×10^{-22}	9.3×10^{46}		4.2×10^{-22}	9.7×10^{46}	
2673	Swift J1818.0 1607	7.0×10^{-22}	1.2×10^{48}		7.3×10^{-22}	1.4×10^{48}	
2674	Swift J1818.0 1607	4.5×10^{-22}	5.1×10^{47}		4.8×10^{-22}	5.9×10^{47}	

Note. We calculate the energies using the source distances given in the caption of Table 1, and conservatively assuming a distance of 8.1 kpc for Swift J1818.0–1607. Because the gravitational-wave energy is proportional to the distance squared, the $E_{\rm GW}^{90\%}$ upper limits pertaining to Swift J1818.0–1607 could scale by a factor as low as 0.35 if the source is at its nearest distance of 4.8 kpc. The burst numbers are consistent with those used in the catalog: http: www.ssl.berkeley.edu ipn3 sgrlist.txt.

This table is available in machine-readable form.)

Since the delayed on-source window starts just after the end of the centered on-source window and has a 500 s duration, it overlaps the off-source window for the centered on-source search. This introduces the possibility of a signal detected in the delayed on-source window being included in the background of the centered on-source window. We mitigate this possibility by examining the results of the delayed on-source window and verifying the absence of a signal before viewing the results of the centered on-source window. A summary of the pipeline, time window, and frequency range for the short-duration searches and long-duration search) is reported in Table 2.

2.2. Long duration Search

Following previous searches Quitzow-James 2016; Quitzow-James et al. 2017; Abbott et al. 2019), we use the Stochastic Transient Analysis Multidetector Pipeline STAMP; Thrane et al. 2011) to analyze data for the long-duration search. STAMP builds signal-to-noise ratio S N) time–frequency maps using the cross-power between two detectors. We then use STAMP s seedless clustering algorithm, which generates clusters with quadratic Bézier curves Thrane & Coughlin 2013), to search for long-duration transient gravitational-wave signals. Restricting the variation of the clusters in frequency to a maximum of 10 allows us to target nearly monochromatic gravitational-wave signals potentially emitted from the mechanisms responsible for QPOs while reducing computational resources Abbott et al. 2019). Clusters are ranked according to their S N, de ned as the sum of the S N of the pixels that compose the cluster Thrane & Coughlin 2013).

The on-source window starts 4 s before the burst time and ends 1600 s after, for 1604 s in total. Additional details are provided in Appendix B and in Thrane et al. 2011). The frequency range is 24–2500 Hz, limited by seismic noise at low frequencies, and going to just above the QPO s highest frequency observed in the tail of the 2004 giant flare Mereghetti et al. 2005). Data from LHO and LLO are used when available, with data from Virgo used for bursts that also have data from either LHO or LLO see Table 1 for the available detectors for each burst).

The background for each burst is estimated using 59,040 s of off-source data as close as possible to the burst s on-source window while excluding the on-source windows of all of the other bursts. These data are broken up into 36 off-source analysis windows. We combine the data from one detector from each of these analysis windows with the data from the other detector from every other analysis window to create 1260 $36^2 - 36$) S N time–frequency maps which we will refer to as background segments) in order to produce a background cluster distribution for each burst.

3. Results

The results of the short-duration and long-duration searches for each burst are presented in the following sections. Clusters found in the on-source windows of the short-duration search are ranked by their *p*-value, which is the probability of having a cluster of such signi cance in the on-source window under the null hypothesis. They are calculated considering the clusters in the background with a ranking statistic larger than the on-source cluster. Similarly we characterize the signi cance of the on-source clusters of the long-duration search with the fraction of background segments FBS) as

$$\mathrm{FBS} = N_{\geqslant}/N_{\rm Total}, \tag{1}$$

where N is the number of segments in the respective burst s background whose loudest cluster has an S N greater than or equal to the on-source cluster s S N, and $N_{\rm Total}$ is the total number of segments in that background. The *p*-value in the short-duration search is found similarly to Equation 1), but where N and $N_{\rm Total}$ include all clusters in the background with

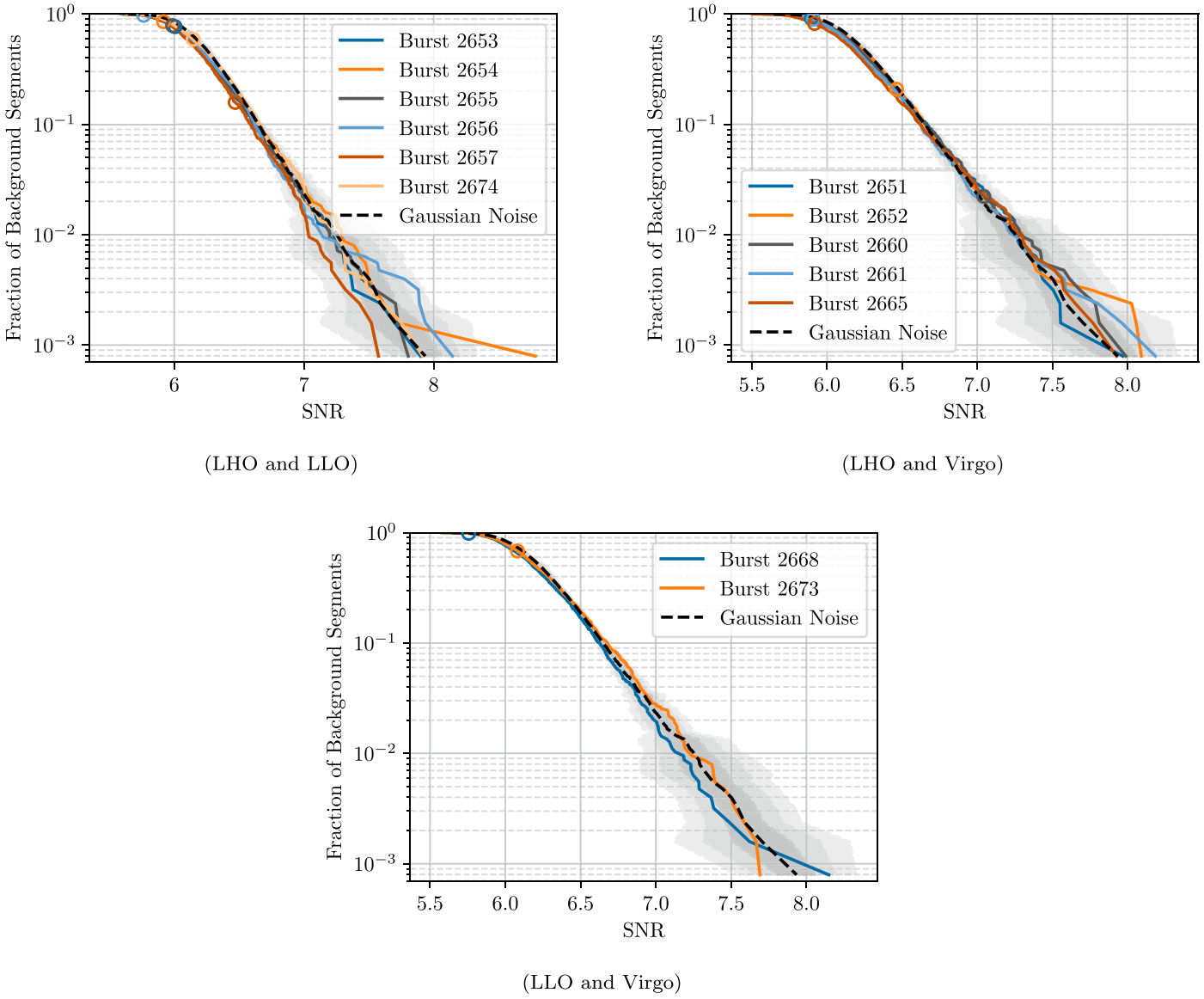

Figure 5. Distributions of background and on-source clusters found by the long-duration search for each burst analyzed with data from LHO, LLO, and Virgo. The background of each burst is displayed along with the S N of its on-source cluster, denoted by a circle. The dashed black line is the mean, and the gray contours are the one, two, and three standard deviations of the distribution of FBS obtained simulating Gaussian noise colored with the Advanced LIGO design sensitivity curve Barsotti et al. 2018).

a S N higher than the on-source cluster rather than only the loudest cluster from each time segment.

The upper limit $h_{\rm rss}^{90\%}$ $E_{\rm GW}^{90\%}$) is the value of the root-sum-square strain gravitational-wave energy) of the magnetar signal such that 90 of a population of signals with that amplitude energy) would have given rise to gravitational-wave candidates more signi cant than those found by our search. We also present the analogous upper limits pertaining to a 50 detection ef ciency, $h_{\rm rss}^{50\%}$ and $E_{\rm GW}^{50\%}$. To estimate $h_{\rm rss}^{50\%}$ and $h_{\rm rss}^{90\%}$ for each burst, we inject waveforms into the data and calculate the amplitudes for which 50 and 90 of the signals have a detection statistic equal to or greater than the respective most signi cant on-source cluster. These waveforms are meant to encapsulate a broad range of different signals that could be produced in association with magnetar bursts, but are not associated with speci c emission mechanisms.

We then derive the rms of the integrated incident gravitational-wave strain $h_{\rm rss}$) and gravitational-wave energy $E_{\rm GW}$) for these amplitudes. The de nition of $h_{\rm rss}$ is

$$h_{\rm rss} = \sqrt{\int_{-\infty}^{\infty} |h_+(t)|^2 + |h_\times(t)|^2 dt}\,, \tag{2}$$

where h_+ t) and $h_\times$ t) are the two signal polarizations. In Appendix C we derive $h_{\rm rss}$ and $E_{\rm GW}$ for the different waveforms used in the analysis.

When calculating $E_{\rm GW}$, we use 9 kpc for SGR 1935+2154 Zhong et al. 2020). The distance to Swift J1818.0 1607 is estimated to be in the range of 4.8–8.1 kpc Karuppusamy et al. 2020); we calculate $E_{\rm GW}$ with the larger distance of 8.1 kpc to be conservative. For the magnetar bursts with unknown source s), we consider 1 RXS J170849 as the source and use 3.8 kpc for the distance Olausen & Kaspi 2014). The gravitational-wave energy upper limits corresponding to the $h_{\rm rss}$ upper limits are calculated according to the discussion in Appendix C, and in all cases the energy is proportional to the source distance

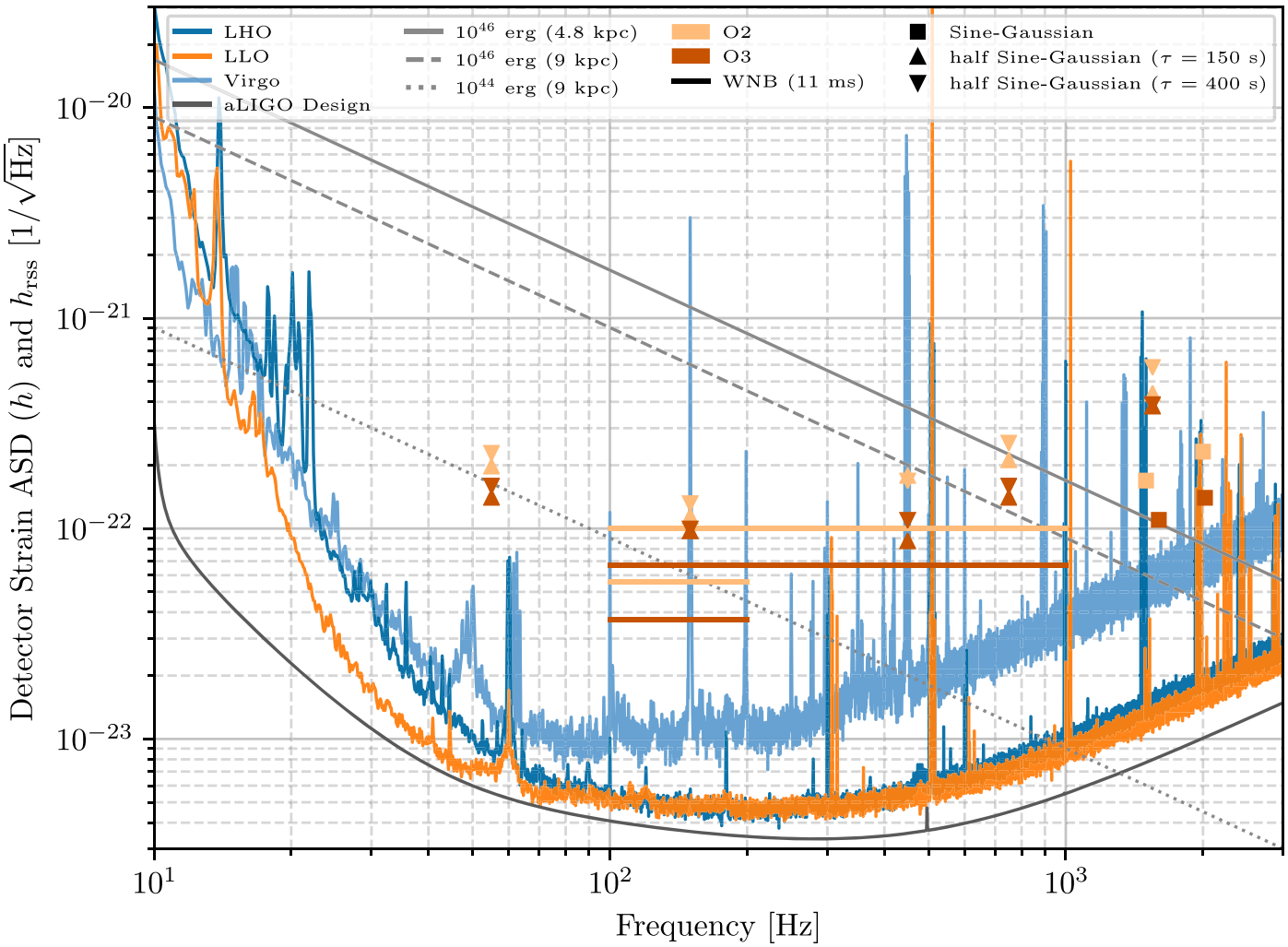

Figure 6. The lowest $h_{\rm rss}^{50\%}$ value across all bursts with known sources are displayed and compared to O2 results for the long-duration search. The detectors amplitude strain density curves correspond to the representative sensitivity for each detector during O3 Buikema et al. 2020; Kissel 2020; Verkindt 2021).

squared. Any uncertainty in these distances will also effect the energy upper limits.

3.1. Short duration Search Results

All bursts listed in Table 1 have been considered by the short-duration search except bursts 2651 and 2665 because of missing data in the on-source windows. For the bursts considered, the short-duration centered and delayed on-source searches nd clusters whose p-values are reported in Table 3. The cumulative distribution of these p-values is represented in Figure 1. The two most signi cant p-value < 1) clusters found for bursts 2653 and 2656 by the short-duration search are discussed.

Burst 2653. Two signi cant clusters are detected by the delayed on-source search. The most signi cant cluster has a p-value of 3.5×10^{-3}, a peak frequency of 97 Hz, and duration of 31 ms. This is the outlier displayed in Figure 2. X-pipeline identi es another loud cluster 50 s earlier with the same p-value, a peak frequency of 228 Hz, and a duration of 7.8 ms. Given their frequency and duration, each of these clusters is only a couple of cycles long. Both clusters display similar characteristics in the LHO data, appearing in spectrograms as a short-duration, low-frequency spike. In both cases, another high-S N spike is seen in the data ∼0.3 s from the time of the cluster as shown in Figure 2. Several other of these high-S N features are detected on the same day as trigger 2653, and these are also in groups of two spaced out by ∼0.3 s. While X-pipeline does not reconstruct either of these neighboring spikes in a coherent cluster, their presence at such a consistent and short time separation from the cluster strongly suggests that each of these clusters has a terrestrial origin. While X-pipeline conducts a coherent search, there remains poor coherence across the two-detector network for these clusters. When the energy per time–frequency pixel is standardized to be 1 unit for Gaussian data, this signal is detected with 165.3 units in LHO, and only 6.2 units and 12.8 units of energy in LLO and Virgo, respectively. The ratio between the LHO and LLO energies is more than can be accounted for by the ratio of antenna factors squared, which gives a measure of the directional sensitivity 4.8 for LHO–LLO and 1.3 for LHO–Virgo) at the time of the burst. Finally, neither of these clusters is visibly identi able in the LLO nor the Virgo time–frequency maps, meaning they are likely instrumental artifacts in LHO only.

Burst 2656. The most signi cant cluster found by the centered on-source search has a p-value of 8.6×10^{-3}. This cluster is 63 ms long, and its frequency extends from 1560 to

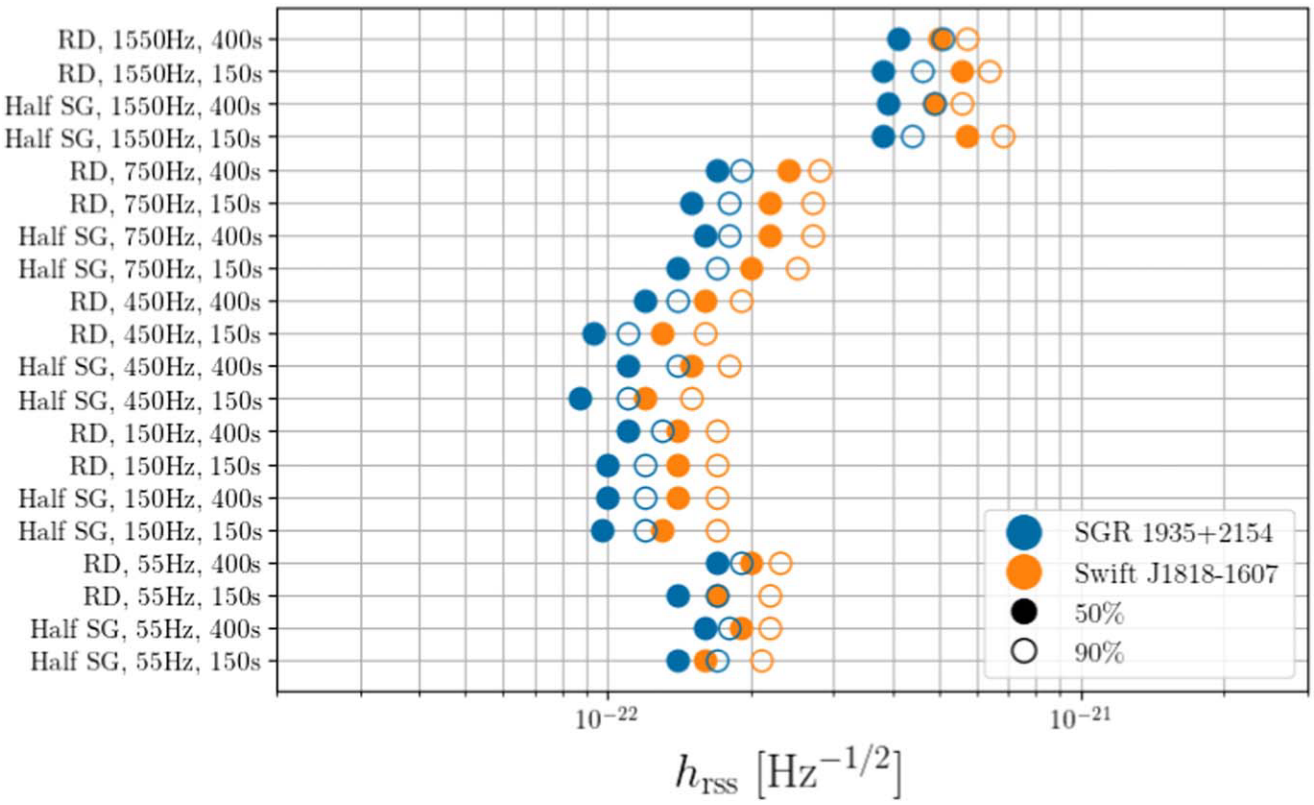

Figure 7. For each injection, we display the $h_{\rm rss}^{50\%}$ values of the burst with the lowest value at 50 detection ef ciency from each source in the long-duration search, and the $h_{\rm rss}^{90\%}$ values for the same burst. The $h_{\rm rss}^{50\%}$ values are marked by lled-in shapes, and the $h_{\rm rss}^{90\%}$ values are not lled in. The vertical axis notes the waveform, where "Half SG" means half sine-Gaussian and "RD" means ringdown. The frequency and duration of each injection are given as well. In general the $h_{\rm rss}^{90\%}$ values are less than a factor of 1.5 greater than their corresponding $h_{\rm rss}^{50\%}$. The numerical values of the upper limits pertaining to SGR 1935+2154 can be found in Table 12, while the upper limits for Swift J1818.0–1607 can be found in Table 13.

1608 Hz, which matches the expected frequency range of neutron star *f*-mode oscillations. The cluster appears ∼3.1 s before the burst time. There are no known physical mechanisms to produce gravitational waves so long before the electromagnetic emission; while this does not rule out this cluster being astrophysical, it makes it less plausible.

Unlike the clusters found for burst 2653, this one is only visible in the LLO data spectrogram shown in Figure 3, which also illustrates that no high-S N glitches are present in the ambient noise at the time of the burst. The imbalance in detector energies for this cluster also suggests that it is an instrumental artifact.

When considering the number of analyses in the long-duration and short-duration searches 40 in total across the three on-source windows of 16 bursts), the probability of having a *p*-value as low as that of burst 2656 is 29 . This, and the high probability that the cluster is due to an instrumental artifact, imply it is highly unlikely to be a signal of astrophysical origin. Nevertheless, we can calculate the strain and gravitational-wave energy required for such a signal assuming it is of astrophysical origin. Using the ringdown waveform with a 100 ms damping time and 1590 Hz frequency, $h_{\rm rss}^{50\%}$ and $E_{\rm GW}^{50\%}$ are 2.2×10^{-22} Hz $^{-1/2}$ and 1×10^{47} erg, respectively. This implies a ratio of gravitational-wave energy to electromagnetic energy of $E_{\rm GW}^{50\%}/E_{\rm EM}^{\rm iso} = 6 \times 10^{6}$. It is dif cult to imagine a physical scenario whereby this much more energy is deposited into gravitational rather than electromagnetic waves, adding further weight to the conclusion that this cluster is not of astrophysical origin.

In the short-duration searches, simulated signals are added into the on-source data and the resulting time–frequency maps are processed similarly to the on-source time–frequency maps. The injected signals are chosen such that they adequately model a short-duration transient consistent with a magnetar *f*-mode signal, and also such that they cover a reasonable range of frequencies outside of the *f*-mode frequency range. We inject sine-Gaussian waveforms, described in Appendix C, at a range of frequencies between 70 and 3560 Hz and standardize the damping time of each injection to be the inverse of the frequency. We also inject a series of ringdown waveforms characterized by sinusoids with an exponentially decaying amplitude as described in Appendix C. These ringdown waveforms have damping times of 100 ms and 200 ms, and frequencies ranging from 1500 to 2020 Hz for consistency with previous searches. We also include a series of white noise burst WNB) signals ranging in frequency from 100 to 1000 Hz to probe $h_{\rm rss}$ upper limits at lower frequencies. The ringdown and sine-Gaussian waveforms are eliptically polarized such that the analysis makes no assumptions on the source orientation. The exception to this are two circularly polarized sine-Gaussian waveforms injected at 1600 and 2020 Hz, which assume an optimally oriented source and are used for comparison with previous searches.

In Figure 4, we present the $h_{\rm rss}^{50\%}$ and $h_{\rm rss}^{90\%}$ values of the most sensitive burst from each source for the short-duration search. Overall, the $h_{\rm rss}$ upper limits follow the detectors sensitivity frequency evolution and we also see that for most waveforms, $h_{\rm rss}^{90\%}$ is approximately a factor of 2 greater than the

Table 5
Parameters Used in the Centered On-source and Delayed On-source Short-duration Searches

Burst	Parameters of the Delayed On-source Search	Parameters of the Centered On-source Search
2652	Background asymmetry factor = 0.3726, background length = 8090 s, frequency range = 300 Hz to 4000 Hz	Background asymmetry factor = 0.3858, background length = 9056 s
2653	Background asymmetry factor = 0.4711, background length = 10,790 s, frequency range = 65 Hz to 4000 Hz, error region = 1°	
2655	Background asymmetry factor = 0.5677, background length = 10,790 s	Background asymmetry factor = 0.5225, background length = 10,790 s
2656	Background asymmetry factor = 0.4331, background length = 10,790 s	Background asymmetry factor = 0.4775, background length = 10,790 s
2660	Background asymmetry factor = 0.3421, background length = 10,790 s	Background asymmetry factor = 0.3403, background length = 10,790 s
2661	Error region = 1°	
2668	Error region = 1°	Frequency range = 85 Hz to 4000 Hz
2669	Background asymmetry factor = 0.8993, background length = 10,790 s	Background asymmetry factor = 0.854, background length = 10,790 s
2670	Background asymmetry factor = 0.1015, background length = 10,790 s	Background asymmetry factor = 0.1459, background length = 10,790 s
2671		Background length = 10,790 s
2673	Frequency range = 60–4000 Hz, error region = 1°	

Note. When no value is speci ed, the search was run with the default parameters, including frequency ranging from 50 to 4000 Hz, a symmetric background window 10,800 s in length, and a 0° error region. The background asymmetry factor is de ned as the fraction of the background time before the burst time, with 0.5 corresponding to a symmetric background. The error region is de ned as the 1 uncertainty in the sky position of the source. Using a nonzero error region on a point source can sometimes optimize the $h_{\rm rss}$ and $E_{\rm GW}$ upper limits because it counters the effects of the Earth s rotation during the on-source window.

Table 6
$h_{\rm rss}^{50\%}$ and $E_{\rm GW}^{50\%}$ for the Most Sensitive Burst from SGR 1935+2154 for Each Injected Waveform in the Centered and Delayed On-source Windows of the Short-duration Search

Injection Type	Frequency	Duration	Centered 8 s)			Delayed 500 s)		
	Hz)	τ ms)	Burst	$h_{\rm rss}^{50\%}$ Hz ^{1} ^{2})	$E_{\rm GW}^{50\%}$ $\frac{d^2}{(9\ {\rm kpc})^2}$ erg)	Burst	$h_{\rm rss}^{50\%}$ Hz ^{1} ^{2})	$E_{\rm GW}^{50\%}$ $\frac{d^2}{(9\ {\rm kpc})^2}$ erg)
Sine-Gaussian	70	14.3	2655	7.3×10^{-23}	3.2×10^{43}	2656	8.5×10^{-23}	4.4×10^{43}
Sine-Gaussian	90	11.1	2668	5.8×10^{-23}	3.3×10^{43}	2656	7.4×10^{-23}	5.5×10^{43}
Sine-Gaussian	145	6.89	2668	5.7×10^{-23}	8.4×10^{43}	2656	6.6×10^{-23}	1.1×10^{44}
Sine-Gaussian	290	3.45	2655	5.8×10^{-23}	3.5×10^{44}	2656	6.7×10^{-23}	4.7×10^{44}
Sine-Gaussian	1100	0.909	2655	1.3×10^{-22}	2.6×10^{46}	2656	1.5×10^{-22}	3.4×10^{46}
Sine-Gaussian	1600	0.625	2655	1.9×10^{-22}	1.1×10^{47}	2656	2.2×10^{-22}	1.6×10^{47}
Sine-Gaussian	2020	0.495	2655	2.4×10^{-22}	3.0×10^{47}	2656	2.9×10^{-22}	4.3×10^{47}
Sine-Gaussian	2600	0.385	2655	3.3×10^{-22}	9.2×10^{47}	2656	4.0×10^{-22}	1.3×10^{48}
Sine-Gaussian	3100	0.323	2655	4.1×10^{-22}	2.0×10^{48}	2652	5.2×10^{-22}	3.1×10^{48}
Sine-Gaussian	3560	0.281	2655	5.1×10^{-22}	4.0×10^{48}	2652	6.2×10^{-22}	6.0×10^{48}
Sine-Gaussian	1600	0.625	2655	1.1×10^{-22}	3.8×10^{46}	2656	1.3×10^{-22}	5.2×10^{46}
Sine-Gaussian	2020	0.495	2655	1.4×10^{-22}	9.6×10^{46}	2656	1.7×10^{-22}	1.4×10^{47}
Ringdown	1590	100	2655	1.9×10^{-22}	1.1×10^{47}			
Ringdown	1590	200	2655	1.8×10^{-22}	9.6×10^{46}			
Ringdown	1500	100	2668	2.5×10^{-22}	1.8×10^{47}			
Ringdown	1500	200	2668	2.3×10^{-22}	1.5×10^{47}			
Ringdown	2020	100	2655	2.2×10^{-22}	2.4×10^{47}			
Ringdown	2020	200	2655	2.2×10^{-22}	2.3×10^{47}			
WNB	100–200	11	2668	3.8×10^{-23}	1.0×10^{44}	2656	4.1×10^{-23}	1.2×10^{44}
WNB	100–200	100	2668	5.3×10^{-23}	2.0×10^{44}	2656	6.1×10^{-23}	2.7×10^{44}
WNB	100–1000	11	2655	6.7×10^{-23}	5.1×10^{45}	2656	7.5×10^{-23}	6.4×10^{45}
WNB	100–1000	100	2655	1.1×10^{-22}	1.5×10^{46}	2656	1.5×10^{-22}	2.4×10^{46}

Note. The energy is calculated assuming a distance of 9 kpc. Taking into account the uncertainty on the distance to SGR 1935+2154 given in the caption of Table 1, the energies could scale by a factor ranging from 0.52 to 1.6. All waveforms are elliptically polarized, except those denoted by an " ," which have circular polarization, and the WNBs, which are unpolarized.

This table is available in machine-readable form.)

Table 7

$h_{\rm rss}^{50\%}$ and $E_{\rm GW}^{50\%}$ for the Most Sensitive Burst from Swift J1818.0 1607 for Each Injected Waveform in the Centered and Delayed On-source Windows of the Short-duration Search

Injection Type	Frequency	Duration	Centered 8 s)			Delayed 500 s)		
	Hz)	τ ms)	Burst	$h_{\rm rss}^{50\%}$ Hz ^{1} ^{2})	$E_{\rm GW}^{50\%}$ $\frac{d^2}{(8.1\ {\rm kpc})^2}$ erg)	Burst	$h_{\rm rss}^{50\%}$ Hz ^{1} ^{2})	$E_{\rm GW}^{50\%}$ $\frac{d^2}{(8.1\ {\rm kpc})^2}$ erg)
Sine-Gaussian	70	14.3	2674	6.9×10^{23}	2.3×10^{43}	2673	9.2×10^{23}	4.1×10^{43}
Sine-Gaussian	90	11.1	2674	6.1×10^{23}	3.0×10^{43}	2673	8.7×10^{23}	6.1×10^{43}
Sine-Gaussian	145	6.89	2674	5.7×10^{23}	6.9×10^{43}	2674	8.5×10^{23}	1.5×10^{44}
Sine-Gaussian	290	3.45	2674	5.9×10^{23}	3.0×10^{44}	2674	9.1×10^{23}	6.9×10^{44}
Sine-Gaussian	1100	0.909	2674	1.3×10^{22}	2.1×10^{46}	2674	2.0×10^{22}	4.8×10^{46}
Sine-Gaussian	1600	0.625	2674	2.0×10^{22}	1.0×10^{47}	2674	2.9×10^{22}	2.1×10^{47}
Sine-Gaussian	2020	0.495	2674	2.7×10^{22}	3.0×10^{47}	2674	3.9×10^{22}	6.1×10^{47}
Sine-Gaussian	2600	0.385	2674	3.5×10^{22}	8.2×10^{47}	2674	4.9×10^{22}	1.6×10^{48}
Sine-Gaussian	3100	0.323	2674	4.4×10^{22}	1.8×10^{48}	2674	6.1×10^{22}	3.5×10^{48}
Sine-Gaussian	3560	0.281	2674	5.3×10^{22}	3.5×10^{48}	2674	7.1×10^{22}	6.3×10^{48}
Sine-Gaussian	1600	0.625	2674	1.2×10^{22}	3.5×10^{46}	2674	1.7×10^{22}	7.4×10^{46}
Sine-Gaussian	2020	0.495	2674	1.5×10^{22}	9.0×10^{46}	2674	2.1×10^{22}	1.8×10^{47}
Ringdown	1590	100	2674	2.1×10^{22}	1.1×10^{47}			
Ringdown	1590	200	2674	2.1×10^{22}	1.1×10^{47}			
Ringdown	1500	100	2673	2.6×10^{22}	1.5×10^{47}			
Ringdown	1500	200	2673	2.6×10^{22}	1.5×10^{47}			
Ringdown	2020	100	2674	2.6×10^{22}	2.6×10^{47}			
Ringdown	2020	200	2674	2.5×10^{22}	2.5×10^{47}			
WNB	100–200	11	2674	3.7×10^{23}	8.1×10^{43}	2673	5.6×10^{23}	1.8×10^{44}
WNB	100–200	100	2674	5.3×10^{23}	1.6×10^{44}	2673	7.8×10^{23}	3.5×10^{44}
WNB	100–1000	11	2674	7.0×10^{23}	4.5×10^{45}	2674	1.0×10^{22}	9.4×10^{45}
WNB	100–1000	100	2674	1.2×10^{22}	1.3×10^{46}	2674	1.8×10^{22}	3.1×10^{46}

Note. The energy is calculated assuming a distance of 8.1 kpc, the most conservative value in the range of accepted distances. Taking into account the distance range to Swift J1818.0 1607 given in the caption of Table 1, the energies could scale by a factor as low as 0.35. All waveforms are elliptically polarized, except those denoted by an " ," which have circular polarization, and the WNBs, which are unpolarized.

This table is available in machine-readable form.)

Table 8

$h_{\rm rss}^{50\%}$ and $E_{\rm GW}^{50\%}$ for the Most Sensitive Burst from the Unknown Source for Each Injected Waveform in the Centered and Delayed On-source Windows of the Short-duration Search

Injection Type	Frequency	Duration	Centered 8 s)			Delayed 500 s)		
	Hz)	τ ms)	Burst	$h_{\rm rss}^{50\%}$ Hz ^{1} ^{2})	$E_{\rm GW}^{50\%}$ $\frac{d^2}{(3.8\ {\rm kpc})^2}$ erg)	Burst	$h_{\rm rss}^{50\%}$ Hz ^{1} ^{2})	$E_{\rm GW}^{50\%}$ $\frac{d^2}{(3.8\ {\rm kpc})^2}$ erg)
Sine-Gaussian	70	14.3	2669	4.2×10^{23}	1.9×10^{42}	2669	5.0×10^{23}	2.7×10^{42}
Sine-Gaussian	90	11.1	2669	4.0×10^{23}	2.8×10^{42}	2669	4.6×10^{23}	3.8×10^{42}
Sine-Gaussian	145	6.89	2669	3.3×10^{23}	5.1×10^{42}	2669	3.9×10^{23}	7.0×10^{42}
Sine-Gaussian	290	3.45	2669	3.6×10^{23}	2.4×10^{43}	2669	4.1×10^{23}	3.1×10^{43}
Sine-Gaussian	1100	0.909	2669	7.7×10^{23}	1.6×10^{45}	2669	8.8×10^{23}	2.1×10^{45}
Sine-Gaussian	1600	0.625	2669	1.1×10^{22}	7.1×10^{45}	2670	1.3×10^{22}	9.5×10^{45}
Sine-Gaussian	2020	0.495	2669	1.5×10^{22}	1.9×10^{46}	2669	1.7×10^{22}	2.5×10^{46}
Sine-Gaussian	2600	0.385	2669	2.0×10^{22}	5.9×10^{46}	2669	2.4×10^{22}	8.8×10^{46}
Sine-Gaussian	3100	0.323	2669	2.5×10^{22}	1.3×10^{47}	2670	3.0×10^{22}	1.9×10^{47}
Sine-Gaussian	3560	0.281	2669	2.9×10^{22}	2.3×10^{47}	2670	4.0×10^{22}	4.5×10^{47}
Sine-Gaussian	1600	0.625	2669	6.2×10^{23}	2.2×10^{45}	2669	7.7×10^{23}	3.3×10^{45}
Sine-Gaussian	2020	0.495	2669	8.6×10^{23}	6.6×10^{45}	2670	9.5×10^{23}	8.1×10^{45}
Ringdown	1590	100	2670	1.1×10^{22}	6.8×10^{45}			
Ringdown	1590	200	2670	1.1×10^{22}	7.0×10^{45}			
Ringdown	1500	100	2669	1.8×10^{22}	1.6×10^{46}			
Ringdown	1500	200	2671	2.7×10^{22}	3.6×10^{46}			
Ringdown	2020	100	2670	1.3×10^{22}	1.6×10^{46}			
Ringdown	2020	200	2670	1.3×10^{22}	1.6×10^{46}			
WNB	100–200	11	2669	2.2×10^{23}	6.2×10^{42}	2669	2.5×10^{23}	8.2×10^{42}
WNB	100–200	100	2669	3.2×10^{23}	1.3×10^{43}	2670	3.6×10^{23}	1.7×10^{43}
WNB	100–1000	11	2669	3.9×10^{23}	3.0×10^{44}	2669	4.6×10^{23}	4.4×10^{44}
WNB	100–1000	100	2669	7.1×10^{23}	1.0×10^{45}	2669	8.2×10^{23}	1.4×10^{45}

Note. The energy is calculated assuming a distance of 3.8 kpc. Taking into account the uncertainty on the distance to 1 RXS J170849 given in the caption of Table 1, the energies could scale by a factor ranging from 0.75 to 1.3. All waveforms are elliptically polarized, except those denoted by an " ," which have circular polarization, and the WNBs, which are unpolarized.

This table is available in machine-readable form.)

Table 9

$h_{\rm rss}^{90\%}$ and $E_{\rm GW}^{90\%}$ for the Most Sensitive Burst from SGR 1935+2154 for Each Injected Waveform in the Centered and Delayed On-source Windows of the Short-duration Search

Injection Type	Frequency	Duration	Centered 8 s)			Delayed 500 s)		
	Hz)	τ ms)	Burst	$h_{\rm rss}^{90\%}$ Hz ^{1} ^{2})	$E_{\rm GW}^{90\%}$ $\frac{d^2}{(9\ {\rm kpc})^2}$ erg)	Burst	$h_{\rm rss}^{90\%}$ Hz ^{1} ^{2})	$E_{\rm GW}^{90\%}$ $\frac{d^2}{(9\ {\rm kpc})^2}$ erg)
Sine-Gaussian	70	14.3	2655	1.6×10^{22}	1.5×10^{44}	2656	1.9×10^{22}	2.1×10^{44}
Sine-Gaussian	90	11.1	2655	1.4×10^{22}	1.9×10^{44}	2656	1.7×10^{22}	2.9×10^{44}
Sine-Gaussian	145	6.89	2655	1.0×10^{22}	2.8×10^{44}	2655	1.4×10^{22}	5.1×10^{44}
Sine-Gaussian	290	3.45	2655	1.3×10^{22}	1.7×10^{45}	2656	1.4×10^{22}	2.0×10^{45}
Sine-Gaussian	1100	0.909	2655	2.8×10^{22}	1.2×10^{47}	2656	3.2×10^{22}	1.5×10^{47}
Sine-Gaussian	1600	0.625	2655	4.2×10^{22}	5.5×10^{47}	2656	5.1×10^{22}	8.1×10^{47}
Sine-Gaussian	2020	0.495	2655	4.9×10^{22}	1.2×10^{48}	2652	6.6×10^{22}	2.2×10^{48}
Sine-Gaussian	2600	0.385	2655	7.0×10^{22}	4.0×10^{48}	2656	8.7×10^{22}	6.3×10^{48}
Sine-Gaussian	3100	0.323	2655	8.1×10^{22}	7.8×10^{48}	2652	1.1×10^{21}	1.3×10^{49}
Sine-Gaussian	3560	0.281	2656	1.1×10^{21}	2.0×10^{49}	2652	1.5×10^{21}	3.3×10^{49}
Sine-Gaussian	1600	0.625	2655	1.5×10^{22}	7.0×10^{46}	2656	1.9×10^{22}	1.1×10^{47}
Sine-Gaussian	2020	0.495	2655	2.0×10^{22}	2.1×10^{47}	2656	2.3×10^{22}	2.6×10^{47}
Ringdown	1590	100	2655	3.9×10^{22}	4.7×10^{47}			
Ringdown	1590	200	2655	3.9×10^{22}	4.8×10^{47}			
Ringdown	1500	100	2655	6.5×10^{22}	1.2×10^{48}			
Ringdown	1500	200	2668	6.3×10^{22}	1.1×10^{48}			
Ringdown	2020	100	2655	4.5×10^{22}	1.0×10^{48}			
Ringdown	2020	200	2655	4.8×10^{22}	1.2×10^{48}			
WNB	100–200	11	2655	6.4×10^{23}	2.9×10^{44}	2656	7.6×10^{23}	4.1×10^{44}
WNB	100–200	100	2655	8.3×10^{23}	4.9×10^{44}	2656	8.7×10^{23}	5.4×10^{44}
WNB	100–1000	11	2655	9.0×10^{23}	9.2×10^{45}	2656	1.1×10^{22}	1.4×10^{46}
WNB	100–1000	100	2655	1.7×10^{22}	3.3×10^{46}	2656	1.9×10^{22}	4.0×10^{46}

Note. The energy is calculated assuming a distance of 9 kpc. Taking into account the uncertainty on the distance to SGR 1935+2154 given in Table 1, the energies could scale by a factor ranging from 0.52 to 1.6. All waveforms are elliptically polarized, except those denoted by an " ," which have circular polarization, and the WNBs, which are unpolarized.

This table is available in machine-readable form.)

Table 10

$h_{\rm rss}^{90\%}$ and $E_{\rm GW}^{90\%}$ for the Most Sensitive Burst from Swift J1818.0 1607 for Each Injected Waveform in the Centered and Delayed On-source Windows of the Short-duration Search

Injection Type	Frequency	Duration	Centered 8 s)			Delayed 500 s)		
	Hz)	τ ms)	Burst	$h_{\rm rss}^{90\%}$ Hz ^{1} ^{2})	$E_{\rm GW}^{90\%}$ $\frac{d^2}{(8.1\ {\rm kpc})^2}$ erg)	Burst	$h_{\rm rss}^{90\%}$ Hz ^{1} ^{2})	$E_{\rm GW}^{90\%}$ $\frac{d^2}{(8.1\ {\rm kpc})^2}$ erg)
Sine-Gaussian	70	14.3	2674	1.4×10^{22}	9.4×10^{43}	2673	2.1×10^{22}	2.1×10^{44}
Sine-Gaussian	90	11.1	2674	1.3×10^{22}	1.4×10^{44}	2673	1.8×10^{22}	2.7×10^{44}
Sine-Gaussian	145	6.89	2674	1.3×10^{22}	3.6×10^{44}	2673	2.0×10^{22}	8.2×10^{44}
Sine-Gaussian	290	3.45	2674	1.3×10^{22}	1.4×10^{45}	2674	2.0×10^{22}	3.4×10^{45}
Sine-Gaussian	1100	0.909	2674	3.4×10^{22}	1.4×10^{47}	2674	4.8×10^{22}	2.7×10^{47}
Sine-Gaussian	1600	0.625	2674	4.8×10^{22}	5.9×10^{47}	2674	7.5×10^{22}	1.4×10^{48}
Sine-Gaussian	2020	0.495	2674	6.1×10^{22}	1.5×10^{48}	2674	8.8×10^{22}	3.1×10^{48}
Sine-Gaussian	2600	0.385	2674	7.3×10^{22}	3.6×10^{48}	2674	1.0×10^{21}	7.1×10^{48}
Sine-Gaussian	3100	0.323	2674	9.8×10^{22}	9.2×10^{48}	2674	1.4×10^{21}	1.8×10^{49}
Sine-Gaussian	3560	0.281	2674	1.1×10^{21}	1.5×10^{49}	2674	1.6×10^{21}	3.1×10^{49}
Sine-Gaussian	1600	0.625	2674	1.6×10^{22}	6.9×10^{46}	2674	2.2×10^{22}	1.3×10^{47}
Sine-Gaussian	2020	0.495	2674	2.2×10^{22}	2.0×10^{47}	2674	3.1×10^{22}	3.9×10^{47}
Ringdown	1590	100	2674	4.5×10^{22}	5.1×10^{47}			
Ringdown	1590	200	2674	4.6×10^{22}	5.2×10^{47}			
Ringdown	1500	100	2673	6.6×10^{22}	9.8×10^{47}			
Ringdown	1500	200	2673	6.2×10^{22}	8.5×10^{47}			
Ringdown	2020	100	2674	5.4×10^{22}	1.2×10^{48}			
Ringdown	2020	200	2674	5.2×10^{22}	1.1×10^{48}			
WNB	100–200	11	2673	7.9×10^{23}	3.6×10^{44}	2673	9.7×10^{23}	5.4×10^{44}
WNB	100–200	100	2674	8.2×10^{23}	3.9×10^{44}	2673	1.2×10^{22}	9.0×10^{44}
WNB	100–1000	11	2674	1.0×10^{22}	9.4×10^{45}	2674	1.6×10^{22}	2.4×10^{46}
WNB	100–1000	100	2674	1.8×10^{22}	2.9×10^{46}	2674	2.8×10^{22}	7.4×10^{46}

Note. The energy is calculated assuming a distance of 8.1 kpc, the most conservative value in the range of accepted distances. Taking into account the distance range to Swift J1818.0 1607 given in the caption of Table 1, the energies could scale by a factor as low as 0.35. All waveforms are elliptically polarized, except those denoted by an " ," which have circular polarization, and the WNBs, which are unpolarized.

This table is available in machine-readable form.)

Table 11

$h_{\rm rss}^{90\%}$ and $E_{\rm GW}^{90\%}$ for the Most Sensitive Burst from the Unknown Source for Each Injected Waveform in the Centered and Delayed On-source Windows of the Short-duration Search

Injection Type	Frequency	Duration	Centered 8 s)			Delayed 500 s)		
	Hz)	τ ms)	Burst	$h_{\rm rss}^{90\%}$ Hz $^{1\ 2}$)	$E_{\rm GW}^{90\%}$ $\frac{d^2}{(3.8\ {\rm kpc})^2}$ erg)	Burst	$h_{\rm rss}^{90\%}$ Hz $^{1\ 2}$)	$E_{\rm GW}^{90\%}$ $\frac{d^2}{(3.8\ {\rm kpc})^2}$ erg)
Sine-Gaussian	70	14.3	2669	9.2×10^{23}	9.1×10^{42}	2669	1.1×10^{22}	1.2×10^{43}
Sine-Gaussian	90	11.1	2669	8.7×10^{23}	1.3×10^{43}	2669	9.9×10^{23}	1.7×10^{43}
Sine-Gaussian	145	6.89	2669	6.5×10^{23}	2.0×10^{43}	2669	7.7×10^{23}	2.7×10^{43}
Sine-Gaussian	290	3.45	2670	7.4×10^{23}	1.0×10^{44}	2669	8.6×10^{23}	1.4×10^{44}
Sine-Gaussian	1100	0.909	2669	1.4×10^{22}	5.5×10^{45}	2669	1.6×10^{22}	6.8×10^{45}
Sine-Gaussian	1600	0.625	2669	2.2×10^{22}	2.6×10^{46}	2669	2.4×10^{22}	3.1×10^{46}
Sine-Gaussian	2020	0.495	2669	3.0×10^{22}	8.0×10^{46}	2669	3.4×10^{22}	1.0×10^{47}
Sine-Gaussian	2600	0.385	2669	3.7×10^{22}	2.1×10^{47}	2670	5.1×10^{22}	3.8×10^{47}
Sine-Gaussian	3100	0.323	2669	4.8×10^{22}	4.8×10^{47}	2669	6.9×10^{22}	1.0×10^{48}
Sine-Gaussian	3560	0.281	2669	6.1×10^{22}	1.0×10^{48}	2670	1.4×10^{21}	5.8×10^{48}
Sine-Gaussian	1600	0.625	2669	9.1×10^{23}	4.6×10^{45}	2670	1.0×10^{22}	6.0×10^{45}
Sine-Gaussian	2020	0.495	2669	1.1×10^{22}	1.1×10^{46}	2670	1.4×10^{22}	1.8×10^{46}
Ringdown	1590	100	2670	2.3×10^{22}	3.0×10^{46}			
Ringdown	1590	200	2670	2.2×10^{22}	2.6×10^{46}			
Ringdown	1500	100	2671	4.7×10^{22}	1.1×10^{47}			
Ringdown	1500	200	2671	6.0×10^{22}	1.8×10^{47}			
Ringdown	2020	100	2670	2.8×10^{22}	6.9×10^{46}			
Ringdown	2020	200	2670	2.9×10^{22}	7.6×10^{46}			
WNB	100–200	11	2669	3.6×10^{23}	1.7×10^{43}	2669	4.1×10^{23}	2.1×10^{43}
WNB	100–200	100	2669	4.2×10^{23}	2.2×10^{43}	2669	5.3×10^{23}	3.6×10^{43}
WNB	100–1000	11	2669	5.6×10^{23}	6.4×10^{44}	2669	6.0×10^{23}	7.4×10^{44}
WNB	100–1000	100	2669	8.9×10^{23}	1.6×10^{45}	2669	1.2×10^{22}	2.9×10^{45}

Note. The energy is calculated assuming a distance of 3.8 kpc. Taking into account the uncertainty on the distance to 1 RXS J170849 given in Table 1, the energies could scale by a factor ranging from 0.75 to 1.3. All waveforms are elliptically polarized, except those denoted by an " ," which have circular polarization, and the WNBs, which are unpolarized.

This table is available in machine-readable form.)

Table 12

Upper Limits for $h_{\rm rss}$ and $E_{\rm GW}$ for Half Sine-Gaussian and Ringdown Waveforms for Burst 2656 from SGR 1935+2154 for the Long-duration Search

Frequency Hz)	τ s)	Detection Ef ciency	Half Sine-Gaussian		Ringdown	
			$h_{\rm rss}$ Hz $^{1\ 2}$)	$E_{\rm GW}$ erg)	$h_{\rm rss}$ Hz $^{1\ 2}$)	$E_{\rm GW}$ erg)
55	150	50	1.4×10^{22}	7.3×10^{43}	1.4×10^{22}	7.8×10^{43}
		90	1.7×10^{22}	1.0×10^{44}	1.7×10^{22}	1.1×10^{44}
	400	50	1.6×10^{22}	9.3×10^{43}	1.7×10^{22}	1.0×10^{44}
		90	1.8×10^{22}	1.3×10^{44}	1.9×10^{22}	1.4×10^{44}
150	150	50	9.7×10^{23}	2.6×10^{44}	1.0×10^{22}	2.9×10^{44}
		90	1.2×10^{22}	3.8×10^{44}	1.2×10^{22}	4.1×10^{44}
	400	50	1.0×10^{22}	2.9×10^{44}	1.1×10^{22}	3.3×10^{44}
		90	1.2×10^{22}	3.8×10^{44}	1.3×10^{22}	4.4×10^{44}
450	150	50	8.7×10^{23}	1.9×10^{45}	9.3×10^{23}	2.1×10^{45}
		90	1.1×10^{22}	2.8×10^{45}	1.1×10^{22}	3.2×10^{45}
-	400	50	1.1×10^{22}	3.1×10^{45}	1.2×10^{22}	3.5×10^{45}
		90	1.4×10^{22}	4.7×10^{45}	1.4×10^{22}	5.0×10^{45}
750	150	50	1.4×10^{22}	1.4×10^{46}	1.5×10^{22}	1.7×10^{46}
		90	1.7×10^{22}	1.9×10^{46}	1.8×10^{22}	2.2×10^{46}
	400	50	1.6×10^{22}	1.7×10^{46}	1.7×10^{22}	1.9×10^{46}
		90	1.8×10^{22}	2.2×10^{46}	1.9×10^{22}	2.6×10^{46}
1550	150	50	3.8×10^{22}	4.2×10^{47}	3.8×10^{22}	4.2×10^{47}
		90	4.4×10^{22}	5.8×10^{47}	4.6×10^{22}	6.2×10^{47}
	400	50	3.9×10^{22}	4.4×10^{47}	4.1×10^{22}	5.0×10^{47}
		90	4.9×10^{22}	7.0×10^{47}	5.1×10^{22}	7.7×10^{47}

Note. Burst 2656 had the lowest upper limits for 50 detection ef ciency. The value of $E_{\rm GW}$ is proportional to d^2, where d is the distance to the source. The energies are calculated assuming a distance of 9 kpc the distance to SGR 1935+2154 is 9.0 ± 2.5 kpc; Zhong et al. 2020); given the uncertainty on the distance to SGR 1935 +2154, the energies could scale by a factor ranging from 0.52 to 1.6.

This table is available in machine-readable form.)

Table 13
Upper Limits for $h_{\rm rss}$ and $E_{\rm GW}$ for Half Sine-Gaussian and Ringdown Waveforms for Swift J1818.0 1607 for the Long-duration Search

Frequency Hz)	τ s)	Detection Ef ciency	Half Sine-Gaussian		Ringdown	
			$h_{\rm rss}$ Hz ^{1} ^{2})	$E_{\rm GW}$ erg)	$h_{\rm rss}$ Hz ^{1} ^{2})	$E_{\rm GW}$ erg)
55	150	50	1.6×10^{22}	7.9×10^{43}	1.7×10^{22}	8.8×10^{43}
		90	2.1×10^{22}	1.3×10^{44}	2.2×10^{22}	1.5×10^{44}
	400	50	1.9×10^{22}	1.1×10^{44}	2.0×10^{22}	1.2×10^{44}
		90	2.2×10^{22}	1.5×10^{44}	2.3×10^{22}	1.6×10^{44}
150	150	50	1.3×10^{22}	3.8×10^{44}	1.4×10^{22}	4.2×10^{44}
		90	1.7×10^{22}	6.1×10^{44}	1.7×10^{22}	6.7×10^{44}
	400	50	1.4×10^{22}	4.2×10^{44}	1.4×10^{22}	4.5×10^{44}
		90	1.7×10^{22}	6.2×10^{44}	1.7×10^{22}	6.7×10^{44}
450	150	50	1.2×10^{22}	3.0×10^{45}	1.3×10^{22}	3.5×10^{45}
		90	1.5×10^{22}	4.5×10^{45}	1.6×10^{22}	5.1×10^{45}
	400	50	1.5×10^{22}	4.5×10^{45}	1.6×10^{22}	5.0×10^{45}
		90	1.8×10^{22}	6.6×10^{45}	1.9×10^{22}	7.5×10^{45}
750	150	50	2.0×10^{22}	2.3×10^{46}	2.2×10^{22}	2.7×10^{46}
		90	2.5×10^{22}	3.4×10^{46}	2.7×10^{22}	4.0×10^{46}
	400	50	2.2×10^{22}	2.8×10^{46}	2.4×10^{22}	3.2×10^{46}
		90	2.7×10^{22}	4.1×10^{46}	2.8×10^{22}	4.4×10^{46}
1550	150	50	5.7×10^{22}	7.8×10^{47}	5.6×10^{22}	7.5×10^{47}
		90	6.8×10^{22}	1.1×10^{48}	6.4×10^{22}	9.9×10^{47}
	400	50	4.9×10^{22}	5.7×10^{47}	5.0×10^{22}	6.0×10^{47}
		90	5.6×10^{22}	7.5×10^{47}	5.7×10^{22}	7.9×10^{47}

Note. The upper limits are given for burst 2673 for 55 Hz waveforms with $\tau = 400$ s and given for burst 2674 for all other waveforms; these bursts had the lowest upper limits for 50 detection ef ciency for these respective waveforms. The energy upper limits are calculated conservatively assuming a distance of 8.1 kpc for Swift J1818.0–1607, although we note that these upper limits could scale by a factor as low as 0.35 if the source is at the close end of its distance range 4.8 kpc).

This table is available in machine-readable form.)

corresponding $h_{\rm rss}^{50\%}$. In Table 4 we provide $h_{\rm rss}^{90\%}$ and $E_{\rm GW}^{90\%}$ for two waveforms that best model the *f*-mode for each burst. Finally, in Appendix D we give for each waveform the lowest value of $h_{\rm rss}^{50\%}$ and $E_{\rm GW}^{50\%}$ considering all bursts from SGR 1935 +2154, Swift J1818.0 1607, and the unknown source for each waveform in Tables 6–8, respectively. The lowest values of $h_{\rm rss}^{90\%}$ and $E_{\rm GW}^{90\%}$ are in Tables 9–11.

3.2. Long duration Search Results

All bursts from Table 1 have been analyzed by the long-duration search except the three bursts from the unknown source s). The search results for each burst are shown in Table 3, which lists the FBS of the most signi cant cluster for each burst. No interesting cluster has been found as the most signi cant cluster has an FBS of 0.02. Figure 5 compares the most signi cant on-source cluster to the corresponding background distribution for each burst.

As in the O2 search Abbott et al. 2019), two families of waveforms, half sine-Gaussians and ringdowns, are injected at ve frequencies 55, 150, 450, 750, and 1550 Hz) and two damping times 150 and 400 s). The lowest value of $h_{\rm rss}^{50\%}$ comes from burst 2656, identi ed with SGR 1935+2154, which has the largest sum squared antenna factors. The results for burst 2656 indicate an improvement in $h_{\rm rss}^{50\%}$ from O2 to O3, ranging from a factor of 1.25–2, which follow roughly the detectors sensitivity improvement between the runs, although it also depends on additional considerations such as the detector antenna factors at the time of the burst. The half sine-Gaussian $h_{\rm rss}^{50\%}$ values for burst 2656 are plotted against representative sensitivity curves of LHO, LLO, and Virgo during O3 Buikema et al. 2020; Kissel 2020; Verkindt 2021) in Figure 6, along with $h_{\rm rss}^{50\%}$ from O2 as a comparison.

In Figure 7, we plot $h_{\rm rss}^{50\%}$ and $h_{\rm rss}^{90\%}$ for bursts 2656 and 2674 2673 for waveforms at 55 Hz with a damping time of 400 s for Swift J1818.0 1607), which provide the lowest values at 50 detection ef ciency among all bursts emitted by SGR 1935 +2154 and Swift J1818.0 1607, respectively. Tables 12 and 13 provide the 50 and 90 detection ef ciency upper limits on $h_{\rm rss}$ and $E_{\rm GW}$ for these same bursts for each waveform.

4. Conclusions

In this study, we search for and nd no evidence of gravitational waves coincident with 16 bursts 13 magnetar short bursts and three electromagnetic bursts thought to be magnetar short bursts but with no identi ed source object) during O3. We search for both short-duration signals produced by excited *f*-modes in the neutron star s core, and for long-duration signals that may be generated from core buoyancy or Alfvén modes. The detection statistics for both the short-duration and long-duration searches are consistent with background noise: the most signi cant cluster found that was not clearly identi ed as an instrumental artifact has a *p*-value of 0.00857; a cluster with this *p*-value or lower has a 29 probability of appearing in one or more of the 40 searches performed over all of the bursts under the null hypothesis.

For bursts with known sources, the lowest $E_{\rm GW}^{50\%}$ in the short-duration search for waveforms with frequencies from 1500 to 2020 Hz ranged from 4×10^{46} to 6×10^{47} erg. The $E_{\rm GW}^{90\%}$

values of these waveforms ranged from 7×10^{46} erg to 3×10^{48} erg. In Tables 6–8, we report the lowest $h_{\rm rss}^{50\%}$ values over all bursts for each waveform; the lowest $h_{\rm rss}^{90\%}$ values are given in Tables 9–11. The only injected waveforms with exactly the same parameters as the O2 search are the WNBs; we see a factor of improvement in $h_{\rm rss}^{50\%}$ of 1.1 for the 100 200 Hz, 11 ms WNB. To obtain an approximate metric of improvement, we compare injected circularly polarized sine-Gaussian waveforms at 1600 Hz and 2020 Hz from O3 to sine-Gaussian waveforms of 1500 Hz and 2000 Hz in O2 and see factors of improvement of 1.5 and 1.7 in $h_{\rm rss}^{50\%}$, respectively. This is roughly in agreement with the detector s sensitivity improvement between O2 and O3.

The long-duration search sets the lowest upper limits on long-duration gravitational-wave emission from magnetar bursts to date. We report the long-duration upper limits for each waveform for the burst which had the lowest $h_{\rm rss}$ values at 50 detection ef ciency in Table 12 for SGR 1935+2154 and in Table 13 for Swift J1818.0 1607. Of these results, the half sine-Gaussian waveform injected into burst 2656 from SGR 1935+2154) at 450 Hz produced the lowest $h_{\rm rss}^{90\%}$ upper limit of $1.1 \times 10^{-22}/\sqrt{\rm Hz}$. This corresponds to a gravitational-wave energy of 2.8×10^{45} erg. The lowest $E_{\rm GW}^{90\%}$ values from these results for SGR 1935+2154 and Swift J1818.0–1607 are measured by the sine-Gaussian waveform at 55 Hz, and are 1.0×10^{44} erg and $0.5–1.3 \times 10^{44}$ erg, respectively. The energy upper limits scale with the distance squared to the source, and here we give the full range of $E_{\rm GW}^{90\%}$ for Swift J1818.0–1607 that corresponds to the distance range of 4.9–8.1 kpc.

We also place upper limits on the ratio of gravitational-wave energy to electromagnetic energy emitted by SGR 1935+2154 the only source whose bursts have published electromagnetic fluences) using the calculated isotropic electromagnetic energies given in Table 1. For the short-duration search, the most constraining ratio when taking the gravitational-wave energy from the 1590 Hz, 100 ms ringdown waveform is $E_{\rm GW}^{90\%}/E_{\rm EM}^{\rm iso} = 3.0 \times 10^{7}$. For the long-duration search, the lowest ratio from burst 2656 is $E_{\rm GW}^{90\%}/E_{\rm EM}^{\rm iso} = 4.5 \times 10^{3}$, which comes from a half sine-Gaussian at 55 Hz with $\tau = 150$ s. These upper limits are less constraining than those of the 2004 giant flare from SGR 1806 20, which had $E_{\rm GW}^{90\%}/E_{\rm EM}^{\rm iso} = 9 \times 10^{4}$ for a 200 ms ringdown waveform at 1590 Hz Abbott et al. 2008a) and $E_{\rm GW}^{90\%}/E_{\rm EM}^{\rm iso} \approx 5$ for a band surrounding the 92.5 Hz QPO in the giant flare s tail Abbott et al. 2007, 2008a).

With the current sensitivities of the LIGO and Virgo detectors, we can now probe well below the potential energy budgets available to generate gravitational waves from catastrophic rearrangements of the star s internal magnetic eld Ioka 2001; Corsi & Owen 2011). However, even the lowest upper limits provided here are well above the expected gravitational-wave energy one would expect from f-mode emission from giant flares e.g., Levin 2007; Ciol & Rezzolla 2012; Zink et al. 2012), let alone the lower-energy bursts being considered here. As gravitational-wave observatories continue to improve in sensitivity, and more observatories such as KAGRA Akutsu et al. 2019) reach comparable sensitivity, searches for gravitational waves from magnetar bursts will eventually probe several orders of magnitude below the electromagnetic energy of giant flares, increasing the probability of a discovery of gravitational waves from magnetar flares.

Acknowledgments

This material is based upon work supported by NSF s LIGO Laboratory, which is a major facility fully funded by the National Science Foundation. The authors also gratefully acknowledge the support of the Science and Technology Facilities Council STFC) of the United Kingdom, the Max-Planck-Society MPS), and the State of Niedersachsen Germany for support of the construction of Advanced LIGO and construction and operation of the GEO 600 detector. Additional support for Advanced LIGO was provided by the Australian Research Council. The authors gratefully acknowledge the Italian Istituto Nazionale di Fisica Nucleare INFN), the French Centre National de la Recherche Scienti que CNRS) and the Netherlands Organization for Scienti c Research NWO), for the construction and operation of the Virgo detector and the creation and support of the EGO consortium. The authors also gratefully acknowledge research support from these agencies as well as by the Council of Scienti c and Industrial Research of India, the Department of Science and Technology, India, the Science & Engineering Research Board SERB), India, the Ministry of Human Resource Development, India, the Spanish Agencia Estatal de Investigación AEI), the Spanish Ministerio de Ciencia e Innovación and Ministerio de Universidades, the Conselleria de Fons Europeus, Universitat i Cultura and the Direcció General de Política Universitaria i Recerca del Govern de les Illes Balears, the Conselleria d Innovació Universitats, Ciència i Societat Digital de la Generalitat Valenciana and the CERCA Programme Generalitat de Catalunya, Spain, the National Science Centre of Poland and the European Union—European Regional Development Fund, Foundation for Polish Science FNP), the Swiss National Science Foundation SNSF), the Russian Foundation for Basic Research, the Russian Science Foundation, the European Commission, the European Social Funds ESF), the European Regional Development Funds ERDF), the Royal Society, the Scottish Funding Council, the Scottish Universities Physics Alliance, the Hungarian Scienti c Research Fund OTKA), the French Lyon Institute of Origins LIO), the Belgian Fonds de la Recherche Scienti que FRS-FNRS), Actions de Recherche Concertées ARC) and Fonds Wetenschappelijk Onderzoek—Vlaanderen FWO), Belgium, the Paris Ile-de-France Region, the National Research, Development and Innovation Of ce Hungary NKFIH), the National Research Foundation of Korea, the Natural Science and Engineering Research Council Canada, Canadian Foundation for Innovation CFI), the Brazilian Ministry of Science, Technology, and Innovations, the International Center for Theoretical Physics South American Institute for Fundamental Research ICTP-SAIFR), the Research Grants Council of Hong Kong, the National Natural Science Foundation of China NSFC), the Leverhulme Trust, the Research Corporation, the Ministry of Science and Technology MOST), Taiwan, the United States Department of Energy, and the Kavli Foundation. The authors gratefully acknowledge the support of the NSF, STFC, INFN, and CNRS for provision of computational resources.

This work was supported by MEXT, JSPS Leading-edge Research Infrastructure Program, JSPS Grant-in-Aid for Specially Promoted Research 26000005, JSPS Grant-in-Aid for Scienti c Research on Innovative Areas 2905 JP17H06358, JP17H06361, and JP17H06364), JSPS Core-to-Core Program A. Advanced Research Networks, JSPS Grant-in-Aid for Scienti c

Research S) 17H06133 and 20H05639, JSPS Grant-in-Aid for Transformative Research Areas A) 20A203: JP20H05854, the joint research program of the Institute for Cosmic Ray Research, University of Tokyo, National Research Foundation NRF), Computing Infrastructure Project of KISTI-GSDC, Korea Astronomy and Space Science Institute KASI), and Ministry of Science and ICT MSIT) in Korea, Academia Sinica AS), AS Grid Center ASGC) and the Ministry of Science and Technology MoST) in Taiwan under grants including AS-CDA-105-M06, Advanced Technology Center ATC) of NAOJ, and Mechanical Engineering Center of KEK.

The McGill Online Magnetar Catalog at https: www. physics.mcgill.ca ~pulsar magnetar main.html was very useful as a catalog with updated information on magnetars.

This project has made use of the data of the Interplanetary Network ssl.berkeley.edu ipn3 index.html), which was maintained by Kevin Hurley. We would like to remember all of the contributions Kevin made to many LIGO–Virgo–KAGRA searches over the years.

We would like to thank all of the essential workers who put their health at risk during the COVID-19 pandemic, without whom we would not have been able to complete this work.

Appendix A
Modi cations to the Parameters of the Short duration Search

It should be noted that the burst times are distributed such that the standard 3 hr symmetric background in the short-duration searches would in some cases include the time of the previous or subsequent burst. We mitigate this by either reducing the background length or adjusting the background asymmetry factor the fraction of background time before the burst) to optimize the amount of background data that could be used for each burst. Full details of these modi cations are provided in Table 5.

In addition to modifying the length and background asymmetry factor to exclude neighboring bursts, there are also modi cations to the search that we do in order to optimize the upper limits of $h_{\rm rss}^{50\%}$ and $h_{\rm rss}^{90\%}$ for each burst. These include vetoing events in speci c frequency bands that display high non-Gaussianity and introducing an error region around the source direction to adjust for the motion of the Earth during the on-source window. A full list of these changes is given in Table 5.

Appendix B
Data Removed from Long duration Search Windows

Data are required both before and after each pixel in the long-duration time–frequency map to estimate the pixel background see Thrane et al. 2011 for details). In this search, we use 18 s of data before and after each pixel, as was done in Quitzow-James 2016), Quitzow-James et al. 2017), and Abbott et al. 2019). Thus, any data removed from the long-duration on-source window include up to an additional 36 s, with 18 s both before and after the interval to be removed. We note that 1640 s of data are required for the full 1604 s long-duration on-source window.

Two on-source windows are missing data. One of these is the on-source window of burst 2651, which starts 87 s after the burst; since the on-source window starts 4 s before the burst and 18 s is needed to estimate the pixel background, the time–frequency map starts 109 s after the start of the on-source window 105 s after the burst). Data are available for the rst 1121 s of the on-source window of burst 2665, leading to the time–frequency map ending after 1103 s. The on-source windows for bursts 2652, 2660, and 2665 each had 8 s of data removed due to data quality issues, leading to gaps of 44 s in the time–frequency maps. As was done in previous searches including the O2 search; Abbott et al. 2019), noisy spectral lines, such as 60 Hz power-line harmonics, are identi ed and removed from the time–frequency maps for each detector pair. Of special note, 55 and 150 Hz are removed for the LHO Virgo detector pair and 150 Hz for LLO Virgo; thus, these detector pairs are not sensitive to injected waveforms in these respective frequencies. The Bezier curves for the clusters are generated identically to the other windows, with the missing times and data removed due to noisy lines) not included in the calculation of the cluster S N. The background segments are treated identically to their respective on-source windows.

Appendix C
Injected Waveforms and Upper Limit Calculations

For both short-duration and long-duration searches, we consider sine-Gaussian and ringdown waveforms whose plus +) and cross ×) polarizations are given respectively by

$$\begin{bmatrix} h_+^{\rm SG}(t) \\ h_\times^{\rm SG}(t) \end{bmatrix} = \frac{h_0}{\sqrt{2}} \begin{bmatrix} \frac{1+\cos^2\iota}{2} \times \cos(2\pi f_0 t) \\ \cos\iota \times \sin(2\pi f_0 t) \end{bmatrix} e^{-\frac{t^2}{\tau^2}}, \tag{C1}$$

and

$$\begin{bmatrix} h_+^{\rm RD}(t) \\ h_\times^{\rm RD}(t) \end{bmatrix} = \frac{h_0}{\sqrt{2}} \begin{bmatrix} \frac{1+\cos^2\iota}{2} \times \cos(2\pi f_0 t) \\ \cos\iota \times \sin(2\pi f_0 t) \end{bmatrix} e^{-\frac{t}{\tau}} \qquad \text{for t} > 0, \tag{C2}$$

where ι is the inclination angle and τ is the damping time. An injection is circularly polarized in the case where $\cos\iota$ is 1 or 1, linearly polarized when $\cos\iota = 0$, and elliptically polarized when $\cos\iota$ is between 1 and 1. All waveforms in the long-duration search half sine-Gaussians and ringdowns) have circular polarization. For the short-duration search, the ringdown and most of the sine-Gaussian waveforms are elliptically polarized so as not to assume a source orientation. The polarization angle around the line of sight to the source is set to zero for the long-duration search which results in an overall phase shift for circularly polarized waveforms), and is uniformly distributed from 0 to π for the waveforms in the short-duration search.

We calculate $E_{\rm GW}^{50\%}$ $E_{\rm GW}^{90\%}$) for the short-duration search from the corresponding $h_{\rm rss}^{50\%}$ $h_{\rm rss}^{90\%}$) using the rotating system emission formula in the narrow-band approximation given by Equation 17) of Sutton 2013)

$$E_{\rm GW} \approx \frac{2}{5}\frac{c^3\pi^2}{G} d^2 f_0^2 h_{\rm rss}^2, \tag{C3}$$

where d is the distance to the source and f_0 is the central frequency. We note that Equation 17) of Sutton 2013) is valid regardless of waveform polarization.

We calculate the $E_{\rm GW}^{50\%}$ and $E_{\rm GW}^{90\%}$ of the WNB waveforms using Equation 11) of Sutton 2013) for isotropic emission,

with correction factors to account for our waveforms being broadband. Speci cally, we use

$$E_{\rm GW} = 1.0370 \times \frac{c^3\pi^2}{G} d^2 f_0^2 h_{\rm rss}^2, \tag{C4}$$

for WNBs with a frequency range from 100 to 200 Hz, and

$$E_{\rm GW} = 1.2231 \times \frac{c^3\pi^2}{G} d^2 f_0^2 h_{\rm rss}^2, \tag{C5}$$

for WNBs with a frequency range of 100–1000 Hz.

The $h_{\rm rss}$ of a sine-Gaussian waveform derived from Equation 2) is Quitzow-James 2016)

$$h_{\rm rss}^{\rm SG} = h_0 \tau^{1/2} \frac{\pi^{1/4}}{2(2^{1/4})} \sqrt{\left(\frac{(1+\cos^2\iota)^2}{4} + \cos^2\iota\right) + \left(\frac{(1+\cos^2\iota)^2}{4} - \cos^2\iota\right) e^{-2\pi^2 f_0^2 \tau^2}}. \tag{C6}$$

The $h_{\rm rss}$ of a sine-Gaussian when the inclination angle $\iota = 0$ is

$$h_{{\rm rss},\iota=0}^{\rm SG} = h_0 \sqrt{\tau} \frac{\pi^{1/4}}{2^{3/4}}. \tag{C7}$$

The $E_{\rm GW}$ of a sine-Gaussian waveform is Quitzow-James 2016)

$$E_{\rm GW}^{\rm SG} = \frac{c^3\pi^{5/2}}{5\sqrt{2}\ G} h_0{}^2 d^2 f_0{}^2 \tau \times \left[1 + \frac{1}{4\pi^2 f_0^2 \tau^2}\left(1 + \frac{1}{6} e^{-2\pi^2 f_0^2 \tau^2}\right)\right]. \tag{C8}$$

For $Q = \sqrt{2}\pi f_0 \tau \gg 1$, this can be approximated as

$$E_{\rm GW}^{\rm SG} \approx \frac{c^3\pi^{5/2}}{5\sqrt{2}\ G} h_0{}^2 d^2 f_0{}^2 \tau. \tag{C9}$$

The $E_{\rm GW}$ of a half sine-Gaussian is half of the $E_{\rm GW}$ of a sine-Gaussian, and the $h_{\rm rss}$ of a half sine-Gaussian is the $h_{\rm rss}$ of a sine-Gaussian divided by $\sqrt{2}$. The $h_{\rm rss}$ of a half sine-Gaussian with $\iota = 0$ is Quitzow-James 2016)

$$h_{{\rm rss},\iota=0}^{\rm hSG} = \frac{h_{{\rm rss},\iota=0}^{\rm SG}}{\sqrt{2}} = h_0 \sqrt{\tau} \frac{\pi^{1/4}}{2^{5/4}}. \tag{C10}$$

The $E_{\rm GW}$ of a half sine-Gaussian waveform with $Q = \sqrt{2}\pi f_0 \tau \gg 1$ can be approximated as Quitzow-James 2016)

$$E_{\rm GW}^{\rm hSG} \approx \frac{c^3\pi^{5/2}}{10\sqrt{2}\ {\rm G}} h_0{}^2 d^2 f_0{}^2 \tau. \tag{C11}$$

The $h_{\rm rss}$ of a ringdown waveform can be derived from Equation 2) as

$$h_{\rm rss}^{\rm ringdown} = \frac{h_0}{2}\sqrt{\frac{\tau}{2}} \left[\left(\frac{(1+\cos^2\iota)^2}{4} + \cos^2\iota\right) + \frac{1}{1+4\pi^2 f_0^2 \tau^2}\left(\frac{(1+\cos^2\iota)^2}{4} - \cos^2\iota\right)\right]^{1/2}. \tag{C12}$$

For $\iota = 0$ this becomes

$$h_{{\rm rss},\iota=0}^{\rm ringdown} = \frac{h_0}{2}\sqrt{\tau}. \tag{C13}$$

$E_{\rm GW}$ can be calculated as

$$E_{\rm GW}^{\rm ringdown} = \frac{c^3}{40G} h_0^2 d^2 \left(\frac{1 + 4\pi^2 f_0^2 \tau^2}{\tau}\right) \times \left(1 + \left(\frac{1}{6}\right)\frac{1}{1+4\pi^2 f_0^2 \tau^2}\right). \tag{C14}$$

For $Q = \sqrt{2}\pi f_0 \tau \gg 1$

$$E_{\rm GW}^{\rm ringdown} \approx \frac{\pi^2 c^3}{10\ {\rm G}} d^2 f_0^2 h_0^2 \tau. \tag{C15}$$

It is important to note that the short-duration ringdown waveforms include a ringup right before the injection time for the purpose of avoiding a discontinuous jump in the signal. This ringup has a rise time that is one-tenth of the ringdown damping time. When including this ringup, the $h_{\rm rss}$ of the total waveform is the $h_{\rm rss}$ of the ringup and ringdown added in quadrature while the $E_{\rm GW}$ of the ringup and ringdown are add linearly. This gives

$$h_{{\rm rss},\iota=0}^{\rm ringup+ringdown} = \frac{h_0}{2}\sqrt{\tau + \tau\frac{1}{10}} = \frac{h_0}{2}\sqrt{\tau\frac{11}{10}}, \tag{C16}$$

and for $\sqrt{2}\pi f_0 \tau \gg 1$)

$$E_{\rm GW}^{\rm ringup+ringdown} \approx \frac{\pi^2 c^3}{10G} d^2 f_0^2 h_0^2 \tau (11/10). \tag{C17}$$

Appendix D
Search Upper Limit Tables

This section of the appendix contains the tables whose values are displayed in Figures 4, 6 and 7. The upper limits pertaining to both a 50 and 90 detection ef ciency are included in Tables 6–13 to provide a complete picture of the search sensitivity.

ORCID iDs

K. Ackley https: orcid.org 0000-0002-8648-0767
N. Adhikari https: orcid.org 0000-0002-4559-8427
R. X. Adhikari https: orcid.org 0000-0002-5731-5076
M. Agathos https: orcid.org 0000-0002-9072-1121
K. Agatsuma https: orcid.org 0000-0002-3952-5985
O. D. Aguiar https: orcid.org 0000-0002-2139-4390
L. Aiello https: orcid.org 0000-0003-2771-8816
P. Ajith https: orcid.org 0000-0001-7519-2439
T. Akutsu https: orcid.org 0000-0003-0733-7530
A. Allocca https: orcid.org 0000-0002-5288-1351

P. A. Altin https: orcid.org 0000-0001-8193-5825
A. Amato https: orcid.org 0000-0001-9557-651X
S. B. Anderson https: orcid.org 0000-0003-2219-9383
W. G. Anderson https: orcid.org 0000-0003-0482-5942
N. Andres https: orcid.org 0000-0002-5360-943X
M. Andrés-Carcasona https: orcid.org 0000-0002-8738-1672
T. Andri https: orcid.org 0000-0002-9277-9773
J. M. Antelis https: orcid.org 0000-0003-3377-0813
S. Antier https: orcid.org 0000-0002-7686-3334
K. Arai https: orcid.org 0000-0001-8916-8915
A. Araya https: orcid.org 0000-0002-6884-2875
M. C. Araya https: orcid.org 0000-0002-6018-6447
J. S. Areeda https: orcid.org 0000-0003-0266-7936
N. Aritomi https: orcid.org 0000-0003-4424-7657
N. Arnaud https: orcid.org 0000-0001-6589-8673
H. Asada https: orcid.org 0000-0001-9442-6050
G. Ashton https: orcid.org 0000-0001-7288-2231
Y. Aso https: orcid.org 0000-0002-1902-6695
P. Astone https: orcid.org 0000-0003-4981-4120
F. Aubin https: orcid.org 0000-0003-1613-3142
K. AultONeal https: orcid.org 0000-0002-6645-4473
S. Babak https: orcid.org 0000-0001-7469-4250
F. Badaracco https: orcid.org 0000-0001-8553-7904
S. Bae https: orcid.org 0000-0003-2429-3357
S. Bagnasco https: orcid.org 0000-0001-6062-6505
R. Bajpai https: orcid.org 0000-0003-0495-5720
G. Baltus https: orcid.org 0000-0002-0304-8152
S. Banagiri https: orcid.org 0000-0001-7852-7484
B. Banerjee https: orcid.org 0000-0002-8008-2485
D. Bankar https: orcid.org 0000-0002-6068-2993
P. Barneo https: orcid.org 0000-0002-8883-7280
F. Barone https: orcid.org 0000-0002-8069-8490
B. Barr https: orcid.org 0000-0002-5232-2736
L. Barsotti https: orcid.org 0000-0001-9819-2562
M. Barsuglia https: orcid.org 0000-0002-1180-4050
D. Barta https: orcid.org 0000-0001-6841-550X
M. A. Barton https: orcid.org 0000-0002-9948-306X
R. Bassiri https: orcid.org 0000-0001-8171-6833
M. Bawaj https: orcid.org 0000-0003-3611-3042
J. C. Bayley https: orcid.org 0000-0003-2306-4106
B. Bécsy https: orcid.org 0000-0003-0909-5563
F. Beirnaert https: orcid.org 0000-0002-4003-7233
M. Bejger https: orcid.org 0000-0002-4991-8213
J. D. Bentley https: orcid.org 0000-0002-4736-7403
M. Berbel https: orcid.org 0000-0001-6345-1798
B. K. Berger https: orcid.org 0000-0002-4845-8737
S. Bernuzzi https: orcid.org 0000-0002-2334-0935
D. Bersanetti https: orcid.org 0000-0002-7377-415X
J. Betzwieser https: orcid.org 0000-0003-1533-9229
D. Beveridge https: orcid.org 0000-0002-1481-1993
U. Bhardwaj https: orcid.org 0000-0003-1233-4174
D. Bhattacharjee https: orcid.org 0000-0001-6623-9506
S. Bhaumik https: orcid.org 0000-0001-8492-2202
G. Billingsley https: orcid.org 0000-0002-4141-2744
O. Birnholtz https: orcid.org 0000-0002-7562-9263
S. Biscoveanu https: orcid.org 0000-0001-7616-7366
B. Biswas https: orcid.org 0000-0003-2131-1476
M.-A. Bizouard https: orcid.org 0000-0002-4618-1674
J. K. Blackburn https: orcid.org 0000-0002-3838-2986
G. N. Bolingbroke https: orcid.org 0000-0002-7350-5291
E. Bonilla https: orcid.org 0000-0002-6284-9769
R. Bonnand https: orcid.org 0000-0001-5013-5913
V. Boschi https: orcid.org 0000-0001-8665-2293
V. Boudart https: orcid.org 0000-0001-9923-4154
P. R. Brady https: orcid.org 0000-0002-4611-9387
M. Branchesi https: orcid.org 0000-0003-1643-0526
J. E. Brau https: orcid.org 0000-0003-1292-9725
M. Breschi https: orcid.org 0000-0002-3327-3676
T. Briant https: orcid.org 0000-0002-6013-1729
A. F. Brooks https: orcid.org 0000-0003-4295-792X
R. Bruntz https: orcid.org 0000-0002-0840-8567
A. Buonanno https: orcid.org 0000-0002-5433-1409
R. Buscicchio https: orcid.org 0000-0002-7387-6754
C. Buy https: orcid.org 0000-0003-2872-8186
G. S. Cabourn Davies https: orcid.org 0000-0002-4289-3439
G. Cabras https: orcid.org 0000-0002-6852-6856
R. Cabrita https: orcid.org 0000-0003-0133-1306
L. Cadonati https: orcid.org 0000-0002-9846-166X
G. Cagnoli https: orcid.org 0000-0002-7086-6550
K. C. Cannon https: orcid.org 0000-0003-4068-6572
Z. Cao https: orcid.org 0000-0002-1932-7295
E. Capocasa https: orcid.org 0000-0003-3762-6958
J. B. Carlin https: orcid.org 0000-0001-5694-0809
G. Carullo https: orcid.org 0000-0001-9090-1862
M. Cavaglià https: orcid.org 0000-0002-3835-6729
F. Cavalier https: orcid.org 0000-0002-3658-7240
R. Cavalieri https: orcid.org 0000-0001-6064-0569
G. Cella https: orcid.org 0000-0002-0752-0338
E. Cesarini https: orcid.org 0000-0001-9127-3167
S. Chalathadka Subrahmanya https: orcid.org 0000-0002-9207-4669
E. Champion https: orcid.org 0000-0002-7901-4100
C. L. Chan https: orcid.org 0000-0002-3377-4737
P. Chanial https: orcid.org 0000-0003-1753-524X
C. Chapman-Bird https: orcid.org 0000-0002-2728-9612
P. Charlton https: orcid.org 0000-0002-4263-2706
E. A. Chase https: orcid.org 0000-0003-1005-0792
E. Chassande-Mottin https: orcid.org 0000-0003-3768-9908
C. Chatterjee https: orcid.org 0000-0001-8700-3455
Debarati Chatterjee https: orcid.org 0000-0002-0995-2329
Deep Chatterjee https: orcid.org 0000-0003-0038-5468
S. Chaty https: orcid.org 0000-0002-5769-8601
C. Chen https: orcid.org 0000-0002-3354-0105
D. Chen https: orcid.org 0000-0003-1433-0716
H. Y. Chen https: orcid.org 0000-0001-5403-3762
F. Chiadini https: orcid.org 0000-0002-9339-8622
A. Chincarini https: orcid.org 0000-0003-4094-9942
A. Chiummo https: orcid.org 0000-0003-2165-2967
S. Choudhary https: orcid.org 0000-0003-0949-7298
N. Christensen https: orcid.org 0000-0002-6870-4202
S. S. Y. Chua https: orcid.org 0000-0001-8026-7597
G. Ciani https: orcid.org 0000-0003-4258-9338
M. Cieślar https: orcid.org 0000-0001-8912-5587
R. Ciol https: orcid.org 0000-0003-3140-8933
J. A. Clark https: orcid.org 0000-0003-3243-1393
E. Codazzo https: orcid.org 0000-0001-7170-8733
P.-F. Cohadon https: orcid.org 0000-0003-3452-9415
D. E. Cohen https: orcid.org 0000-0002-0583-9919
M. Colleoni https: orcid.org 0000-0002-7214-9088
A. Colombo https: orcid.org 0000-0002-7439-4773
L. Conti https: orcid.org 0000-0003-2731-2656

T. R. Corbitt https: orcid.org 0000-0002-5520-8541
I. Cordero-Carrión https: orcid.org 0000-0002-1985-1361
N. J. Cornish https: orcid.org 0000-0002-7435-0869
S. Cortese https: orcid.org 0000-0002-6504-0973
M. W. Coughlin https: orcid.org 0000-0002-8262-2924
B. Cousins https: orcid.org 0000-0002-7026-1340
P. Couvares https: orcid.org 0000-0002-2823-3127
D. C. Coyne https: orcid.org 0000-0002-6427-3222
R. Coyne https: orcid.org 0000-0002-5243-5917
J. D. E. Creighton https: orcid.org 0000-0003-3600-2406
A. W. Criswell https: orcid.org 0000-0002-9225-7756
M. Croquette https: orcid.org 0000-0002-8581-5393
J. R. Cudell https: orcid.org 0000-0002-2003-4238
R. Cummings https: orcid.org 0000-0002-8042-9047
T. Dal Canton https: orcid.org 0000-0001-5078-9044
S. Dall Osso https: orcid.org 0000-0003-4366-8265
G. Dálya https: orcid.org 0000-0003-3258-5763
B. D Angelo https: orcid.org 0000-0001-9143-8427
S. Danilishin https: orcid.org 0000-0001-7758-7493
C. Darsow-Fromm https: orcid.org 0000-0001-9602-0388
Sayantani Datta https: orcid.org 0000-0001-9200-8867
D. Davis https: orcid.org 0000-0001-5620-6751
M. C. Davis https: orcid.org 0000-0001-7663-0808
E. J. Daw https: orcid.org 0000-0002-3780-5430
J. Degallaix https: orcid.org 0000-0002-1019-6911
S. Deléglise https: orcid.org 0000-0002-8680-5170
F. De Lillo https: orcid.org 0000-0003-4977-0789
D. Dell Aquila https: orcid.org 0000-0001-5895-0664
T. Dent https: orcid.org 0000-0003-1354-7809
A. Depasse https: orcid.org 0000-0003-1014-8394
R. De Pietri https: orcid.org 0000-0003-1556-8304
R. De Rosa https: orcid.org 0000-0002-4004-947X
R. DeSalvo https: orcid.org 0000-0002-4818-0296
M. C. Díaz https: orcid.org 0000-0002-7555-8856
T. Dietrich https: orcid.org 0000-0003-2374-307X
C. Di Giorgio https: orcid.org 0000-0003-2127-3991
F. Di Giovanni https: orcid.org 0000-0001-8568-9334
T. Di Girolamo https: orcid.org 0000-0003-2339-4471
A. Di Lieto https: orcid.org 0000-0002-4787-0754
A. Di Michele https: orcid.org 0000-0002-0357-2608
S. Di Pace https: orcid.org 0000-0001-6759-5676
I. Di Palma https: orcid.org 0000-0003-1544-8943
F. Di Renzo https: orcid.org 0000-0002-5447-3810
A. Dmitriev https: orcid.org 0000-0002-0314-956X
L. D Onofrio https: orcid.org 0000-0001-9546-5959
S. Doravari https: orcid.org 0000-0001-8750-8330
M. Drago https: orcid.org 0000-0002-3738-2431
J. C. Driggers https: orcid.org 0000-0002-6134-7628
D. D Urso https: orcid.org 0000-0002-8215-4542
T. Eckhardt https: orcid.org 0000-0002-1224-4681
G. Eddolls https: orcid.org 0000-0002-5895-4523
B. Edelman https: orcid.org 0000-0001-7648-1689
O. Edy https: orcid.org 0000-0001-9617-8724
A. Effler https: orcid.org 0000-0001-8242-3944
S. Eguchi https: orcid.org 0000-0003-2814-9336
J. Eichholz https: orcid.org 0000-0002-2643-163X
A. Ejlli https: orcid.org 0000-0002-4149-4532
Y. Enomoto https: orcid.org 0000-0001-6426-7079
R. C. Essick https: orcid.org 0000-0001-8196-9267
D. Estevez https: orcid.org 0000-0002-3021-5964
M. Evans https: orcid.org 0000-0001-8459-4499
F. Fabrizi https: orcid.org 0000-0002-3809-065X
V. Fafone https: orcid.org 0000-0003-1314-1622
P. C. Fan https: orcid.org 0000-0003-3988-9022
A. M. Farah https: orcid.org 0000-0002-6121-0285
B. Farr https: orcid.org 0000-0002-2916-9200
W. M. Farr https: orcid.org 0000-0003-1540-8562
G. Favaro https: orcid.org 0000-0002-0351-6833
M. Favata https: orcid.org 0000-0001-8270-9512
M. Fays https: orcid.org 0000-0002-4390-9746
E. Fenyvesi https: orcid.org 0000-0003-2777-3719
D. L. Ferguson https: orcid.org 0000-0002-4406-591X
A. Fernandez-Galiana https: orcid.org 0000-0002-8940-9261
I. Ferrante https: orcid.org 0000-0002-0083-7228
F. Fidecaro https: orcid.org 0000-0002-6189-3311
P. Figura https: orcid.org 0000-0002-8925-0393
A. Fiori https: orcid.org 0000-0003-3174-0688
I. Fiori https: orcid.org 0000-0002-0210-516X
M. Fishbach https: orcid.org 0000-0002-1980-5293
J. A. Font https: orcid.org 0000-0001-6650-2634
B. Fornal https: orcid.org 0000-0003-3271-2080
F. Frasconi https: orcid.org 0000-0003-4204-6587
Z. Frei https: orcid.org 0000-0002-0181-8491
A. Freise https: orcid.org 0000-0001-6586-9901
R. Frey https: orcid.org 0000-0003-0341-2636
G. G. Fronzé https: orcid.org 0000-0003-0966-4279
B. U. Gadre https: orcid.org 0000-0002-1534-9761
J. R. Gair https: orcid.org 0000-0002-1671-3668
D. Ganapathy https: orcid.org 0000-0003-3028-4174
A. Ganguly https: orcid.org 0000-0001-7394-0755
D. Gao https: orcid.org 0000-0002-1697-7153
B. Garaventa https: orcid.org 0000-0003-2490-404X
F. Garu https: orcid.org 0000-0003-1391-6168
G.-G. Ge https: orcid.org 0000-0003-2601-6484
G. Gemme https: orcid.org 0000-0002-1127-7406
A. Gennai https: orcid.org 0000-0003-0149-2089
O. Gerberding https: orcid.org 0000-0001-7740-2698
L. Gergely https: orcid.org 0000-0003-3146-6201
S. Ghonge https: orcid.org 0000-0002-5476-938X
Abhirup Ghosh https: orcid.org 0000-0002-2112-8578
Archisman Ghosh https: orcid.org 0000-0003-0423-3533
Shaon Ghosh https: orcid.org 0000-0001-9901-6253
Tathagata Ghosh https: orcid.org 0000-0001-9848-9905
B. Giacomazzo https: orcid.org 0000-0002-6947-4023
J. A. Giaime https: orcid.org 0000-0002-3531-817X
M. Giesler https: orcid.org 0000-0003-2300-893X
P. Giri https: orcid.org 0000-0002-4628-2432
S. Gkaitatzis https: orcid.org 0000-0001-9420-7499
E. Goetz https: orcid.org 0000-0003-2666-721X
R. Goetz https: orcid.org 0000-0002-9617-5520
B. Goncharov https: orcid.org 0000-0003-3189-5807
G. González https: orcid.org 0000-0003-0199-3158
A. Grado https: orcid.org 0000-0002-0501-8256
M. Granata https: orcid.org 0000-0003-3275-1186
R. Gray https: orcid.org 0000-0002-5556-9873
A. C. Green https: orcid.org 0000-0002-6287-8746
W. L. Grif ths https: orcid.org 0000-0001-8366-0108
H. L. Griggs https: orcid.org 0000-0001-5018-7908
A. Grimaldi https: orcid.org 0000-0002-6956-4301
H. Grote https: orcid.org 0000-0002-0797-3943
D. Guerra https: orcid.org 0000-0003-0029-5390
G. M. Guidi https: orcid.org 0000-0002-3061-9870
H.-K. Guo https: orcid.org 0000-0002-3777-3117

Anuradha Gupta https: orcid.org 0000-0002-5441-9013
F. Guzman https: orcid.org 0000-0001-9136-929X
L. Haegel https: orcid.org 0000-0002-3680-5519
O. Halim https: orcid.org 0000-0003-1326-5481
E. D. Hall https: orcid.org 0000-0001-9018-666X
W.-B. Han https: orcid.org 0000-0002-2039-0726
M. Haney https: orcid.org 0000-0001-7554-3665
J. Harms https: orcid.org 0000-0002-7332-9806
G. M. Harry https: orcid.org 0000-0002-8905-7622
I. W. Harry https: orcid.org 0000-0002-5304-9372
D. Hartwig https: orcid.org 0000-0002-9742-0794
C.-J. Haster https: orcid.org 0000-0001-8040-9807
J. Healy https: orcid.org 0000-0002-5233-3320
A. Heidmann https: orcid.org 0000-0002-0784-5175
J. Heinze https: orcid.org 0000-0001-8692-2724
H. Heitmann https: orcid.org 0000-0003-0625-5461
F. Hellman https: orcid.org 0000-0002-9135-6330
A. F. Helmling-Cornell https: orcid.org 0000-0002-7709-8638
G. Hemming https: orcid.org 0000-0001-5268-4465
M. Hendry https: orcid.org 0000-0001-8322-5405
E. Hennes https: orcid.org 0000-0002-2246-5496
M. H. Hennig https: orcid.org 0000-0003-1531-8460
M. Heurs https: orcid.org 0000-0002-5577-2273
A. L. Hewitt https: orcid.org 0000-0002-1255-3492
D. G. Holcomb https: orcid.org 0000-0001-5987-769X
I. J. Hollows https: orcid.org 0000-0002-3404-6459
Z. J. Holmes https: orcid.org 0000-0003-1311-4691
D. E. Holz https: orcid.org 0000-0002-0175-5064
E. J. Howell https: orcid.org 0000-0001-7891-2817
C. G. Hoy https: orcid.org 0000-0002-8843-6719
H-F. Hsieh https: orcid.org 0000-0002-8947-723X
H-Y. Huang https: orcid.org 0000-0002-1665-2383
P. Huang https: orcid.org 0000-0002-3812-2180
Y-C. Huang https: orcid.org 0000-0001-8786-7026
Y.-J. Huang https: orcid.org 0000-0002-2952-8429
M. T. Hübner https: orcid.org 0000-0002-9642-3029
D. C. Y. Hui https: orcid.org 0000-0003-1753-1660
V. Hui https: orcid.org 0000-0002-0233-2346
B. Idzkowski https: orcid.org 0000-0001-5869-2714
K. Inayoshi https: orcid.org 0000-0001-9840-4959
P. Iosif https: orcid.org 0000-0003-1621-7709
M. Isi https: orcid.org 0000-0001-8830-8672
Y. Itoh https: orcid.org 0000-0003-2694-8935
B. R. Iyer https: orcid.org 0000-0002-4141-5179
V. JaberianHamedan https: orcid.org 0000-0003-3605-4169
T. Jacqmin https: orcid.org 0000-0002-0693-4838
P.-E. Jacquet https: orcid.org 0000-0001-9552-0057
S. P. Jadhav https: orcid.org 0000-0003-0554-0084
A. L. James https: orcid.org 0000-0001-9165-0807
A. Z. Jan https: orcid.org 0000-0003-2050-7231
K. Janssens https: orcid.org 0000-0001-8760-4429
P. Jaranowski https: orcid.org 0000-0001-8085-3414
R. Jaume https: orcid.org 0000-0001-8691-3166
A. C. Jenkins https: orcid.org 0000-0003-1785-5841
J. Jiang https: orcid.org 0000-0002-0154-3854
H.-B. Jin https: orcid.org 0000-0002-6217-2428
A. W. Jones https: orcid.org 0000-0002-0395-0680
L. Ju https: orcid.org 0000-0002-7951-4295
P. Jung https: orcid.org 0000-0003-2974-4604
J. Junker https: orcid.org 0000-0002-3051-4374
T. Kajita https: orcid.org 0000-0003-1207-6638
M. Kakizaki https: orcid.org 0000-0003-1430-3339
V. Kalogera https: orcid.org 0000-0001-9236-5469
M. Kamiizumi https: orcid.org 0000-0001-7216-1784
N. Kanda https: orcid.org 0000-0001-6291-0227
S. Kandhasamy https: orcid.org 0000-0002-4825-6764
G. Kang https: orcid.org 0000-0002-6072-8189
D. P. Kapasi https: orcid.org 0000-0001-8189-4920
C. Karathanasis https: orcid.org 0000-0002-0642-5507
M. Kasprzack https: orcid.org 0000-0003-4618-5939
S. Katsanevas https: orcid.org 0000-0003-0324-0758
K. Kawaguchi https: orcid.org 0000-0003-4443-6984
D. Keitel https: orcid.org 0000-0002-2824-626X
J. S. Key https: orcid.org 0000-0003-0123-7600
F. Y. Khalili https: orcid.org 0000-0001-7068-2332
S. Khan https: orcid.org 0000-0003-4953-5754
N. Kijbunchoo https: orcid.org 0000-0002-2874-1228
C. Kim https: orcid.org 0000-0003-3040-8456
J. Kim https: orcid.org 0000-0001-9145-0530
K. Kim https: orcid.org 0000-0003-1653-3795
Y.-M. Kim https: orcid.org 0000-0001-8720-6113
M. Kinley-Hanlon https: orcid.org 0000-0002-7367-8002
R. Kirchhoff https: orcid.org 0000-0003-0224-8600
J. S. Kissel https: orcid.org 0000-0002-1702-9577
A. M. Knee https: orcid.org 0000-0003-0703-947X
K. Kokeyama https: orcid.org 0000-0002-2896-1992
S. Koley https: orcid.org 0000-0002-5793-6665
P. Kolitsidou https: orcid.org 0000-0002-6719-8686
M. Kolstein https: orcid.org 0000-0002-5482-6743
A. K. H. Kong https: orcid.org 0000-0002-5105-344X
A. Kontos https: orcid.org 0000-0002-1347-0680
M. Korobko https: orcid.org 0000-0002-3839-3909
C. Kozakai https: orcid.org 0000-0003-2853-869X
N. V. Krishnendu https: orcid.org 0000-0002-3483-7517
A. Królak https: orcid.org 0000-0003-4514-7690
P. Kuijer https: orcid.org 0000-0002-6987-2048
Prayush Kumar https: orcid.org 0000-0001-5523-4603
K. Kuns https: orcid.org 0000-0003-0630-3902
S. Kuroyanagi https: orcid.org 0000-0001-6538-1447
K. Kwak https: orcid.org 0000-0002-2304-7798
D. Laghi https: orcid.org 0000-0001-7462-3794
R. N. Lang https: orcid.org 0000-0002-4804-5537
B. Lantz https: orcid.org 0000-0002-7404-4845
P. D. Lasky https: orcid.org 0000-0003-3763-1386
M. Laxen https: orcid.org 0000-0001-7515-9639
A. Lazzarini https: orcid.org 0000-0002-5993-8808
P. Leaci https: orcid.org 0000-0002-3997-5046
S. Leavey https: orcid.org 0000-0001-8253-0272
Y. K. Lecoeuche https: orcid.org 0000-0002-9186-7034
H. M. Lee https: orcid.org 0000-0003-4412-7161
H. W. Lee https: orcid.org 0000-0002-1998-3209
K. Lee https: orcid.org 0000-0003-0470-3718
R. Lee https: orcid.org 0000-0002-7171-7274
M. Lenti https: orcid.org 0000-0002-2765-3955
M. Leonardi https: orcid.org 0000-0002-7641-0060
N. Leroy https: orcid.org 0000-0002-2321-1017
K. L. Li https: orcid.org 0000-0001-8229-2024
X. Li https: orcid.org 0000-0002-3780-7735
C-Y. Lin https: orcid.org 0000-0002-7489-7418
E. T. Lin https: orcid.org 0000-0002-0030-8051
F-L. Lin https: orcid.org 0000-0002-4277-7219
H. L. Lin https: orcid.org 0000-0002-3528-5726

L. C.-C. Lin https: orcid.org 0000-0003-4083-9567
G. C. Liu https: orcid.org 0000-0001-5663-3016
J. Liu https: orcid.org 0000-0001-6726-3268
R. K. L. Lo https: orcid.org 0000-0003-1561-6716
A. Longo https: orcid.org 0000-0003-4254-8579
M. Lorenzini https: orcid.org 0000-0002-2765-7905
G. Losurdo https: orcid.org 0000-0003-0452-746X
J. D. Lough https: orcid.org 0000-0002-5160-0239
C. O. Lousto https: orcid.org 0000-0002-6400-9640
D. Lumaca https: orcid.org 0000-0002-3628-1591
L.-W. Luo https: orcid.org 0000-0002-2761-8877
R. Macas https: orcid.org 0000-0002-6096-8297
D. M. Macleod https: orcid.org 0000-0002-1395-8694
I. A. O. MacMillan https: orcid.org 0000-0002-6927-1031
C. Magazzù https: orcid.org 0000-0002-9913-381X
R. M. Magee https: orcid.org 0000-0001-9769-531X
R. Maggiore https: orcid.org 0000-0001-5140-779X
M. Magnozzi https: orcid.org 0000-0003-4512-8430
E. Majorana https: orcid.org 0000-0002-2383-3692
V. Mandic https: orcid.org 0000-0001-6333-8621
V. Mangano https: orcid.org 0000-0001-7902-8505
M. Manske https: orcid.org 0000-0002-7778-1189
M. Mantovani https: orcid.org 0000-0002-4424-5726
M. Mapelli https: orcid.org 0000-0001-8799-2548
D. Marín Pina https: orcid.org 0000-0001-6482-1842
S. Márka https: orcid.org 0000-0002-3957-1324
Z. Márka https: orcid.org 0000-0003-1306-5260
S. Marsat https: orcid.org 0000-0001-9449-1071
I. W. Martin https: orcid.org 0000-0001-7300-9151
H. Masalehdan https: orcid.org 0000-0002-4589-0815
M. Masso-Reid https: orcid.org 0000-0001-6177-8105
S. Mastrogiovanni https: orcid.org 0000-0003-1606-4183
M. Mateu-Lucena https: orcid.org 0000-0003-4817-6913
M. Matiushechkina https: orcid.org 0000-0002-9957-8720
N. Mavalvala https: orcid.org 0000-0003-0219-9706
D. E. McClelland https: orcid.org 0000-0001-6210-5842
J. McIver https: orcid.org 0000-0003-0316-1355
D. Meacher https: orcid.org 0000-0001-5882-0368
M. Mehmet https: orcid.org 0000-0001-9432-7108
C. S. Menoni https: orcid.org 0000-0001-9185-2572
K. Merfeld https: orcid.org 0000-0003-1773-5372
C. Messenger https: orcid.org 0000-0001-7488-5022
P. M. Meyers https: orcid.org 0000-0002-2689-0190
F. Meylahn https: orcid.org 0000-0002-9556-142X
A. Miani https: orcid.org 0000-0001-7737-3129
I. Michaloliakos https: orcid.org 0000-0003-2980-358X
C. Michel https: orcid.org 0000-0003-0606-725X
Y. Michimura https: orcid.org 0000-0002-2218-4002
H. Middleton https: orcid.org 0000-0001-5532-3622
D. P. Mihaylov https: orcid.org 0000-0002-8820-407X
M. Miravet-Tenés https: orcid.org 0000-0002-8766-1156
T. Mishra https: orcid.org 0000-0002-7881-1677
S. Mitra https: orcid.org 0000-0002-0800-4626
V. P. Mitrofanov https: orcid.org 0000-0002-6983-4981
G. Mitselmakher https: orcid.org 0000-0001-5745-3658
O. Miyakawa https: orcid.org 0000-0002-9085-7600
K. Miyo https: orcid.org 0000-0001-6976-1252
S. Miyoki https: orcid.org 0000-0002-1213-8416
Geoffrey Mo https: orcid.org 0000-0001-6331-112X
L. M. Modafferi https: orcid.org 0000-0002-3422-6986
S. R. Mohite https: orcid.org 0000-0003-1356-7156
M. Molina-Ruiz https: orcid.org 0000-0003-4892-3042
A. More https: orcid.org 0000-0001-7714-7076
C. Moreno https: orcid.org 0000-0002-0496-032X
S. Morisaki https: orcid.org 0000-0002-8445-6747
B. Mours https: orcid.org 0000-0002-6444-6402
C. M. Mow-Lowry https: orcid.org 0000-0002-0351-4555
S. Mozzon https: orcid.org 0000-0002-8855-2509
D. Mukherjee https: orcid.org 0000-0001-7335-9418
Suvodip Mukherjee https: orcid.org 0000-0002-3373-5236
N. Mukund https: orcid.org 0000-0002-8666-9156
E. A. Muñiz https: orcid.org 0000-0001-8844-421X
P. G. Murray https: orcid.org 0000-0002-8218-2404
R. Musenich https: orcid.org 0000-0002-2168-5462
K. Nagano https: orcid.org 0000-0001-6686-1637
K. Nakamura https: orcid.org 0000-0001-6148-4289
H. Nakano https: orcid.org 0000-0001-7665-0796
I. Nardecchia https: orcid.org 0000-0001-5558-2595
L. Naticchioni https: orcid.org 0000-0003-2918-0730
R. K. Nayak https: orcid.org 0000-0002-6814-7792
S. W. S. Ng https: orcid.org 0000-0001-5843-1434
C. Nguyen https: orcid.org 0000-0001-8623-0306
L. Nguyen Quynh https: orcid.org 0000-0002-1828-3702
W.-T. Ni https: orcid.org 0000-0001-6792-4708
A. Nishizawa https: orcid.org 0000-0003-3562-0990
E. Nitoglia https: orcid.org 0000-0001-8906-9159
L. K. Nuttall https: orcid.org 0000-0002-8599-8791
Y. Obayashi https: orcid.org 0000-0001-8791-2608
E. Oelker https: orcid.org 0000-0002-3916-1595
J. J. Oh https: orcid.org 0000-0001-5417-862X
K. Oh https: orcid.org 0000-0002-9672-3742
S. H. Oh https: orcid.org 0000-0003-1184-7453
M. Ohashi https: orcid.org 0000-0001-8072-0304
M. Ohkawa https: orcid.org 0000-0002-1380-1419
F. Ohme https: orcid.org 0000-0003-0493-5607
K. Oohara https: orcid.org 0000-0002-7518-6677
B. O Reilly https: orcid.org 0000-0002-3874-8335
R. O Shaughnessy https: orcid.org 0000-0001-5832-8517
E. O Shea https: orcid.org 0000-0002-0230-9533
S. Oshino https: orcid.org 0000-0002-2794-6029
S. Ossokine https: orcid.org 0000-0002-2579-1246
D. J. Ottaway https: orcid.org 0000-0001-6794-1591
C. Palomba https: orcid.org 0000-0002-4450-9883
K.-C. Pan https: orcid.org 0000-0002-1473-9880
F. Pannarale https: orcid.org 0000-0002-7537-3210
F. Paoletti https: orcid.org 0000-0001-8898-1963
A. Parisi https: orcid.org 0000-0003-0251-8914
J. Park https: orcid.org 0000-0002-7510-0079
W. Parker https: orcid.org 0000-0002-7711-4423
D. Pascucci https: orcid.org 0000-0003-1907-0175
R. Passaquieti https: orcid.org 0000-0003-4753-9428
B. Patricelli https: orcid.org 0000-0001-6709-0969
S. Paul https: orcid.org 0000-0002-4449-1732
F. E. Peña Arellano https: orcid.org 0000-0002-8516-5159
S. Penn https: orcid.org 0000-0003-4956-0853
T. Pereira https: orcid.org 0000-0003-1856-6881
A. Perreca https: orcid.org 0000-0002-6269-2490
J. Petermann https: orcid.org 0000-0002-8949-3803
H. P. Pfeiffer https: orcid.org 0000-0001-9288-519X
K. A. Pham https: orcid.org 0000-0002-7650-1034
K. S. Phukon https: orcid.org 0000-0003-1561-0760
O. J. Piccinni https: orcid.org 0000-0001-5478-3950
M. Pichot https: orcid.org 0000-0002-4439-8968
L. Pierini https: orcid.org 0000-0003-0945-2196

V. Pierro https: orcid.org 0000-0002-6020-5521
M. D. Pitkin https: orcid.org 0000-0003-4548-526X
A. Placidi https: orcid.org 0000-0001-8032-4416
M. L. Planas https: orcid.org 0000-0001-8278-7406
W. Plastino https: orcid.org 0000-0002-5737-6346
R. Poggiani https: orcid.org 0000-0002-9968-2464
E. Polini https: orcid.org 0000-0003-4059-0765
R. Poulton https: orcid.org 0000-0003-2049-520X
G. Pratten https: orcid.org 0000-0003-4984-0775
G. A. Prodi https: orcid.org 0000-0001-5256-915X
M. Punturo https: orcid.org 0000-0001-8722-4485
M. Pürrer https: orcid.org 0000-0002-3329-9788
H. Qi https: orcid.org 0000-0001-6339-1537
R. Quitzow-James https: orcid.org 0000-0003-1233-633X
P. Raffai https: orcid.org 0000-0001-7576-0141
K. E. Ramirez https: orcid.org 0000-0003-2194-7669
A. Ramos-Buades https: orcid.org 0000-0002-6874-7421
V. Raymond https: orcid.org 0000-0003-0066-0095
N. Raza https: orcid.org 0000-0002-8549-9124
M. Razzano https: orcid.org 0000-0003-4825-1629
L. Rei https: orcid.org 0000-0002-8690-9180
P. Relton https: orcid.org 0000-0003-2756-3391
P. Rettegno https: orcid.org 0000-0001-8088-3517
B. Revenu https: orcid.org 0000-0002-7629-4805
J. W. Richardson https: orcid.org 0000-0002-1472-4806
K. Riles https: orcid.org 0000-0002-6418-5812
S. Rinaldi https: orcid.org 0000-0001-5799-4155
K. Rink https: orcid.org 0000-0002-1494-3494
A. Rocchi https: orcid.org 0000-0002-1382-9016
L. Rolland https: orcid.org 0000-0003-0589-9687
J. G. Rollins https: orcid.org 0000-0002-9388-2799
A. Romero https: orcid.org 0000-0003-2275-4164
S. Ronchini https: orcid.org 0000-0003-0020-687X
M. P. Ross https: orcid.org 0000-0002-8955-5269
D. Rozza https: orcid.org 0000-0002-7378-6353
J. Sadiq https: orcid.org 0000-0001-5931-3624
S. Saha https: orcid.org 0000-0002-3333-8070
M. Sakellariadou https: orcid.org 0000-0002-2715-1517
O. S. Sala a https: orcid.org 0000-0003-4924-7322
F. Salces-Carcoba https: orcid.org 0000-0001-7049-4438
M. Saleem https: orcid.org 0000-0002-3836-7751
F. Salemi https: orcid.org 0000-0002-9511-3846
A. Samajdar https: orcid.org 0000-0002-0857-6018
N. Sanchis-Gual https: orcid.org 0000-0001-5375-7494
A. Sanuy https: orcid.org 0000-0002-5767-3623
B. S. Sathyaprakash https: orcid.org 0000-0003-3845-7586
O. Sauter https: orcid.org 0000-0003-2293-1554
R. L. Savage https: orcid.org 0000-0003-3317-1036
T. Sawada https: orcid.org 0000-0001-5726-7150
M. G. Schiworski https: orcid.org 0000-0001-9298-004X
P. Schmidt https: orcid.org 0000-0003-1542-1791
R. Schnabel https: orcid.org 0000-0003-2896-4218
E. Schwartz https: orcid.org 0000-0001-8922-7794
J. Scott https: orcid.org 0000-0001-6701-6515
S. M. Scott https: orcid.org 0000-0002-9875-7700
M. Seglar-Arroyo https: orcid.org 0000-0001-8654-409X
Y. Sekiguchi https: orcid.org 0000-0002-2648-3835
Y. Setyawati https: orcid.org 0000-0003-3718-4491
M. S. Shahriar https: orcid.org 0000-0002-7981-954X
M. A. Shaikh https: orcid.org 0000-0003-0826-6164
L. Shao https: orcid.org 0000-0002-1334-8853
P. Shawhan https: orcid.org 0000-0002-8249-8070
N. S. Shcheblanov https: orcid.org 0000-0001-8696-2435
Y. Shikano https: orcid.org 0000-0003-2107-7536
H. Shimizu https: orcid.org 0000-0002-4221-0300
K. Shimode https: orcid.org 0000-0002-5682-8750
H. Shinkai https: orcid.org 0000-0003-1082-2844
A. Shoda https: orcid.org 0000-0002-0236-4735
D. H. Shoemaker https: orcid.org 0000-0002-4147-2560
D. M. Shoemaker https: orcid.org 0000-0002-9899-6357
D. Sigg https: orcid.org 0000-0003-4606-6526
L. Silenzi https: orcid.org 0000-0001-7316-3239
L. P. Singer https: orcid.org 0000-0001-9898-5597
D. Singh https: orcid.org 0000-0001-9675-4584
M. K. Singh https: orcid.org 0000-0001-8081-4888
N. Singh https: orcid.org 0000-0002-1135-3456
A. Singha https: orcid.org 0000-0002-9944-5573
A. M. Sintes https: orcid.org 0000-0001-9050-7515
B. J. J. Slagmolen https: orcid.org 0000-0002-2471-3828
J. R. Smith https: orcid.org 0000-0003-0638-9670
R. J. E. Smith https: orcid.org 0000-0001-8516-3324
J. Soldateschi https: orcid.org 0000-0002-5458-5206
S. N. Somala https: orcid.org 0000-0003-2663-3351
K. Somiya https: orcid.org 0000-0003-2601-2264
I. Song https: orcid.org 0000-0002-4301-8281
K. Soni https: orcid.org 0000-0001-8051-7883
N. Sorrentino https: orcid.org 0000-0002-1855-5966
A. P. Spencer https: orcid.org 0000-0003-4418-3366
M. Spera https: orcid.org 0000-0003-0930-6930
D. A. Steer https: orcid.org 0000-0002-8781-1273
S. Steinlechner https: orcid.org 0000-0003-4710-8548
K. A. Strain https: orcid.org 0000-0002-2066-5355
G. Stratta https: orcid.org 0000-0003-1055-7980
A. L. Stuver https: orcid.org 0000-0003-0324-5735
S. Sudhagar https: orcid.org 0000-0001-8578-4665
V. Sudhir https: orcid.org 0000-0002-5397-6950
R. Sugimoto https: orcid.org 0000-0001-6705-3658
H. G. Suh https: orcid.org 0000-0003-2662-3903
A. G. Sullivan https: orcid.org 0000-0002-9545-7286
T. Z. Summerscales https: orcid.org 0000-0002-4522-5591
L. Sun https: orcid.org 0000-0001-7959-892X
A. Sur https: orcid.org 0000-0001-6635-5080
J. Suresh https: orcid.org 0000-0003-2389-6666
P. J. Sutton https: orcid.org 0000-0003-1614-3922
Takamasa Suzuki https: orcid.org 0000-0003-3030-6599
B. L. Swinkels https: orcid.org 0000-0002-3066-3601
M. J. Szczepańczyk https: orcid.org 0000-0002-6167-6149
S. C. Tait https: orcid.org 0000-0003-0327-953X
H. Takahashi https: orcid.org 0000-0003-0596-4397
R. Takahashi https: orcid.org 0000-0003-1367-5149
H. Takeda https: orcid.org 0000-0001-9937-2557
Takahiro Tanaka https: orcid.org 0000-0001-8406-5183
S. Tanioka https: orcid.org 0000-0003-3321-1018
L. Tao https: orcid.org 0000-0003-4382-5507
E. N. Tapia San Martín https: orcid.org 0000-0002-4817-5606
A. Taruya https: orcid.org 0000-0002-4016-1955
J. D. Tasson https: orcid.org 0000-0002-4777-5087
R. Tenorio https: orcid.org 0000-0002-3582-2587
J. E. S. Terhune https: orcid.org 0000-0001-9078-4993
L. Terkowski https: orcid.org 0000-0003-4622-1215
J. E. Thompson https: orcid.org 0000-0002-0419-5517
Shubhanshu Tiwari https: orcid.org 0000-0003-1611-6625

V. Tiwari https: orcid.org 0000-0002-1602-4176
A. E. Tolley https: orcid.org 0000-0001-9841-943X
T. Tomaru https: orcid.org 0000-0002-8927-9014
T. Tomura https: orcid.org 0000-0002-7504-8258
A. Torres-Forné https: orcid.org 0000-0001-8709-5118
I. Tosta e Melo https: orcid.org 0000-0001-5833-4052
A. Trapananti https: orcid.org 0000-0001-7763-5758
F. Travasso https: orcid.org 0000-0002-4653-6156
M. C. Tringali https: orcid.org 0000-0001-5087-189X
A. Tripathee https: orcid.org 0000-0002-6976-5576
A. Trovato https: orcid.org 0000-0002-9714-1904
L. Trozzo https: orcid.org 0000-0002-8803-6715
T. Tsang https: orcid.org 0000-0003-3666-686X
T. Tsutsui https: orcid.org 0000-0002-2909-0471
K. Turbang https: orcid.org 0000-0002-9296-8603
D. Tuyenbayev https: orcid.org 0000-0002-4378-5835
A. S. Ubhi https: orcid.org 0000-0002-3240-6000
N. Uchikata https: orcid.org 0000-0003-0030-3653
T. Uchiyama https: orcid.org 0000-0003-2148-1694
T. Uehara https: orcid.org 0000-0003-4375-098X
K. Ueno https: orcid.org 0000-0003-3227-6055
T. Ushiba https: orcid.org 0000-0002-5059-4033
A. Utina https: orcid.org 0000-0003-2975-9208
G. Vajente https: orcid.org 0000-0002-7656-6882
G. Valdes https: orcid.org 0000-0001-5411-380X
M. Valentini https: orcid.org 0000-0003-1215-4552
M. van Beuzekom https: orcid.org 0000-0002-0500-1286
J. F. J. van den Brand https: orcid.org 0000-0003-4434-5353
H. van Haevermaet https: orcid.org 0000-0003-2386-957X
J. V. van Heijningen https: orcid.org 0000-0002-8391-7513
N. van Remortel https: orcid.org 0000-0003-4180-8199
V. Varma https: orcid.org 0000-0002-9994-1761
M. Vasúth https: orcid.org 0000-0003-4573-8781
A. Vecchio https: orcid.org 0000-0002-6254-1617
J. Veitch https: orcid.org 0000-0002-6508-0713
P. J. Veitch https: orcid.org 0000-0002-2597-435X
J. Venneberg https: orcid.org 0000-0002-2508-2044
G. Venugopalan https: orcid.org 0000-0003-4414-9918
D. Verkindt https: orcid.org 0000-0003-4344-7227
Y. Verma https: orcid.org 0000-0003-4147-3173
S. M. Vermeulen https: orcid.org 0000-0003-4227-8214
D. Veske https: orcid.org 0000-0003-4225-0895
A. Viceré https: orcid.org 0000-0003-0624-6231
A. D. Viets https: orcid.org 0000-0002-4241-1428
A. Vijaykumar https: orcid.org 0000-0002-4103-0666
V. Villa-Ortega https: orcid.org 0000-0001-7983-1963
S. Vitale https: orcid.org 0000-0003-2700-0767
C. Vorvick https: orcid.org 0000-0003-1591-3358
S. P. Vyatchanin https: orcid.org 0000-0002-6823-911X
M. Wade https: orcid.org 0000-0002-5703-4469
K. J. Wagner https: orcid.org 0000-0002-7255-4251
J. Wang https: orcid.org 0000-0002-1830-8527
M. Was https: orcid.org 0000-0002-1890-1128
T. Washimi https: orcid.org 0000-0001-5792-4907
J. Watchi https: orcid.org 0000-0002-9154-6433
A. J. Weinstein https: orcid.org 0000-0002-0928-6784
R. A. Weller https: orcid.org 0000-0002-2280-219X
K. Wette https: orcid.org 0000-0002-4394-7179
J. T. Whelan https: orcid.org 0000-0001-5710-6576
B. F. Whiting https: orcid.org 0000-0002-8501-8669
C. Whittle https: orcid.org 0000-0002-8833-7438
D. Williams https: orcid.org 0000-0003-3772-198X
M. J. Williams https: orcid.org 0000-0003-2198-2974
A. R. Williamson https: orcid.org 0000-0002-7627-8688
J. L. Willis https: orcid.org 0000-0002-9929-0225
B. Willke https: orcid.org 0000-0003-0524-2925
G. Woan https: orcid.org 0000-0003-0381-0394
J. K. Wofford https: orcid.org 0000-0002-4301-2859
I. C. F. Wong https: orcid.org 0000-0003-2166-0027
C. Wu https: orcid.org 0000-0003-3191-8845
D. S. Wu https: orcid.org 0000-0003-2849-3751
L. Xiao https: orcid.org 0000-0003-2703-449X
H. Yamamoto https: orcid.org 0000-0002-3033-2845
K. Yamamoto https: orcid.org 0000-0001-6919-9570
T. Yamamoto https: orcid.org 0000-0002-0808-4822
F. W. Yang https: orcid.org 0000-0001-9873-6259
K. Z. Yang https: orcid.org 0000-0001-8083-4037
L. Yang https: orcid.org 0000-0002-8868-5977
Y. Yang https: orcid.org 0000-0002-3780-1413
A. B. Yelikar https: orcid.org 0000-0002-8065-1174
J. Yokoyama https: orcid.org 0000-0001-7127-4808
Hang Yu https: orcid.org 0000-0002-6011-6190
Haocun Yu https: orcid.org 0000-0002-7597-098X
S. Zeidler https: orcid.org 0000-0001-7949-1292
M. Zevin https: orcid.org 0000-0002-0147-0835
J. Zhang https: orcid.org 0000-0002-3931-3851
R. Zhang https: orcid.org 0000-0001-8095-483X
C. Zhao https: orcid.org 0000-0001-5825-2401
Y. Zhao https: orcid.org 0000-0003-2542-4734
X. J. Zhu https: orcid.org 0000-0001-7049-6468
Z.-H. Zhu https: orcid.org 0000-0002-3567-6743
J. Zweizig https: orcid.org 0000-0002-1521-3397

References

Aasi, J., Abbott, B. P., Abbott, R., et al. 2015, CQGra, 32, 074001
Aasi, J., Abbott, B. P., Abbott, R., et al. 2014, PhRvL, 113, 011102
Abadie, J., Abbott, B. P., Abbott, R., et al. 2011, ApJL, 734, L35
Abadie, J., Abbott, B. P., Abbott, R., et al. 2012, ApJ, 755, 2
Abbott, B. P., Abbott, R., Adhikari, R., et al. 2007, PhRvD, 76, 062003
Abbott, B. P., Abbott, R., Abbott, T. D., et al. 2008a, PhRvL, 101, 211102
Abbott, B. P., Abbott, R., Adhikari, R., et al. 2008b, ApJ, 681, 1419
Abbott, B. P., Abbot, R., Adhikari, R., et al. 2009, ApJL, 701, L68
Abbott, B. P., Abbott, R., Abbott, T. D., et al. 2018, LRR, 21, 3
Abbott, B. P., Abbott, R., Abbott, T. D., et al. 2019, ApJ, 874, 163
Abbott, R., Abbott, T. D., Abraham, S., et al. 2021, ApJ, 915, 86
Abbott, R., Abbott, T. D., Acernese, F., et al. 2022, ApJ, 928, 186
Abbott, R., Abbott, T. D., Acerness, F., et al. 2023, ApJ, 955, 155
Acernese, F., Agathos, M., Agatsuma, K., et al. 2015, CQGra, 32, 024001
Ackley, K., Adya, V. B., Agrawal, P., et al. 2020, PASA, 37, e047
Akutsu, T., Ando, M., Arai, K., et al. 2019, NatAs, 3, 35
Akutsu, T., Ando, M., Arai, K., et al. 2021, PTEP, 2021, 05A102
Barat, C., Hayles, R. I., Hurley, K., et al. 1983, A&A, 126, 400
Barsotti, L., Gras, S., Evans, M., & Fritschel, P. 2018, Updated Advanced LIGO Sensitivity Design Curve, https: dcc.ligo.org LIGO-T1800044 public
Boggs, S. E., Zoglauer, A., Bellm, E., et al. 2007, ApJ, 661, 458
Buikema, A., Cahillane, C., Mansell, G. L., et al. 2020, PhRvD, 102, 062003
Burns, E., Svinkin, D., Hurley, K., et al. 2021, ApJL, 907, L28
Ciol , R., Lander, S. K., Manca, G. M., & Rezzolla, L. 2011, ApJL, 736, L6
Ciol , R., & Rezzolla, L. 2012, ApJ, 760, 1
Colaiuda, A., & Kokkotas, K. D. 2011, MNRAS, 414, 3014
Corsi, A., & Owen, B. J. 2011, PhRvD, 83, 104014
Cummings, J., Barthelmy, S., Chester, M., & Page, K. 2014, ATel, 6294, 1
Davis, D., Areeda, J. S., Berger, B. K., et al. 2021, CQGra, 38, 135014
Duncan, R. C. 1998, ApJL, 498, L45
Durant, M., & van Kerkwijk, M. H. 2006, ApJ, 650, 1070
Evans, M., Adhikari, R.X., Afle, C., et al. 2021, arXiv:2109.09882

Evans, P., Gropp, J., Kennea, J., et al. 2020, GCN, 27373, 1, https: gcn.gsfc. nasa.gov gcn gcn3 27373.gcn3
Evans, W. D., Klebesadel, R. W., Laros, J. G., et al. 1980, ApJL, 237, L7
Glampedakis, K., & Jones, D. I. 2014, MNRAS, 439, 1522
Glampedakis, K., Samuelsson, L., & Andersson, N. 2006, MNRAS, 371, L74
Ho, W. C. G., Jones, D. I., Andersson, N., & Espinoza, C. M. 2020, PhRvD, 101, 103009
Huppenkothen, D., D Angelo, C., Watts, A. L., et al. 2014a, ApJ, 787, 128
Huppenkothen, D., Heil, L. M., Watts, A. L., & Göğüş, E. 2014b, ApJ, 795, 114
Hurley, K., Boggs, S. E., Smith, D. M., et al. 2005, Natur, 434, 1098
Hurley, K., Cline, T., Mazets, E., et al. 1999, Natur, 397, 41
Hurley, K. 2021, SGR Burst List, http: www.ssl.berkeley.edu ipn3 sgrlist.txt
Ioka, K. 2001, MNRAS, 327, 639
Israel, G. L., Belloni, T., Stella, L., et al. 2005, ApJL, 628, L53
Kalmus, P. 2009, PhD thesis, Columbia Univ.
Kalmus, P., Cannon, K. C., Márka, S., & Owen, B. J. 2009, PhRvD, 80, 042001
Kalmus, P., Khan, R., Matone, L., & Márka, S. 2007, CQGra, 24, S659
Karuppusamy, R., Desvignes, G., Kramer, M., et al. 2020, ATel, 13553
Kashiyama, K., & Ioka, K. 2011, PhRvD, 83, 081302
Kaspi, V. M., & Beloborodov, A. M. 2017, ARA&A, 55, 261
Kirsten, F., Snelders, M. P., Jenkins, M., et al. 2020, NatAs, 5, 414
Kissel, J. 2020, aLIGO, CAL, Of cial Advanced LIGO Sensitivity Plots, https: dcc.ligo.org LIGO-G1500623 public
Lesage, S. 2020, GCN Circular 26980, https: gcn.gsfc.nasa.gov gcn gcn3 26980.gcn3
Levin, Y. 2007, MNRAS, 377, 159
Levin, Y., & van Hoven, M. 2011, MNRAS, 418, 659
Lin, L., Göğüş, E., Roberts, O. J., et al. 2020, ApJL, 902, L43
Lindblom, L., & Detweiler, S. L. 1983, ApJS, 53, 73
Macquet, A., Bizouard, M. A., Burns, E., et al. 2021, ApJ, 918, 80
Matone, L., & Márka, S. 2007, CQGra, 24, S649
Mazets, E. P., Aptekar, R. L., Cline, T. L., et al. 2008, ApJ, 680, 545
McDermott, P. N., van Horn, H. M., & Hansen, C. J. 1988, ApJ, 325, 725
Meegan, C., Lichti, G., Bhat, P. N., et al. 2009, ApJ, 702, 791
Mereghetti, S., Götz, D., von Kienlin, A., et al. 2005, ApJL, 624, L105
Messios, N., Papadopoulos, D. B., & Stergioulas, N. 2001, MNRAS, 328, 1161
Murphy, D., Tse, M., Raffai, P., et al. 2013, PhRvD, 87, 103008
Olausen, S. A., & Kaspi, V. M. 2014, ApJS, 212, 6
Piro, A. L. 2005, ApJL, 634, L153
Punturo, M., Abernathy, M., Acernese, F., et al. 2010, CQGra, 27, 194002
Quitzow-James, R. 2016, PhD thesis, Univ. of Oregon
Quitzow-James, R., Brau, J., Clarke, J., et al. 2017, CQGra, 34, 164002
Reitze, D., Adhikari, R. X., Ballmer, S., et al. 2019, BAAS, 51, 035
Robinet, F., Arnaud, N., Leroy, N., et al. 2020, SoftX, 12, 100620
Schale, P. 2019, PhD thesis, Univ. of Oregon, https: scholarsbank.uoregon. edu xmlui handle 1794 24835
Strohmayer, T. E., & Watts, A. L. 2005, ApJL, 632, L111
Strohmayer, T. E., & Watts, A. L. 2006, ApJ, 653, 593
Sutton, P. J. 2013, arXiv:1304.0210
Sutton, P. J., Jones, G., Chatterji, S., et al. 2010, NJPh, 12, 053034
Svinkin, D., Frederiks, D., Hurley, K., et al. 2021, Natur, 589, 211
Thrane, E., & Coughlin, M. 2013, PhRvD, 88, 083010
Thrane, E., Kandhasamy, S., Ott, C. D., et al. 2011, PhRvD, 83, 083004
Tsokaros, A., Ruiz, M., Shapiro, S. L., & Uryū, K. 2022, PhRvL, 128, 061101
Verkindt, D., 2021 Sensitivity Curves and BNS Range for Virgo in O2 and O3, Virgo TDS, https: tds.virgo-gw.eu ?content=3&r=19594
Was, M., Sutton, P. J., Jones, G., & Leonor, I. 2012, PhRvD, 86, 022003
Watts, A. L., & Strohmayer, T. E. 2006, ApJL, 637, L117
Wen, D.-H., Li, B.-A., Chen, H.-Y., & Zhang, N.-B. 2019, PhRvC, 99, 045806
Zhong, S.-Q., Dai, Z.-G., Zhang, H.-M., & Deng, C.-M. 2020, ApJL, 898, L5
Zink, B., Lasky, P. D., & Kokkotas, K. D. 2012, PhRvD, 85, 024030